

The role of carbon and oxygen in the transient behaviour of iron catalysts in Fischer-Tropsch synthesis

Citation for published version (APA):

Dijk, van, W. (1981). *The role of carbon and oxygen in the transient behaviour of iron catalysts in Fischer-Tropsch synthesis*. [Phd Thesis 1 (Research TU/e / Graduation TU/e), Chemical Engineering and Chemistry]. Technische Hogeschool Eindhoven. <https://doi.org/10.6100/IR132944>

DOI:

[10.6100/IR132944](https://doi.org/10.6100/IR132944)

Document status and date:

Published: 01/01/1981

Document Version:

Publisher's PDF, also known as Version of Record (includes final page, issue and volume numbers)

Please check the document version of this publication:

- A submitted manuscript is the version of the article upon submission and before peer-review. There can be important differences between the submitted version and the official published version of record. People interested in the research are advised to contact the author for the final version of the publication, or visit the DOI to the publisher's website.
- The final author version and the galley proof are versions of the publication after peer review.
- The final published version features the final layout of the paper including the volume, issue and page numbers.

[Link to publication](#)

General rights

Copyright and moral rights for the publications made accessible in the public portal are retained by the authors and/or other copyright owners and it is a condition of accessing publications that users recognise and abide by the legal requirements associated with these rights.

- Users may download and print one copy of any publication from the public portal for the purpose of private study or research.
- You may not further distribute the material or use it for any profit-making activity or commercial gain
- You may freely distribute the URL identifying the publication in the public portal.

If the publication is distributed under the terms of Article 25fa of the Dutch Copyright Act, indicated by the "Taverne" license above, please follow below link for the End User Agreement:

www.tue.nl/taverne

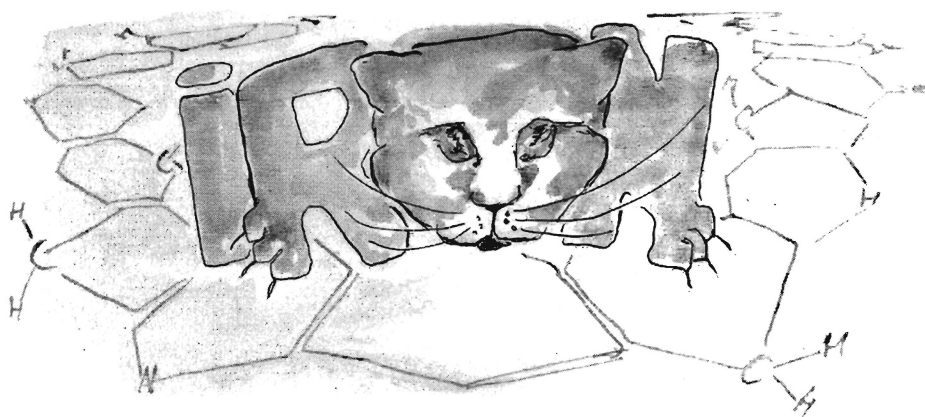
Take down policy

If you believe that this document breaches copyright please contact us at:

openaccess@tue.nl

providing details and we will investigate your claim.

THE ROLE OF CARBON AND OXYGEN IN
THE TRANSIENT BEHAVIOUR OF IRON CATALYSTS
IN FISCHER-TROPSCH SYNTHESIS



W. VAN DIJK

THE ROLE OF CARBON AND OXYGEN IN THE TRANSIENT BEHAVIOUR OF IRON CATALYSTS IN FISCHER-TROPSCH SYNTHESIS

PROEFSCHRIFT

TER VERKRIJGING VAN DE GRAAD VAN DOCTOR IN DE
TECHNISCHE WETENSCHAPPEN AAN DE TECHNISCHE
HOOGESCHOOL EINDHOVEN, OP GEZAG VAN DE
RECTOR MAGNIFICUS, PROF. IR. J. ERKELENS, VOOR
EEN COMMISSIE AANGEWEZEN DOOR HET COLLEGE
VAN DEKANEN IN HET OPENBAAR TE VERDEDIGEN OP
DINSDAG 2 JUNI 1981 TE 16.00 UUR

DOOR

WIM VAN DIJK

GEBOREN TE AMSTERDAM

Dit proefschrift is goedgekeurd
door de promotoren

Prof. Drs. H.S. van der Baan
en
Prof. Dr. V. Ponec

Aan Ineke en Joey

Oom Dagobert: Donald! Pak je spullen! Ik heb een hoogst
belangrijke opdracht voor je!

Donald Duck: Een opdracht?

Oom Dagobert: Kom mee naar buiten! Kijk maar eens naar
de lucht! Is-ie niet prachtig?

Donald Duck: Eh... huh...

Oom Dagobert: Ik bedoel die regenboog, Donald!

Donald Duck: O, ja... prachtig hoor! Maar wat heeft dat
met m'n opdracht te maken?

Oom Dagobert: Dat is je opdracht! Die regenboog!

Donald Duck: Huh?

Oom Dagobert: Ik wil dat je naar het einde van de regen-
boog gaat om de pot met goud voor me te
halen!

CONTENTS

1. INTRODUCTION	
1.1. Coal conversion	1
1.2. Synthesis gas conversion	3
1.3. Production of ethene in Western Europe	5
1.4. Aim and outline of this thesis	7
1.5. References	8
2. LITERATURE SURVEY	
2.1. Introduction	9
2.2. Activation of iron catalysts	12
2.2.1. Pretreatment conditions	12
2.2.2. Formation of iron carbides	12
2.2.3. Bulk composition of an industrial iron catalyst	13
2.3. Crystal structures of iron carbides	14
2.4. Mechanisms proposed for the Fischer-Tropsch reaction	16
2.5. Adsorption studies of H_2 and CO	20
2.6. References	21
3. THE ACTIVITY AND CHARACTERIZATION OF METALLIC IRON CATALYSTS DURING THE FISCHER-TROPSCH SYNTHESIS	
3.1. Introduction	25
3.2. Experimental	26
3.2.1. Catalyst preparation	26
3.2.2. Experimental methods	26
3.2.3. Catalyst characterization	28
3.2.4. Evaluation procedures for the Mössbauer spectra	28
3.2.5. Adsorption apparatus	29
3.3. Results	30
3.3.1. Catalysts before and after reduction	30
3.3.2. Crystallographically different iron carbides	30
3.3.3. Formation of carbides at different temperatures	34

3.3.4. Non-steady state experiments at 513 K	36
3.3.5. Adsorption of hydrogen and carbon monoxide	42
3.4. Discussion	43
3.5. References	49
 4. THE FISCHER-TROPSCH REACTION OVER PROMOTED IRON MANGANESE OXIDE CATALYSTS FOR THE PRODUCTION OF LIGHT OLEFINS	
4.1. Introduction	51
4.2. Experimental	52
4.2.1. Catalyst preparation	52
4.2.2. Outline of experimental methods	53
4.2.3. Catalyst characterization	53
4.3. Results	54
4.3.1. The iron manganese oxide catalyst before reduction	54
4.3.2. The manganese oxide catalyst after reduction	57
4.3.3. The iron manganese oxide catalyst after reduction	58
4.3.4. The Fischer-Tropsch synthesis on an iron manganese oxide catalyst at 513 K	60
4.3.5. The Fischer-Tropsch synthesis on a sulfur containing iron manganese oxide catalyst at 513 K	64
4.3.6. Olefin selective catalyst at 623 K	65
4.4. Discussion	67
4.5. References	70
 5. THE FORMATION OF ACTIVE HYDROGENATION ENSEMBLES DURING THE ACTIVATION OF AN IRON FISCHER-TROPSCH CATALYST	
5.1. Introduction	71
5.2. Experimental	72
5.2.1. Catalyst preparation	72
5.2.2. Magnetic susceptibility apparatus	73
5.2.3. Temperature programmed surface reaction (TPSR) apparatus	75
5.2.4. Thermobalance	75
5.2.5. Isothermal flushing reactions	76
5.3. Results	76
5.3.1. Thermomagnetic analysis	76
5.3.2. Carburization followed in the thermobalance	79

5.3.3. Reactivity of carbon species determined with TPSR experiments	85
5.3.4. Isothermal flushing reactions	89
5.4. Discussion	91
5.5. References	96
 6. A STUDY ON THE FISCHER-TROPSCH SYNTHESIS AT LOW PRESSURES	
6.1. Introduction	99
6.2. Experimental	100
6.2.1. High vacuum apparatus	100
6.2.2. Evaluation of mass spectra	103
6.2.3. Outline of experimental methods	105
6.3. Results	106
6.3.1. CO hydrogenation over clean reduced iron catalysts at very low pressures in a continuous flow fixed- bed reactor	106
6.3.2. CO hydrogenation over clean reduced iron catalysts at low pressures in a batch reactor	109
6.3.3. CO hydrogenation over preoxidized iron catalysts at low pressures in a batch reactor	113
6.4. Discussion	117
6.5. References	120
 SUMMARIZED CONCLUSIONS	121
 SUMMARY	124
 SAMENVATTING	127
 CURRICULUM VITAE	130
 DANKWOORD	131

CHAPTER 1

INTRODUCTION

1.1. COAL CONVERSION

During and shortly after the 'energy crisis' of 1973 there was much concern about the possibility that the shortage in oil availability in the industrialized world and in particular in continental Western Europe would continue in the future. Such a development has as yet not come about (1), as is shown in figure 1.1. The total consumption of oil and gas in the Netherlands has actually increased albeit that we were obliged to pay substantially higher prices for the raw material.

According to most energy scenarios we will have sufficient supply of oil and gas in the Netherlands until 1990, when the maximum of the oil and gas supply is expected; thereafter, it is hoped, we will experience a smooth substitution of oil and gas by coal and other energy sources.

In order to maintain as much as possible of our technical infrastructure, developed for the application of fluid energy carriers, coal will have to be converted into a fluid.

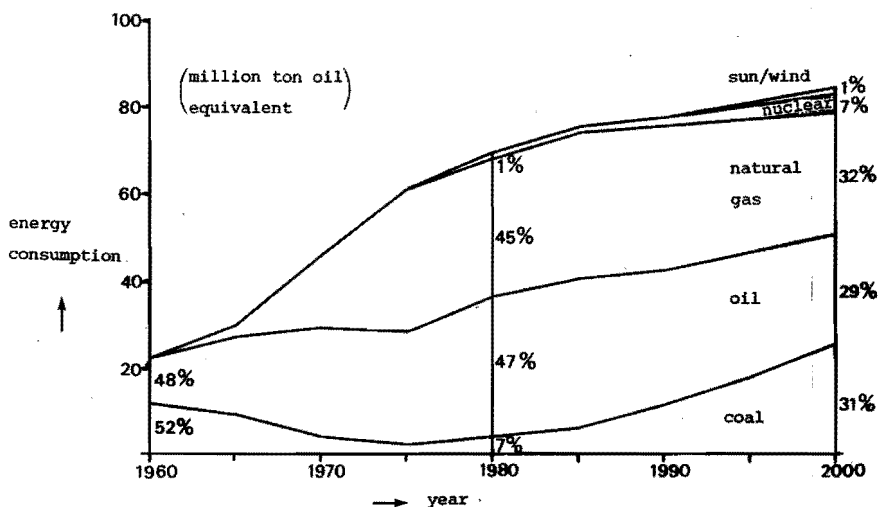


Figure 1.1. Expected contributions of various energy carriers to the energy consumption in Holland.

Several coal technologies are known already for a long time:

a. pyrolysis

In the Char Oil Energy Development (COED) process gases and liquids are produced by thermal decomposition of the coal in 4 consecutive reactors at temperatures varying from 315 to 870°C.

The disadvantage of this process is the low liquid yields and a high char and gas production.

b. direct liquefaction route

This process was developed by Bergius in 1913 in Germany and is now again taken up i.a. in the U.S.A.

Hydrogen gas and an organic solvent are added to the coal; the solvent has two functions:

1. extraction of soluble organic material
2. transfer of hydrogen to the polyaromatic fragments in the coal.

Two processes, which are still in the pilot-plant stadium, apply this system:

- Solvent Refined Coal (SRC) process (started in 1962).

The slurry of coal and hydrogen and solvent is recycled to produce mainly liquids.

- H-coal process (started in 1964).

A cobalt molybdenum catalyst is added to the slurry of coal, solvent and hydrogen. Because the catalyst is quickly deactivated, the catalyst has to be renewed often.

c. extraction with a hydrogen donor solvent

In the Exxon Donor Solvent (EDS) process, hydrogen is added to the coal by the solvent alone. The dehydrogenated donor solvent is catalytically hydrogenated in a separate fixed-bed reactor and then mixed with coal in the extraction vessel.

d. indirect route

The coal is first gasified with steam or oxygen and the synthesis gas (a mixture of H_2 and CO) obtained is then converted into mainly liquid products.

This route has a number of advantages:

- the process is executed at moderate pressures, which means lower investments costs
- simple gas phase catalytic reactions occur in the second step
- high quality products can be made
- the technological know-how is available e.g. from SASOL in South-Africa.

The disadvantage of this route is the gasification process, which does not have a required high overall efficiency, because 30% of the coal is used as heat supplier for the gasification reaction proper.

1.2. SYNTHESIS GAS CONVERSION

The synthesis gas can be used as a raw material for the production of:

- a. pure SNG-gas (Methanation)
- b. methanol (ICI-process)
- c. gasoline (Mobil-process)

If methanol is dehydrated to dimethylether and then passed

over a zeolite catalyst, gasoline with a high-octane number is produced (2) very selectively (90%).

- d. various hydrocarbon fractions from ethene to dieseloil (Fischer-Tropsch process).

The product distribution is determined by the reaction conditions and the catalyst. The Fischer-Tropsch process is attractive, because many valuable products can be made e.g. light olefins (C_2-C_4) as chemical feedstock for the chemical industry, a naphthafraction (C_5-C_{12}) as a substitute for naphthacracker feedstock and a diesel fraction ($C_{13}-C_{18}$) as a competitive motorfuel.

The production costs as estimated by Hiller/Garkisch (3) for the Fischer-Tropsch process and the Mobil-process are shown in table 1.I; the difference between these two processes are not very pronounced. In fact these production processes are becoming already almost competitive with the traditional gasoline manufacture from crude oil, if the gaseous byproduct SNG can be sold at a reasonable price (0.09 \$/m³ gas).

Table 1.I. The production costs of gasoline by different processes

process	starting material	products	price gasoline (\$)/gallon
Fischer-Tropsch	coal \$20/ton	gasoline dieseloil LPG	1.15
Fischer-Tropsch	coal \$20/ton	gasoline dieseloil LPG SNG	0.7
Mobil	coal \$20/ton	gasoline LPG	0.9
Mobil	coal \$20/ton	gasoline LPG SNG	0.6
naphtha cracker (4)	crude oil \$20/barrel	gasoline middle destillate heavy fuel oil	0.58

Recent work (5, 6) has shown, that a combination of an iron Fischer-Tropsch catalyst and the Mobil zeolite can result in an increased gasoline production, while the chain length of the hydrocarbon is limited by the shape of the zeolite.

Thus there are now a number of ways that can be followed to produce gasoline (direct liquefaction, Fischer-Tropsch and/or Mobil-process) and diesel fuel (with the Fischer-Tropsch process) from coal. We will now consider alternatives for the manufacture of ethene and other small olefins, that are in great demand as chemical feedstocks.

1.3. PRODUCTION OF ETHENE IN WESTERN EUROPE

Ethene, still mainly manufactured by cracking of naphtha in Western Europe, is an important feedstock in the chemical industry for the production of:

- a. plastics (65%), like polyethene (44%), polyvinyl chloride (13%) and polystyrene (8%).
- b. etheneoxide (16%), which is used in the production of anti-freeze and polyester fibers.
- c. chemicals (19%), like aliphatic alcohols, α -olefins and vinyl-acetate.

Between 1976-1978 the demand of ethene has increased with 9%/year and it is assumed (7) that after 1980 this increase will be somewhat lower: around 6%/year. The demand for ethene will catch up with the present overcapacity of ethene (8) between 1983-1985.

With naphtha in short supply the ethene producers in Western Europe have turned to other sources like gasoil, C_4 and C_5 fractions and lately towards natural gas liquids (NGL) from North Sea gas fields.

These light fractions can be used as feedstock in an ethane cracker, that is a somewhat less expensive version of a naphtha cracker. That ethane crackers are more attractive than naphtha crackers is illustrated in table 1.II by the comparison of the quantities of feedstock required for the production of e.g. 1 million ton ethene/year (9). Especially the conversion of 22% of the naphtha into residual gas and fuel oil in a naphtha cracker is a serious drawback for this process.

Table 1.II. Production amounts in million ton/year

	ethane feedstock	Kuwait naphtha feedstock
residual gas	0.175	0.484
ethene	1.000	1.000
C ₃ 's	0.031	0.392
C ₄ 's	0.025	0.205
gasoline	0.019	0.644
cracked fuel oil	<u> </u>	<u>0.175</u>
total feedstock	1.250	2.900

The uncertainties concerning ethane crackers in Western Europe are still substantial, because present forecasts envisage a maximum NGL-production from the North Sea gas fields around 1984 and a possible decrease again after the year 1990 (figure 1.1).

At the moment the production costs of ethene from coal are with the Fischer-Tropsch process still higher than from an ethane- or gasoil cracker (see table 1.III).

A comparison with the actual production costs of ethene from crude oil is difficult, as the price of crude oil has increased since 1977 from \$13/barrel to about \$30/barrel nowadays.

The price of ethene is in Western Europe about 25% higher than in the U.S.A., because of differences in the hydrocarbon price structures in the two areas. The Fischer-Tropsch production of ethene with coal from Germany is not an attractive route either, since the price of this coal is extremely high (\$95/ton in 1979).

If the supply of naphtha, gasoil and LPG fuels will decrease in the future, while the ethene price will increase due to an increasing demand the production of ethene from cheaper imported coal will made it all more attractive.

Table 1.III. Production capacity 2 million ton ethene/year

feedstock	price feedstock in 1977 in U.S.A.	net production costs in 1977 in U.S.A. (\$/ton ethene)
coal	\$ 12/ton	275
ethane	\$ 79/ton	161
gasoil	\$ 72/ton	126
crude oil	\$ 13/barrel	220-264

1.4. AIM AND OUTLINE OF THIS THESIS

The production of light olefins from synthesis gas had to be improved by developing more advanced Fischer-Tropsch catalysts, which have a high selectivity for light olefins, combined with a good stability and activity.

Because iron catalysts produce higher hydrocarbons with a rather high olefin content, this metal is chosen as the starting material for the catalyst.

A short literature review of the behaviour and the bulk composition of iron catalysts during industrial Fischer-Tropsch synthesis is given in chapter 2, where also a survey is given of the many reaction intermediates and rate determining steps, that have been proposed for the Fischer-Tropsch reaction.

Kinetic studies on iron catalysts are rather difficult, because the composition of the surface and the bulk of the catalyst change drastically during the synthesis. In the literature a number of different views concerning the bulk composition of iron catalysts can be found. We have endeavoured to shed some more light on these problems in chapter 3. This work is done in co-operation with the IRI laboratory in Delft (Holland), where the Mössbauerspectra of our catalyst samples were measured.

In continuation of the work described in chapter 3 a parallel study on promoted iron catalysts is reported in chapter 4. For these catalysts an improved selectivity for light olefins is demonstrated. Also here we want to mention the fruitful co-operation with the IRI laboratory.

The different carbonaceous deposits formed on the catalyst surface are further studied with the aid of various experimental techniques in chapter 5. The reactivity of the bulk- and surface carbon species towards hydrogen is further discussed.

In chapter 6 we report on the Fischer-Tropsch reaction at low pressures ($10\text{--}10^4$ Pa). In the vacuum equipment more information is obtained about the nature and reactivity of the surface intermediates.

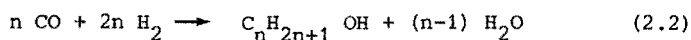
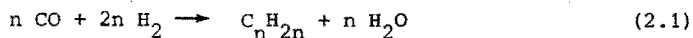
1.5. REFERENCES

1. Essobron, Aug. (1980)
2. Chem. Eng. News 26, Jan. (1978)
3. H. Hiller, O.L. Garkisch, Hydrocarbon Proc., 238, Sept. (1980)
4. H. Grünewald, Chemistry and Industry 806, Dec. (1979)
5. C.D. Chang, W.H. Lang, A.J. Silvestri, J. Catal. 56, 268 (1979)
6. P.D. Caesar, J.A. Brennan, W.E. Garwood, J. Ciric, J. Catal. 56, 274 (1979)
7. L. Wilkinson, C & EN 11, May (1979)
8. Chemical Week, Oct. (1979)
9. S.B. Zdonik, E.J. Bassler, L.P. Hallee, Hydrocarbon Proc. 73, Febr. (1974)

LITERATURE SURVEY

2.1. INTRODUCTION

The results of the thermodynamic calculations of Anderson et al. (1) on the hydrogenation of carbon monoxide are summarized in figure 2.1 for the case that only hydrocarbons and simple oxygenated molecules are formed. The normalized free enthalpy changes ($\Delta G^0/n$) are plotted as a function of temperature for the following reactions, which are coupled with the formation of water:



Because most of the reactions considered are exothermic, the free enthalpy changes are at the usual temperatures of the Fischer-Tropsch reaction generally adequate for the formation of hydrocarbons and simple oxygenated molecules, there are only a few exceptions to this statement e.g. for the formation of acetylene, formaldehyde and also methanol.

However formation of hydrocarbons by the Fischer-Tropsch reaction is in general, in so far as the turnover numbers are considered,

generally exceptionally slow. This is shown e.g. by the difference between the turnover numbers of the hydrogenation (2) of carbon monoxide (0.06 mol/surface atom. sec) and for instance the hydrogenation (3) of cyclohexene to cyclohexane (2.0 mol/surface atom. sec).

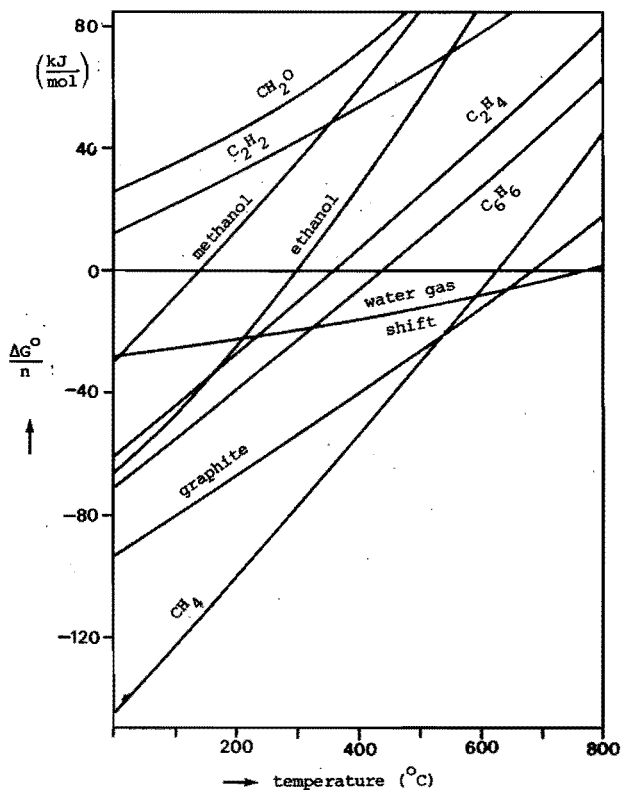


Figure 2.1. Normalized standard free enthalpy changes for the production of various molecules by the Fischer-Tropsch reaction as a function of temperature (ref. 1).

An increase of the reaction rate is obtained at higher reaction temperatures (600 - 700 K), but excessive amounts of elemental carbon (graphite) are usually formed at these reaction temperatures.

Even if ΔG° is positive, higher molecular weight products can be obtained at increased pressures, according to the van het Hoff - Le Chatelier principle. This is demonstrated in figure 2.2 for the formation of alcohols (4).

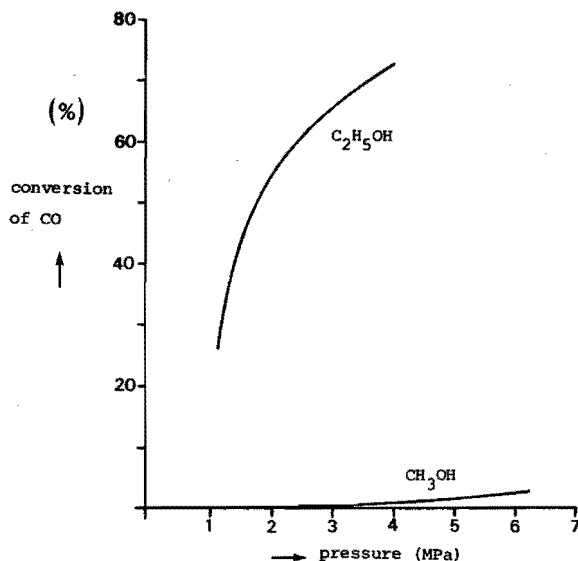


Figure 2.2. The formation of alcohols by the Fischer-Tropsch reaction at 670 K as a function of the pressure (ref. 4).

If specific types of molecules have to be produced with the Fischer-Tropsch reaction, the selectivity of the catalyst becomes important.

Several metals have been applied for the preparation of selective catalysts, since in 1902 Sabatier discovered the CO hydrogenation by Ni catalysts.

Methane is produced at a relatively high rate and selectivity over nickel catalysts.

Cobalt catalysts were already used at the end of 1930 in Germany at medium (0.6 - 1 MPa) pressures for the production of gasoline; at one atmosphere mostly methane and a small amount of saturated hydrocarbons are produced (5).

Ruthenium catalysts are unique in their ability to form high molecu-

lar weight paraffinic waxes, even at atmospheric conditions. During the second world war various iron catalysts were tested in Germany at medium pressures; a broad product distribution with a high olefin content was characteristic for those catalysts. Some alcohols, aldehydes and acids were formed as byproduct. Recently palladium and platinum as well as iridium have been found to be active at medium pressures (1.2 MPa) for the selective production of methanol (6). Poutsma et al. (6) suggested, that the oxygen containing compounds are formed, because these metals do not dissociate carbon monoxide (7), which is generally assumed to be necessary for the initiation step in the Fischer-Tropsch synthesis.

In this thesis iron was chosen as the active metal for catalysts for the Fischer-Tropsch reaction. As the usual broad product distribution had to be avoided, special catalysts were chosen, in order to obtain a narrow product distribution and a reasonable reaction rate.

2.2. ACTIVATION OF IRON CATALYSTS

2.2.1. Pretreatment conditions

Alkalized precipitated iron catalysts were studied by Pichler around 1950 at reaction temperatures between 550 and 570 K and at atmospheric or medium pressures. After a reduction in H_2 at about 630 K the raw material was, at least initially, inactive in the Fischer-Tropsch synthesis. However at the Kaiser-Wilhelm Institute (KWI) the pretreatment conditions were studied for these catalysts and an active catalyst was obtained by treatment with 0.01 MPa of carbon monoxide at 600 K.

In recent patents of Kölbel (8) (and also in the industrial Fischer-Tropsch process at SASOL, South-Africa) the iron catalysts are first pretreated with carbon monoxide or synthesis gas at 0.1 MPa.

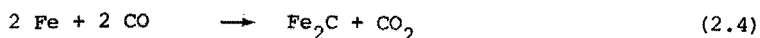
2.2.2. Formation of iron carbides

Table 2.I presents the free enthalpy changes for the formation of iron carbides (9). These carbides have a positive free enthalpy

of formation in the temperature range of the Fischer-Tropsch synthesis i.e. the carbides are unstable as compared with the decomposition into the metal and carbon:



However reactions producing carbides from carbon monoxide such as:



have negative standard free enthalpy changes.

The carbides can also easily be formed with olefins, as is shown by the negative standard free enthalpy changes in table 2.I.

Also for paraffins with carbon numbers higher than 4, the standard free enthalpy changes are negative; however the carbides are produced at a relatively low rate of formation.

Table 2.I. ΔG° (kJ/mol)

temperature (°C)	$2\text{Fe} + \text{C} \rightarrow \text{Fe}_2\text{C}$	$2\text{Fe} + 2\text{CO} \rightarrow \text{Fe}_2\text{C} + \text{CO}_2$	$\text{C}_2\text{H}_4 + 4\text{Fe} \rightarrow 2\text{Fe}_2\text{C} + 2\text{H}_2$
227	+ 16.0	- 67.9	- 49.0
327	+ 14.5	- 51.5	- 59.1

2.2.3. Bulk composition of an industrial iron catalyst

After a reduced industrial iron catalyst (10) was submitted to synthesis gas at 0.8 MPa at a temperature of 530 K, its bulk composition was determined by thermomagnetic analysis (TMA), as is shown in figure 2.3. Initially, reasonable amounts of iron carbide and magnetite (Fe_3O_4) were formed; later on, more magnetite was formed at the expense of $\alpha\text{-Fe}$.

Pichler et al. (11) suggested, that the activity of their catalyst at atmospheric pressure was proportional to the amount of carbide

present. Recently Raupp and Delgass (12) came to the same conclusion from their Mössbauer studies on iron catalysts.

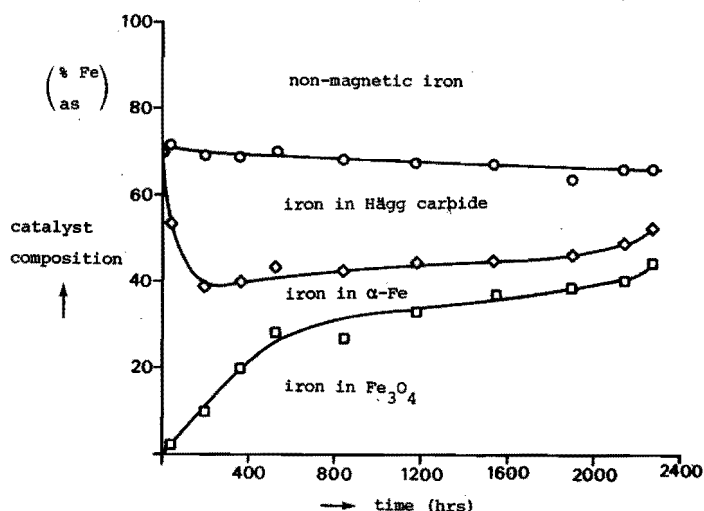


Figure 2.3. The bulk composition of an industrial iron catalyst during the Fischer-Tropsch synthesis at 0.8 MPa and at 530 K (ref. 10).

On the basis of their TMA studies Pichler et al. claimed further, that the hexagonal carbide $\epsilon\text{-Fe}_2\text{C}$ (Curie temperature at 650 K) was more effective in increasing the activity than the Hägg carbide (Curie temperature at 521 K). Herbst et al. (13) agreed partly by stating that the presence of the hexagonal carbide $\epsilon\text{-Fe}_2\text{C}$ was a necessary, but not a sufficient condition for catalysts to be of high activity.

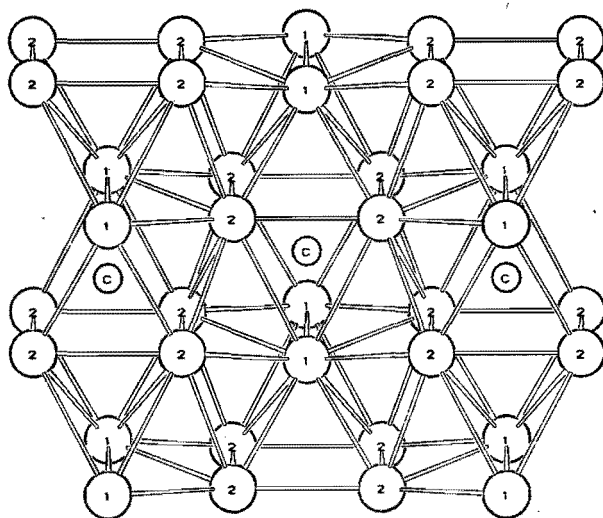
2.3. CRYSTAL STRUCTURES OF IRON CARBIDES

Hägg carbide ($\chi\text{-Fe}_5\text{C}_2$) has a monoclinic structure (14).

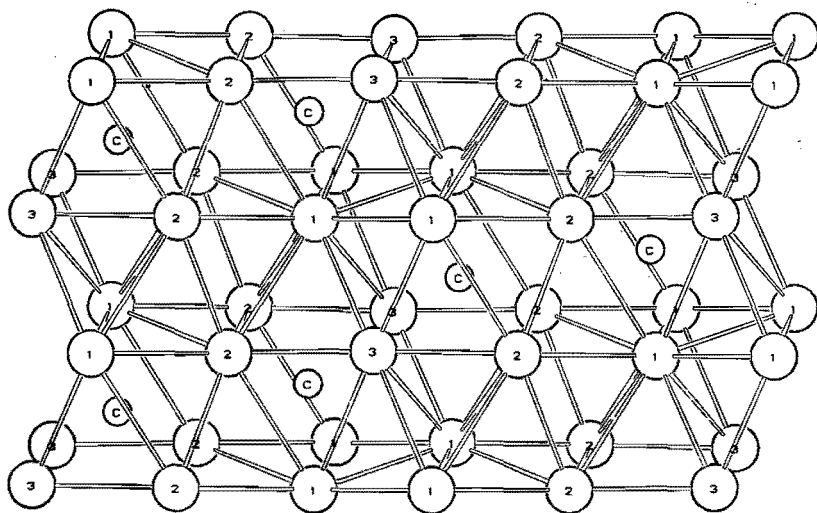
Three different lattice sites for iron are present with the following occupation ratio $\text{Fe}_\text{I} : \text{Fe}_\text{II} : \text{Fe}_\text{III}$ of 2 : 2 : 1.

Hägg carbide is a ferromagnetic compound with a Curie temperature of 521 K.

Cementite ($\theta\text{-Fe}_3\text{C}$) has an orthorhombic structure (15).



$\theta\text{-Fe}_3\text{C}$ (100)-projection



$\chi\text{-Fe}_5\text{C}_2$ (001)-projection

Figure 2.4. A representative part of the structures of $\theta\text{-Fe}_3\text{C}$ and $\chi\text{-Fe}_5\text{C}_2$ (only distances between 1.5 Å and 3.0 Å are drawn) (ref. 16).

Only two different lattice sites are occupied with an occupation ratio $\text{Fe}_I : \text{Fe}_{II}$ of 1 : 2.

Cementite is a ferromagnetic compound with a Curie temperature (485 K) that differs noticeable from that of the Hägg carbide. If a representative part of the projection of 4 unit cells of $\chi\text{-Fe}_5\text{C}_2$ on the (001) plane is compared with a representative part of the projection of 4 unit cells of $\theta\text{-Fe}_3\text{C}$ on the (100) plane (16), the agreement between the two crystal structures becomes evident (figure 2.4).

Hofer (17) synthesized the hexagonal carbide $\epsilon\text{-Fe}_2\text{C}$, which was found to have a Curie temperature of 653 K, while the distorted hexagonal ϵ' -carbide with the stoichiometry $\text{Fe}_{2.2}\text{C}$ was observed at a Curie temperature of 723 K (18).

2.4. MECHANISMS PROPOSED FOR THE FISCHER-TROPSCH REACTION

The first mechanism, proposed by Fischer (19), is the so called carbide mechanism. Carbon monoxide dissociates and forms carbides, which are subsequently hydrogenated to CH_2 -groups. Chain growth proceeds via polymerisation of these CH_2 -groups. Many objections have been raised against this mechanism. Emmett (20) carburized an iron catalyst with ^{12}CO to 60 to 70 percent Fe_2C at 520 K; an additional 10 percent of the catalyst was then carburized with radioactive ^{14}CO . Appreciable amounts of radioactive $^{14}\text{CH}_4$ were produced for a long period during the following Fischer-Tropsch synthesis at 520 K, but only 4.2 percent of the ($\text{C}_3 + \text{C}_4$) fraction was formed from the ^{14}C -carbides. Also Kryukov (21) showed that the ^{14}C atoms of freshly prepared bulk ^{14}C -carbides are hardly inserted in the Fischer-Tropsch chains. Recent work of Raupp and Delgass (12) shows, that the hydrogenation rate of a bulk carbide is about 4 times slower than the corresponding Fischer-Tropsch reaction rate. Because the bulk carbides have a too low reactivity, these compounds are not thought to be plausible intermediates in the Fischer-Tropsch synthesis.

Storch (22) proposed an alcohol-type (hydroxycarbene) complex as the intermediate; the chain growth is taking place via dehydro-

condensation of these complexes. This mechanism was in particular favoured by Anderson (23) and Kölbl (24). Several authors (25, 26, 27) observed after the simultaneous adsorption of H_2 and CO at $50^\circ C$, that H_2 and CO desorbed with a constant 1 : 1 ratio. The proposed reaction intermediate $*CHOH$ satisfied the measured stoichiometric H_2/CO ratio of 1. The validity of this argument has been doubted by authors who pointed out, that this reaction intermediate $*CHOH$ can hardly exist at the reaction temperatures (between 470 and 670 K), when XPS- and UPS show, that the dissociation of carbon monoxide takes place already at room temperature on iron catalysts (28, 29). The addition of methanol to synthesis gas (30) causes hardly any increased chain growth, but this may be caused by the fact, that methanol dissociates into CO and H_2 above reaction temperatures of $250^\circ C$ (31, 32).

The alcoholic intermediates on metallic Fe have as yet not been observed with IR-spectroscopy (33, 34, 35).

Because of the arguments raised against the previous intermediates, Pichler (36) proposed carbonyl species as the reactive intermediates. The propagation would then proceed via the insertion of carbon monoxide in the growing chain. Actually not many experimental results have been put forward to support this intermediate and the support is by inferential arguments.

XPS- and UPS studies on iron catalysts show, that carbon monoxide can dissociate already at room temperature (28, 29), while various authors have shown, that a carbon atom from dissociated CO can form CH_x intermediates with H_2 and finally also methane (37, 38, 39). The chain growth can proceed then as a polymerisation of the CH_x surface species (40, 41). In a kinetic study by Rautavuoma and van der Baan (42) of the Fischer-Tropsch reaction on a Co/Al_2O_3 catalyst, this mechanism, whereby hydrogenation of C^* to CH_2^* was assumed to be the overall rate determining step, was supported by all data.

Van Ho and Harriott (44) deposited carbon on a 2% Ni-silica catalyst by the disproportionation of CO:



When the C^* species were subsequently hydrogenated, the initial gasification rate ($r_{\text{initial}}^{\text{gasification}}$) of these atomic C^* species in pure H_2 appeared to be faster than the rate of methanation reaction in the steady-state ($r_{\text{steady-state}}^{\text{methanation}}$), as is shown in figure 2.5. The disproportionation of CO takes probably place in two steps:



Since according to Van Ho and Harriott the reaction of preadsorbed oxygen with carbon monoxide is very fast on a Ni catalyst, the CO_2 released was taken as a measure of the carbon C^* formed. The rate of CO_2 formation and thus the rate of formation of C^* increased quickly to a maximum ($r_{\text{C-deposition}}^{\text{max}}$) and then declined to a nearly constant value ($r_{\text{steady-state}}^{\text{C-deposition}}$). However even the maximum rate of formation of C^* appeared then to be much lower than the steady-state methanation rate referred to above (see figure 2.5).

Results similar to those of Van Ho and Harriott are also obtained by several other authors (38, 39, 43), who concluded, that the dissociation of CO, possibly assisted by H_2 , might be involved in the rate-determining step of the Fischer-Tropsch synthesis.

One should be rather cautious in interpreting these results. It is known, that CO and H_2 compete for the same sites and that CO is stronger bonded than H_2 . Also the Fischer-Tropsch reaction rate is strongly dependent on the H_2 -partial pressure (first order) and hardly on the CO-partial pressure (almost zero order). It thus remains very well possible, that the surface, obtained after disproportionation of CO, has during the initial gasification with H_2 a higher coverage by H_2 than the surface which operates under the methanation reaction in the steady-state.

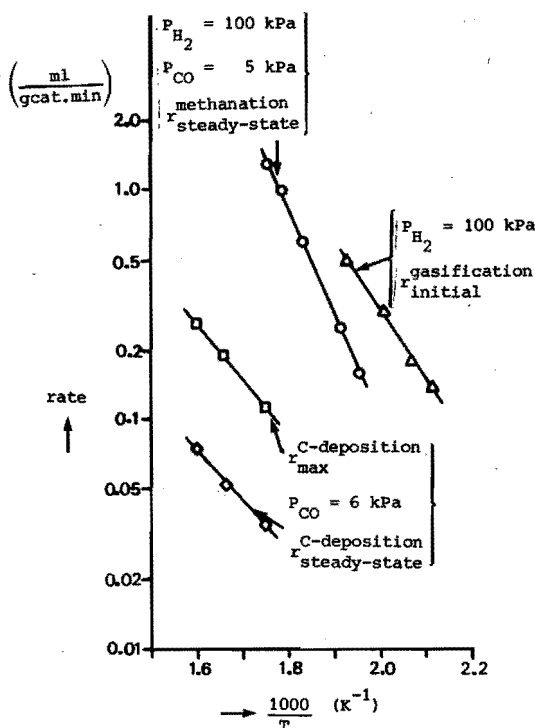


Figure 2.5. Comparison of the methanation rates with the rates of carbon deposition and carbon gasification for a 2% Ni catalyst (ref. 44).

Hydrogen may possibly 'assist' the dissociation of carbon monoxide indirectly. Not only the O-atoms, but also the C-atoms, are removed by H_2 according to the reactions:



So that less inhibition of the CO disproportionation, due to blocking of the surface by C^* or O^* , occurs.

Although Van Ho and Harriott found, that the removal of preadsorbed oxygen was fast with CO on Ni catalysts, this result does not yet prove, that the reaction rate constants of the CO-dissociation (k_1 , k_{-1}) and of the formation of CH_2^* -species (k_4) are lower than the rate constant of the oxygen removal reactions (k_2 and k_3).

The hydrogen assisted dissociation of CO is possibly supported by the experiments of Rabo et al. (36) on Pd catalysts at 300°C. Hardly any disproportionation of CO occurred, when pure CO was pulsed at 300°C over this catalyst. A subsequent H₂-puls produced at once a reasonable amount of methane. One cannot exclude the possibility, that the metals Rh, Pt and Pd, which do not dissociate carbon monoxide easily (7), behave totally different from the metals Fe, Ni, CO and Ru, which can dissociate carbon monoxide easily.

2.5. ADSORPTION STUDIES OF H₂ AND CO

The knowledge of the amounts of carbon monoxide and hydrogen adsorbed at the reaction temperature would be most interesting, but no reproducible adsorption experiments can be carried out at the Fischer-Tropsch reaction temperature. Even at room temperature, a part of CO can already dissociate and deposit carbon on iron catalysts. Nevertheless, the active surface sites are usually determined by adsorption of H₂ and CO at room temperature with the assumption, that carbon monoxide does not dissociate.

The CO-adsorption experiments are usually carried out by measuring the adsorption isotherm up to a carbon monoxide pressure of about 10 kPa; the physically adsorbed CO is evacuated within a few minutes and subsequently a second CO-adsorption isotherm is determined. The difference between the two isotherms is the amount of carbon monoxide chemisorbed firmly on the active sites.

With regard to the adsorption of H₂ it is usually assumed, that H₂ is adsorbed dissociatively at room temperature.

Vannice (45) studied the adsorption of H₂ and CO at room temperature on various alumina supported metal catalysts; in most cases the H₂-adsorption was less than the CO-adsorption, sometimes even several orders of magnitude smaller (see table 2.II).

Recently Topsøe (46) obtained saturation coverages of H₂ on supported iron catalysts, only when the H₂-adsorption was carried out at temperatures around 500 K. These results indicate, that the adsorption of hydrogen is probably an activated process on supported metal catalysts.

Topsøe (46) showed that with CO-adsorption measurements and IR-spectroscopy the stoichiometry Fe : CO was dependent of the particle size. If the average particle diameter was smaller than 50\AA , CO was adsorbed at room temperature on top of a Fe-atom (Fe : CO stoichiometry of 1 : 1), while the larger particles do adsorb CO with a Fe : CO stoichiometry of 2 : 1. The latter stoichiometry is more often observed on iron catalysts (47, 48).

Table 2.II. Chemisorption measurements at 293 K on catalyst samples (Vannice)

catalyst	H ₂ uptake ($\mu\text{mol/g cat}$)	CO uptake ($\mu\text{mol/g cat}$)
15% Fe/Al ₂ O ₃	0	21.5
2% Co/Al ₂ O ₃	1	16
5% Ru/Al ₂ O ₃	17.4	35

Jagannathan et al. (49) studied with XPS- and UPS-equipment at 400 K the adsorption of CO on Fe-films; CO dissociated and an enrichment of oxides was observed in the surface layers, while the carbon atoms diffused away into the interior of the Fe-film. No adsorption of CO is observed on Fe₂O₃ (46), while Fe₃O₄ hardly adsorbs any carbon monoxide at room temperature (50).

Emmett et al. (51) observed also no adsorption of carbon monoxide on the Hägg carbide $\chi\text{-Fe}_5\text{C}_2$.

2.5. REFERENCES

1. R.B. Anderson, C.B. Lee, J.C. Machiels, Can. Journ. of Chem. Eng. 54, 590 (1976)
2. M. Vannice, J. Catal. 37, 462 (1975)
3. M. Boudart, R.L. Burwell jr., Investigation of rates and Mechanisms of Reactions, Part I, 3rd ed., ed. by E.S. Lewis, John Wiley & Sons, New York, 702 (1974)

4. D. Dwyer, K. Yoshida, G.A. Somorjai, Symp. on advances in F.T. Chemistry, Anaheim meeting, March (1978)
5. A.O.I. Rautavuoma, thesis University of Technology Eindhoven (1978)
6. M.L. Poutsma, L.F. Elek, P.A. Ibarbia, A.P. Risch, J.A. Rabo, J. Catal. 52, 157 (1978)
7. B.G. Broden, T.N. Rhodin, C. Brucker, R. Renhow, Z. Hurych, Surf. Science 59, 593 (1976)
8. H. Kölbel, K.D. Tillmetz, Deutsches Offenlegungsschrift 2 507 647 (1976)
9. P.H. Emmett, Catalysis, Vol. IV, 21 (1956)
10. R.B. Anderson, L.J.E. Hofer, E.M. Cohn, B.J. Seligman, J. Am. Chem. Soc. 73, 944 (1951)
11. H. Pichler, H. Merkel, U.S. Bureau of Mines Techn. Paper, 718 (1949)
12. G.B. Raupp, W.N. Delgass, J. Catal. 58, 361 (1979)
13. M. Herbst, F. Haller, R. Brill, FIAT Reel R19, Frames 7, 136-147
14. G. Le Caer, J.M. Dubois, J.P. Senateur, J. of Sol. State Chem. 19, 19 (1976)
15. F. Herbstein, J. Smuts, Acta Cryst. 17, 1331 (1964)
16. G.J. Visser, private communication
17. L.J.E. Hofer, E.M. Cohn, W.C. Peebles, J. Am. Chem. Soc. 71, 189 (1949)
18. S.M. Loktev, L.I. Makarenkova, E.V. Slivinskii, S.D. Entin, Kinet. Katal. 13, 1042 (1972)
19. F. Fischer, H. Tropsch, Ber. Dtsch. Chem. Ges. 59, 830 (1926)
20. P.H. Emmett, J.T. Kummer, T.W. de Witt, J. Am. Chem. Soc. 70, 3632 (1948)
21. Y.B. Kryukov, A.N. Bashkistrov, N.P. Stepanova, Kinet. Katal. 2, 702 (1961)
22. H. Storch, H. Golumbic, R.B. Anderson, Fischer-Tropsch and related synthesis, John Wiley & Sons, New York (1951)
23. R.B. Anderson, Catalysis, Vol. IV, ed. by P.H. Emmett, Reinhold Publishing Corporation, Baltimore 1-371 (1956)
24. H. Kölbel, Chem. Technologie, Band 3, ed. by K. Winnacker and L. Kuchler, Carl Hanser Verlag, München 439 (1959)

25. M.V.E. Sastri, R. Balaji Gupta, B. Viswanathan, J. Catal. 32, 325 (1974)
26. V.M. Vlasenko, L.A. Kukhar, M.T. Rusov, N.P. Sahenko, Kinet. Katal. 5, 301 (1964)
27. H. Kölbl, G. Patzschke, H. Hammer, Brennstoff Chemie 47(1), 4 (1966)
28. K. Kishi, M. Roberts, J. Chem. Soc. Faraday Trans. 71, 1715 (1975)
29. G. Broden, H. Bonzel, G. Gafner, Appl. Phys. 13, 333 (1977)
30. W. Hall, R.J. Kokes, P.H. Emmett, J. Am. Chem. Soc. 79, 2989 (1957)
31. J.B. Benziger, R.J. Madix, J. Catal. 65, 36 (1980)
32. D. Kitzelmann, thesis University of Technology Bonn (1978)
33. G. Blyholder, L.D. Neff, J. Phys. Chem. 66, 1664 (1962)
34. R.A. Dalla Betta, M. Shelef, J. Catal. 48, 111 (1977)
35. D.L. King, J. Catal. 61, 77 (1980)
36. H. Pichler, H. Schulz, Chem. Ing. Techn. 42, 1162 (1970)
37. M. Araki, V. Ponec, J. Catal. 44, 439 (1976)
38. P. Wentrccek, B.J. Wood, H. Wise, J. Catal. 43, 363 (1976)
39. J. Rabo, A.P. Risch, M.L. Poutsma, J. Catal. 53, 295 (1978)
40. P. Biloen, J.M. Helle, W.M.H. Sachtler, J. Catal. 58, 95 (1979)
41. H.P. Bonzel, H.J. Krebs, W. Schwarting, Chem. Phys. Letters 72(1), 165 (1980)
42. A.O.I. Rautavuoma, H.S. van der Baan, to be published
43. H. Bartholomew, D.C. Gardner, J. Catal., in press
44. S. van Ho, P. Harriott, J. Catal. 64, 272 (1980)
45. M. Vannice, J. Catal. 37, 449 (1975)
46. H. Topsøe, N. Topsøe, H. Bohlbro, Int. Cat. Congress Tokyo (1980)
47. P.H. Emmett, S. Brunauer, J. Am. Chem. Soc. 62, 1732 (1940)
48. R.L. Park, H.E. Farnsworth, J. Chem. Phys. 43, 2351 (1965)
49. K. Jagannathan, A. Srinivasan, M.S. Hegde, F.N.R. Rao, Surf. Science 99, 309 (1980)
50. J.E. Kubsch, C.R.F. Lund, S. Yuen, J.A. Dumesic, 72nd annual AIChE meeting San Francisco (1979)
51. H.H. Podgurski, J.T. Kummer, T.W. de Witt, P.H. Emmett, J. Am. Chem. Soc. 72, 5382 (1950)

THE ACTIVITY AND CHARACTERIZATION OF METALLIC IRON CATALYSTS DURING THE FISCHER-TROPSCH SYNTHESIS

3.1. INTRODUCTION

The main conclusion presented in a 1974 study (1) on the economy of the Fischer-Tropsch process was that for this process to become interesting, a major improvement of the selectivity to move valuable products had to be reached. In particular in Germany and in West Europe the interest should be focussed on the development of catalysts for the production of low olefins. In their patents Kölbl (2) and Büssemeier (3) described olefin selective catalysts containing iron metal and various oxides that are difficult to reduce.

Because our aim is to make a catalyst that is highly selective for the production of olefins, we have chosen iron metal as the main component of our catalysts.

Iron containing catalysts are not stable during Fischer-Tropsch synthesis, but are converted into various carbides and covered by deposited carbon. This conversion into carbides has recently been investigated by means of Mössbauer spectroscopy by Raupp and Delgass (4) and Amelse et al. (5), who used iron supported on silica, by Nahon et al. (6), who used iron on alumina and by Maksimov et al. (7), who worked with a fused iron catalyst in which various pro-

motors were present. Also thermomagnetic analysis (8, 9, 10) and X-ray diffraction (9, 11) have been applied to study the formation of carbides in iron catalysts under various conditions of Fischer-Tropsch synthesis. Frequently, comparison between particular studies is difficult, because not all investigators seem to be aware of the existence of at least four different iron carbides. Moreover some confusion exists about the X-ray diffraction spectra of the hexagonal ϵ' -Fe_{2.2}C and the ϵ -Fe₂C, a carbide which has a monoclinic structure which reminds of the hexagonal one. In the present investigation, we have used Mössbauer spectroscopy together with X-ray diffraction analysis, carbon content determination and reaction kinetic measurements to study the conversion of an unpromoted and unsupported metallic catalyst into various carbide phases during the Fischer-Tropsch process.

3.2. EXPERIMENTAL

3.2.1. Catalyst preparation

Iron(III)oxide was precipitated from a 0.25 kmol/m³ iron(III)nitrate solution (Fe(NO₃)₃·9H₂O, Merck P.A.) by slowly adding ammonium hydroxide (12% by wt ammonia, Merck P.A., 2.8 ml/min) to the suspension, which was heated to 363 K. Ammonia addition was stopped when a pH of 8 was reached. The precipitate was filtered off and washed with 100 ml distilled water. Then the catalyst was dried at 393 K for 24 hours and calcined at 673 K for one hour. We used a sieve fraction of 0.2 - 0.6 mm in all experiments. In some experiments a supported catalyst was used, prepared by precipitating iron(III)hydroxide on a mixture of TiO₂ and CaO to a final weight ratio of Fe : TiO₂ : CaO = 39 : 32 : 9.

3.2.2. Experimental methods

The reactor system used for studying the Fischer-Tropsch reaction on iron catalysts is shown in figure 3.1.

The reactor consisted of a 6 mm inside diameter quartz tube, in an electrically heated oven. An Eurotherm thyristor controller and a chromel-alumel thermocouple regulated the temperature in the re-

actor within 2 K. The gases hydrogen (Hoekloos, purity >99.9%), carbon monoxide (Matheson c.p. >99.5%) and helium (Hoekloos, purity >99.995%) were purified over a reduced copper catalyst (BASF RJ-11, BTS catalyst) at 425 K and a molecular sieve (5A, Union Carbide) at room temperature.

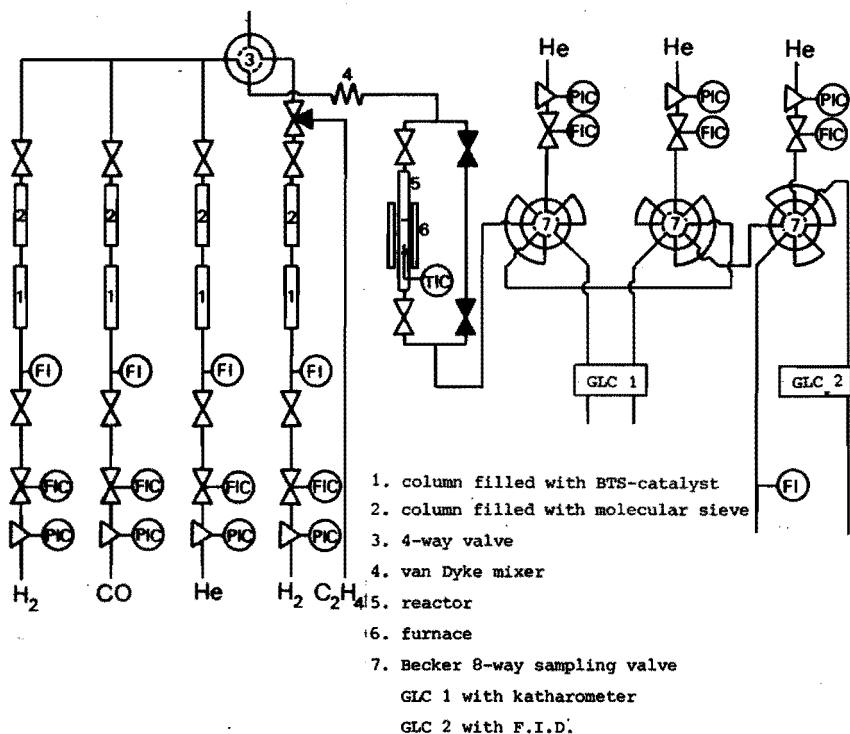


Figure 3.1. The continuous flow fixed bed reactor system.

The hydrocarbons from C_1 to C_3 were analyzed on a Philips Pye series 104 FID gas chromatograph at 298 K with a 3 m phenylisocyanate on a stainless steel Poracil-C column provided with an 8-way inlet valve.

For the analysis of H_2 , CO, CO_2 and H_2O two parallel columns were used in a Hewlett-Packard 5700A gas chromatograph equipped with a katharometer detector. The samples were injected alternately to each column with 8-way valves. A 1.5 m molecular sieve 5A metal column was used to separate hydrogen and carbon monoxide, while the other column, a 2.5 m Porapak Q glass column, was used to separate carbon dioxide and water. Both columns were operated at 343 K and helium was used as carrier gas.

Standard reduction of the catalyst was at 623 K in flowing hydrogen ($100 \text{ cm}^3/\text{min}$) for 16 hours.

Reactions were carried out with 0.5 or 3 gram of catalyst under differential conditions with a maximum conversion of 5%, at 1 atmosphere total pressure with a 1 : 1 : 3 mixture of CO , H_2 and He respectively at a total gas flow rate of $6 \text{ dm}^3/\text{hour}$.

After a certain period of Fischer-Tropsch reaction, the reactor was cooled down to room temperature under a flow of helium. Sometimes, part of the residual iron oxidized in the air after removing the catalyst from the reactor.

The reaction rate is defined as the number of $\mu\text{moles CO}$ converted into C_1 through C_3 hydrocarbons per kg of iron and per second.

3.2.3. Catalyst characterization

The fresh catalysts as well as catalysts after various periods of Fischer-Tropsch synthesis were characterized by X-ray diffraction analysis, Mössbauer spectroscopy and by determination of the carbon content. X-ray diffraction patterns of the samples were taken on a Philips diffractometer Pw 210700 with Mn filtered $\text{Fe K}\alpha$ radiation. Mössbauer spectra were obtained using a constant acceleration spectrometer with a ^{57}Co in Rh source. Isomer shifts (I.S.) are reported relative to the NBS standard sodium nitroprusside (SNP or $\text{Na}_2\text{Fe}(\text{CN})_5 \cdot \text{NO} \cdot 2\text{H}_2\text{O}$) at room temperature, while hyperfine fields (H_{eff}) are calibrated against the 515 kOe field of $\alpha\text{-Fe}_2\text{O}_3$, also at room temperature.

The carbon content of a sample was determined by a CNH analyzer (F & M corporation).

3.2.4. Evaluation procedures for the Mössbauer spectra

Mössbauer spectra of single compounds were analyzed using a least squares program of Lorentzian line shapes. In the final fits all peaks belonging to the same sextuplet were constrained to have equal width and also the intensities of the first and the sixth, the second and the fifth and the third and fourth peak were constrained to be equal. The distances between the peaks in the same sextuplet were constrained to the well known ratios for iron.

In the case that the investigated sample is a mixture of different compounds we preferred to analyze the complex spectrum in such a way that the relative amounts of the compounds present could be obtained. This was done in the following way. Suppose S_k ($k = 1, \dots, 400$) represents the Mössbauer spectra of the mixture, measured in 400 velocity channels. The spectra of the $N-3$ different compounds present in the mixture, corrected for their geometrical background parabola's are represented by B_{ik} ($i = 1, \dots, N-3$ and $k = 1, \dots, 400$). The spectrum S_k has its own background parabola, which can be fitted simultaneously by defining $B_{N-2,k} = k^2$, $B_{N-1,k} = k$ and $B_{N,k} = 1$ ($k = 1, \dots, 400$). Now the problem is to find coefficients a_i for which the combination

$$S_k^{\text{calc}} = \sum_{i=1}^N a_i B_{ik}$$

is the best fit to the measured spectrum S_k . Condition is that the expression

$$\sum_{k=1}^{400} (S_k^{\text{calc}} - S_k)^2$$

has a minimum for the best choice of a_i :

$$\frac{d}{da_j} \sum_{k=1}^{400} (S_k^{\text{calc}} - S_k)^2 = 0 \quad j = 1, \dots, N$$

or

$$\sum_{i=1}^N \sum_{k=1}^{400} B_{jk} B_{ik} a_i = \sum_{k=1}^{400} S_k B_{jk} \quad j = 1, \dots, N$$

This is a set of N linear equations, from which the set of N coefficients a_i can be found. The product of a_i and the spectral area of the normalized spectrum B_{ik} gives the relative spectral contribution of compound i to the measured spectrum S_k .

3.2.5. Adsorption apparatus

The adsorption experiments were performed in a standard adsorption apparatus consisting of a sample holder, gas bulbs for storing the gases to be adsorbed, a two-stage rotary pump and an oil diffusion

pump (both of Leybold-Heraeus) and finally a membrane manometer (Fischer/Porter type 50 DPF 100 - 1 - C).

A known quantity of catalyst is placed in the sample holder, which can be heated by an electric oven. The temperature is measured by a chromel-alumel thermocouple, which is placed in a canal in the middle of the sample holder.

3.3. RESULTS

3.3.1. Catalysts before and after reduction

The unreduced catalysts consisted of pure $\alpha\text{-Fe}_2\text{O}_3$ as we could conclude from their Mössbauer spectra and X-ray diffraction patterns. An average crystallite size of about 30 nm was estimated from the broadening of the X-ray lines.

After reduction, the X-ray experiments showed only the pattern of $\alpha\text{-Fe}$, whereas Mössbauer spectra revealed the presence of a small amount of Fe_3O_4 besides to $\alpha\text{-Fe}$. Since we checked that the reduction conditions were adequate to convert all iron oxide into metallic iron, we believe that the small amount of Fe_3O_4 detected was formed after the catalyst was removed from the reactor.

3.3.2. Crystallographically different iron carbides

First we have tried to find the reaction conditions under which the catalysts are converted into single phase carbides.

The Mössbauer spectrum of a metallic iron catalyst after 1.5 hours Fischer-Tropsch synthesis at 723 K is shown in figure 3.2a. During the initial period of about 15 min, the conversion was above the 5% limit used for differential conversions. This resulted in the formation of graphitic carbon. The Mössbauer spectrum (figure 3.2a) shows some contamination by iron oxides, which is probably formed after the sample was removed from the reactor. The Mössbauer parameters of this sample, presented in table 3.I, agree within the experimental error with the data of Le-Caer et al. (12) for $\theta\text{-Fe}_3\text{C}$. X-ray diffraction data are given in table 3.II and these data agree with the data of Lipson and Petch (13) for $\theta\text{-Fe}_3\text{C}$. This sample had a carbon content of 7.7%

by weight, which is higher than the value of 6.69% calculated for $\theta\text{-Fe}_3\text{C}$. Because the Mössbauer spectrum in figure 3.2a indicates a single phase except for a small oxide contamination, we conclude that some 'free' carbon was deposited on the surface of the catalyst during the reaction.

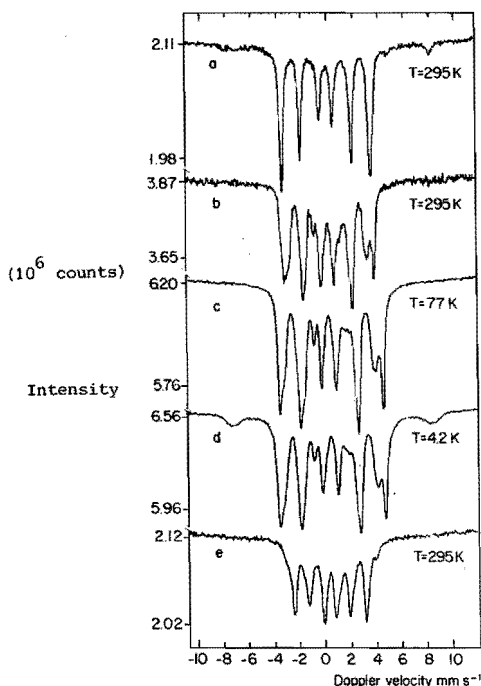


Figure 3.2. Mössbauer spectra of different iron carbides recorded at the indicated temperatures

- A) $\theta\text{-Fe}_3\text{C}$,
- B) , C) and D) $\chi\text{-Fe}_5\text{C}_2$,
- E) $\epsilon'\text{-Fe}_{2.2}\text{C}$ and some $\chi\text{-Fe}_5\text{C}_2$.

A pure iron catalyst after 24 hours of Fischer-Tropsch reaction at 513 K was flushed in helium at 623 K for 1 hour. The data belonging to the X-ray diffraction pattern of this sample (table 3.II) agree with the data for $\chi\text{-Fe}_5\text{C}_2$ as published by Senateur (14). We measured the Mössbauer spectrum of this sample at three temperatures (figure 3.2b-d). The parameters of the room temperature spectrum (table 3.I) agree within experimental error with the parameters of $\chi\text{-Fe}_5\text{C}_2$ reported by Le Caer et al. (12).

Table 3.I. Mössbauer parameters of single phase carbides at
T = 295 K

Carbide	Fe-site	this study		literature data		Ref.
		I.S. (mm/s)	H _{eff} (kOe)	I.S. (mm/s)	H _{eff} (kOe)	
ϵ' -Fe _{2.2} C		.50±.03	173±2	.51±.01	173±1	(5)
χ -Fe ₅ C ₂	I	.43±.03	189±2	.46±.02 *	185±2	
	II	.51±.03	218±2	.49±.02	216±2	(12)
	III	.47±.03	110±5		124±4	
θ -Fe ₃ C	I	.45±.03	212±2	.44±.01	208±2	(12)
	II				206±2	

In the least squares fit of Lorentzian line shapes we found broader lines for the Fe(II) site than for the Fe(I) site. The Mössbauer spectrum at 4.2 K (figure 3.2d) showed two broad lines in positions characteristic for an oxide. These lines are not visible in the spectra at 77 K and 295 K. Repeating the Mössbauer experiments revealed that the spectra did not change during several months. So we must conclude that this oxide was formed either immediately after the sample was removed from the reactor or during the Fischer-Tropsch reaction. In situ experiments will be done to clarify this point.

The Mössbauer spectrum of a Fe/TiO₂/CaO catalyst after 48 hours Fischer-Tropsch reaction at 513 K is shown in figure 3.2e. This spectrum contains a small contribution of χ -Fe₅C₂, for which the small peak at the high positive velocity side is characteristic. From this spectrum we subtracted a contribution of the Mössbauer spectrum of χ -Fe₅C₂ such that the characteristic small peak disappeared. The remaining spectrum was analyzed by means of the Lorentzian line fitting procedure, it contains a sextuplet and a doublet. The Mössbauer parameters for the sextuplet, given in table 3.I, agree with the parameters published by Amelse et al.

(5) for ϵ' -Fe_{2.2}C. The Mössbauer spectrum of this sample recorded at 77 K contained no doublet after the correction for χ -Fe₅C₂ while the intensity of the ϵ' -Fe_{2.2}C sextuplet was stronger than in the room temperature spectrum. So we conclude that the doublet belongs

Table 3.II. X-ray diffraction data of single phase carbides for angles 2θ between 50° and 60° .

$\theta\text{-Fe}_3\text{C}$				$\chi\text{-Fe}_5\text{C}_2$			
this study		Lipson and Petch (13)		this study		Senateur (14)	
2θ	I (%)	2θ	I (%)	2θ	I (%)	2θ	I (%)
50.7	20	50.76	25	50.1	25	50.08	20
51.8	20	52.24	25	52.0	50	52.06	45
54.8	60	55.02	60			52.46	30
				54.5	25	54.46	25
55.9	60	56.10	70	55.4	80	55.46	70
57.0	55	57.39	60	56.4	100	56.38	100
57.5	100	57.62	100	57.5	30	57.54	30
58.7	55	58.90	55	58.3	20	57.58	40

$\epsilon'\text{-Fe}_{2.2}\text{C}$		$\epsilon'\text{-Fe}_2\text{C}^*$	
this study		Barton and Gale (11)	
2θ	I (%)	2θ	I (%)
52.8	25	52.73	21
54.7	100	54.24	
		54.85	100

*) see text

to $\epsilon'\text{-Fe}_{2.2}\text{C}$ in a superparamagnetic state. The contribution of $\epsilon'\text{-Fe}_{2.2}\text{C}$ to the total spectrum of figure 3.2e is 83%. The X-ray diffraction pattern of this sample is shown in figure 3.4c, line positions and intensities are given in table 3.II. Interpretation of these data is less straight forward than the interpretation of the Mössbauer spectrum. The X-ray diffraction pattern measured by us is similar to the one published by Barton and Gale (11) for a carbide $\epsilon\text{-Fe}_2\text{C}$ with an almost hexagonal lattice.

However the Mössbauer spectrum not only shows $\epsilon'\text{-Fe}_{2.2}\text{C}$ as the major phase in this sample, but also excludes $\epsilon\text{-Fe}_2\text{C}$ as a possible constituent. In all other experiments in which Mössbauer spectroscopy revealed the presence of a considerable quantity of $\epsilon'\text{-Fe}_{2.2}\text{C}$, we measured an X-ray diffraction pattern similar to that found by Barton and Gale (11). So we conclude that the X-ray diffraction pattern published by Barton and Gale should not be attributed to almost hexagonal $\epsilon\text{-Fe}_2\text{C}$ but to hexagonal $\epsilon'\text{-Fe}_{2.2}\text{C}$.

Up to now we did not succeed in preparing a single phase of the carbide $\epsilon\text{-Fe}_2\text{C}$.

3.3.3. Formation of carbides at different temperatures

Mössbauer spectra of pure iron catalysts which were used in Fischer-Tropsch synthesis at various temperatures and times are shown in figure 3.3.

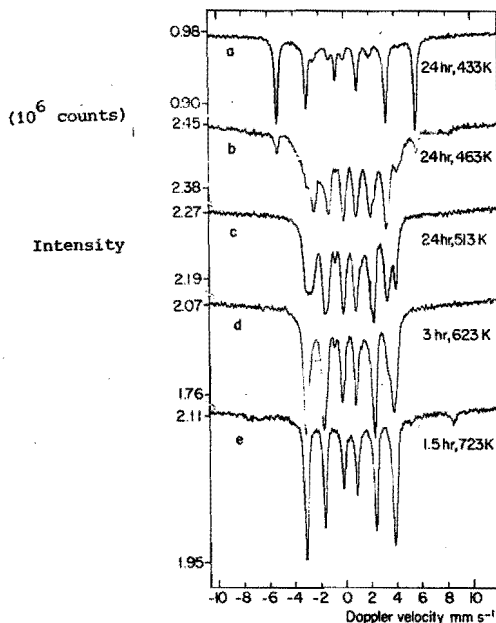


Figure 3.3. Mössbauer spectra of metallic iron catalysts after different periods of Fischer-Tropsch synthesis at various temperatures. Spectra were recorded at room temperature.

Spectra taken at temperatures higher than or equal to 513 K could be analyzed in terms of spectral contributions of the individual constituents as outlined before. The spectra of figure 3.2 were used as the single phase spectra B_{ik} . The spectral contributions obtained are summarized in table 3.III. We have not applied this method to catalysts carbided at temperatures lower than 513 K, because these samples contained a carbide phase which we could not prepare as a single phase.

Table 3.III. Spectral composition of the Mössbauer spectra of metallic iron catalysts at $T = 295$ K after Fischer-Tropsch synthesis at various temperatures.

synthesis temperature (K)	synthesis time (hr)	Spectral contributions (%)				
		α -Fe	Fe_xC	ϵ' - $\text{Fe}_{2.2}\text{C}$	χ - Fe_5C_2	θ - Fe_3C
433	24	87	+	+		
463	24	13	+	+	36	
513	24			35	65	
623	3			12	47	41
723	1.5					100

+ the concerning carbide is clearly visible in the Mössbauer spectrum, although the spectral contribution could not be calculated (see text).

After 24 hours of Fischer-Tropsch synthesis at 433 K (figure 3.3a) only a small part of the catalyst is converted into a carbide. The Mössbauer spectrum of this sample appears to be composed of the spectrum of α -Fe and of a carbide in which a distribution of H_{eff} even up to 275 kOe occurs. Because the contribution of this carbide to the spectrum is too small to be analyzed properly, we confined ourselves to the calculation of the spectral contributions of α -Fe and the total amount of carbide. Since the carbide revealing a distribution in hyperfine fields does not seem to be the same as the ϵ - Fe_2C reported by Maksimov (7), we shall refer to this carbide as Fe_xC . The X-ray diffraction pattern of this sample (figure 3.4a) showed α -Fe as the major phase being present. Also some other weak and broad lines were visible, which we could interpret as a combination of the pattern published by Hofer et al. (9) for ϵ - Fe_2C and by Barton and Gale (11) for ϵ' - $\text{Fe}_{2.2}\text{C}$.

The Mössbauer spectrum of a sample after 24 hours of the synthesis at 463 K showed besides α -Fe, χ - Fe_5C_2 and ϵ' - $\text{Fe}_{2.2}\text{C}$ also the presence of the carbides with hyperfine fields up to 275 kOe, which we attributed to Fe_xC . Under the assumption that the Mössbauer spectrum of Fe_xC has no peaks at the position of the sixth peak of the sextuplet belonging to the Fe(II) site in χ - Fe_5C_2 , the relative

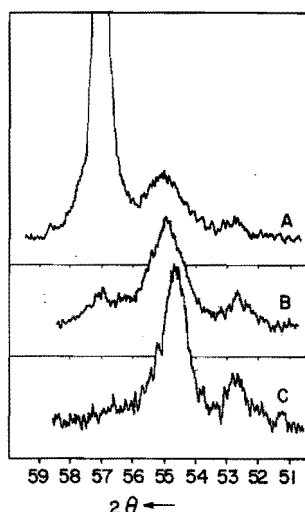


Figure 3.4. Relevant part of the X-ray diffraction patterns of
 A) a metallic iron catalyst after 24 hours of Fischer-Tropsch synthesis at 433 K,
 B) id. at 463 K and
 C) a Fe/TiO₂/CaO catalyst after 48 hours of Fischer-Tropsch synthesis at 513 K.

contribution of χ -Fe₅C₂ and α -Fe were calculated (table 3.III). According to the X-ray diffraction pattern of this sample (figure 3.4b) ϵ' -Fe_{2.2}C is the major constituent, together with χ -Fe₅C₂ and α -Fe.

The X-ray diffraction pattern of the catalyst after synthesis at 513 K during 24 hours showed the presence of χ -Fe₅C₂ and ϵ' -Fe_{2.2}C, while the sample after 3 hours synthesis at 625 K showed χ -Fe₅C₂ and θ -Fe₃C. The X-ray diffraction pattern of a catalyst after 1.5 hour of synthesis at 723 K resembles the data of θ -Fe₃C (13).

3.3.4. Non-steady state experiments at 513 K

The reaction rate achieved with a metallic iron catalyst, obtained after reducing 3 gram of the precipitate, was determined at 513 K as a function of time and the results are presented in figure 3.5. The reaction rate started at zero, the rate reached then a maximum value after 3.5 hours followed by a rather strong deactivation to a level of 40% of the maximum after 24 hours.

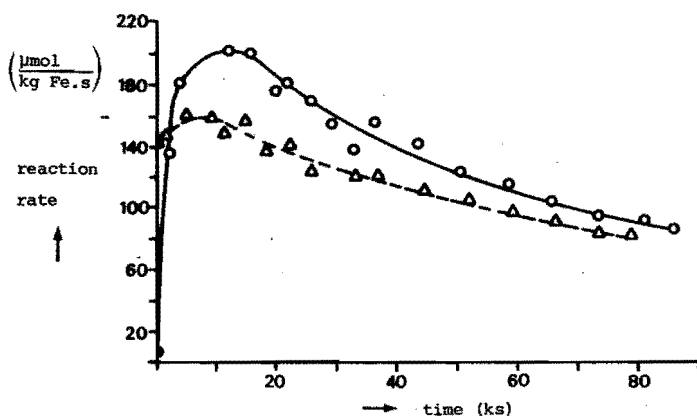


Figure 3.5. Reaction rates during Fischer-Tropsch synthesis at 513 K over a metallic iron catalyst (o) and over a pretreated (with a mixture of CO : He = 1 : 4) iron catalyst (Δ).

After a treatment of the reduced catalyst at 513 K for 2.5 hour with a gas mixture of 20% CO in He, the reaction rate started at a value already near to the maximum activity, which was then achieved after already 2 hours. Although the value of this maximum was slightly lower than in the case of an initially pure iron catalyst, the reaction rates approached each other at increasing times (figure 3.5). The same result was obtained after pretreating the reduced catalyst with a gas mixture of 20% ethylene in helium.

The reaction rate of a Fe/TiO₂/CaO catalyst showed a time dependent behaviour, similar to that of the metallic iron catalyst.

The relation between composition and behaviour of a metallic iron catalyst during Fischer-Tropsch synthesis at 513 K was studied as follows. A sample obtained by reducing 0.5 gram of the precipitate was subjected to synthesis for 0.5 hour. After that the sample was removed from the reactor, a new sample was introduced and subjected to the reaction process for a longer time and so on. We measured reaction rates and product distributions as a function of time for each experiment. No significant differences between various experiments were found for corresponding time intervals. We concluded from this that the reaction process was sufficiently reproducible to justify the procedure used for studying the time dependent behaviour of the catalyst.

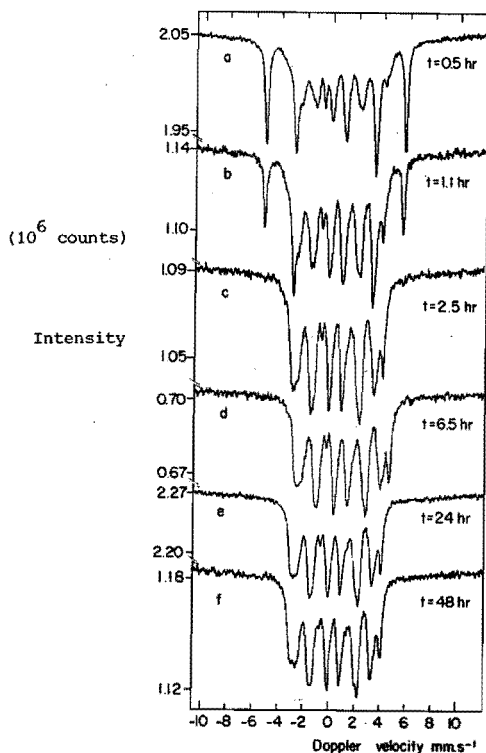


Figure 3.6. Mössbauer spectra of metallic iron catalyst after different periods of Fischer-Tropsch synthesis at 513 K. Spectra were recorded at room temperature.

Mössbauer spectra of the catalyst samples subjected for various periods of time to the Fischer-Tropsch reaction at 513 K are shown in figure 3.6. The spectra were analyzed as discussed in the experimental section and the results are shown in table 3.IV. The

Table 3.IV. Spectral composition of the Mössbauer spectra of metallic iron catalysts at $T = 295$ K after different periods of Fischer-Tropsch synthesis at $T = 513$ K.

synthesis time (hr)	α -Fe (%)	Fe_xC (%)	ϵ -Fe ₅ C ₂ (%)	χ -Fe ₅ C ₂ (%)
0.5	57	14-22	0-8	21
1.1	31	8-23	5-20	41
2.5	0	4-9	25-30	66
6.5	0	0	28	72
24	0	0	35	65
48	0	0	38	62

Mössbauer spectra of samples subjected to synthesis during 2.5 hour. or less indicated the presence of Fe_xC . As the Mössbauer spectrum of this compound, as a single phase could not be obtained, the spectral contributions of some carbides could only be calculated between certain limits (table 3.IV). The spectral contribution of $\chi\text{-Fe}_5\text{C}_2$ has been calculated under the assumption that the Mössbauer spectrum of Fe_xC has no peaks at the position of the sixth peak of the Fe(II) site in $\chi\text{-Fe}_5\text{C}_2$. For comparison, we have plotted the

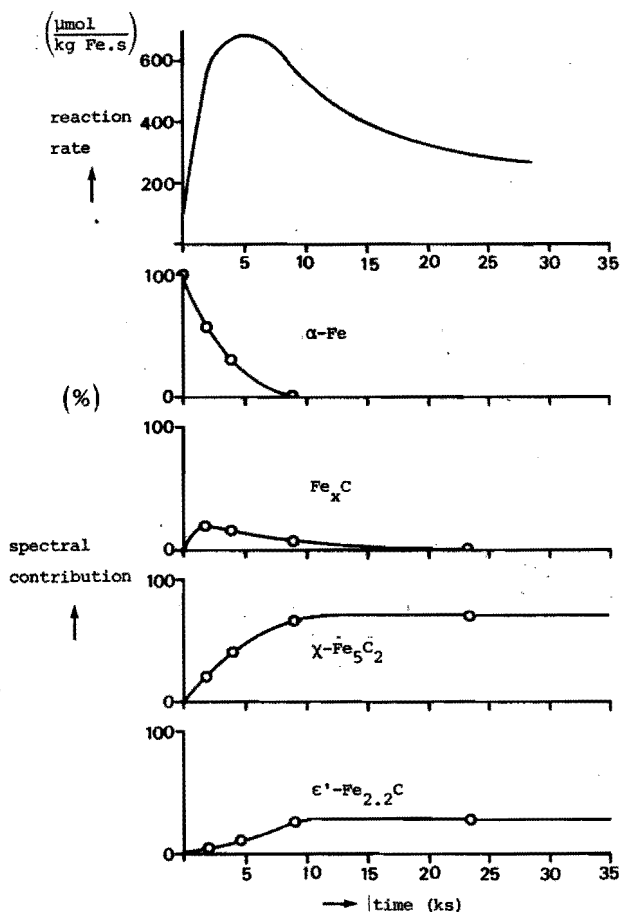


Figure 3.7. Reaction rates (upper curve) and relative contributions of $\alpha\text{-Fe}$ and the various carbides to the Mössbauer spectra during Fischer-Tropsch synthesis over a metallic iron catalyst at 513 K.

catalytic reaction rate together with the relative spectral contributions to the Mössbauer spectra of α -Fe and the different carbides as a function of time in figure 3.7. The results given in this figure will be discussed in the following section.

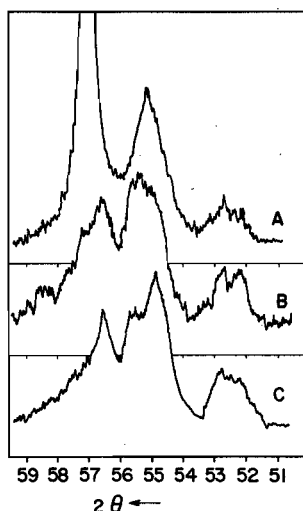


Figure 3.8. Relevant part of the X-ray diffraction patterns of a metallic iron catalyst after Fischer-Tropsch synthesis at 513 K during

- A) 1.1 hours
- B) 6.0 hours
- C) 48 hours.

The X-ray diffraction pattern of the sample after 0.5 hours reaction time showed predominantly α -Fe and furthermore broad lines at diffraction angles 2θ of 55.2° and 52.7° , respectively. We interpret these lines as being due to a combination of the diffraction lines of ϵ -Fe₂C (9) and ϵ' -Fe_{2.2}C (11). After 2.5 hours of synthesis, the α -Fe peak had nearly disappeared and the remaining pattern consisted of broad lines, which can be attributed to contributions of ϵ' -Fe_{2.2}C and χ -Fe₅C₂. The X-ray diffraction patterns of samples after still longer reaction times consisted of narrower lines. They could be identified as a combination of χ -Fe₅C₂ and ϵ' -Fe_{2.2}C. Some of the X-ray diffraction patterns are shown in figure 3.8.

The carbon weight content of the samples is plotted as a function of time in figure 3.9. The value of 8.7% after 48 hours of synthesis

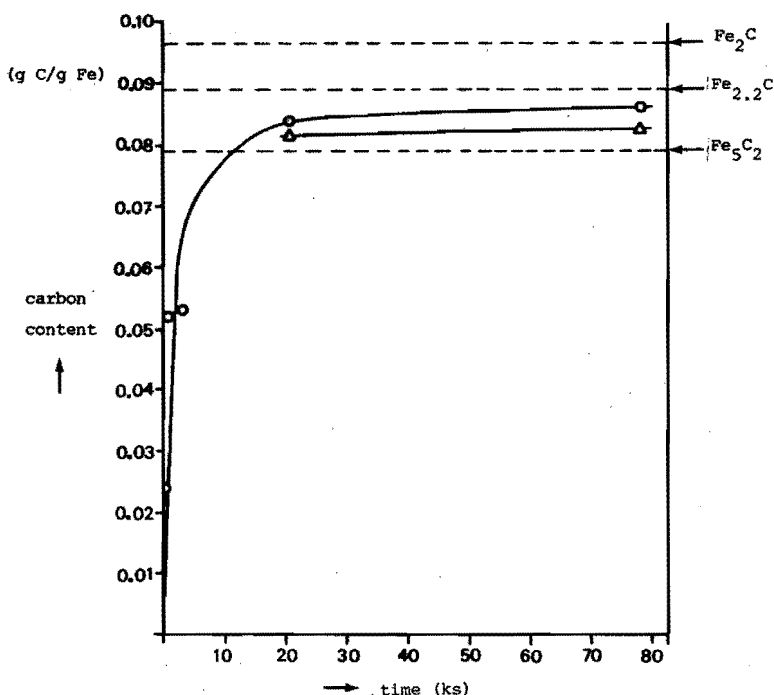


Figure 3.9. Carbon content in metallic iron catalyst during Fischer-Tropsch synthesis at 513 K, experimental values (o) values (Δ) calculated from the spectral composition of the Mössbauer spectra.

lies between the theoretical values for ϵ' -Fe_{2.2}C and χ -Fe₅C₂. When we assume that the carbides ϵ' -Fe_{2.2}C and χ -Fe₅C₂ have the same recoilless Mössbauer fractions, the carbon content due to the present carbide phases could be calculated for this sample also from the analysis of the Mössbauer spectrum. The result is a carbon content of 8.3%, so that apparently a certain amount of 'free' carbon was present on the surface, corresponding to about 0.4% of the sample's total weight. For the samples after 6.5 and 24 hours synthesis the measured carbon content was also higher than the value calculated from the Mössbauer spectra.

3.3.5. Adsorption of hydrogen and carbon monoxide

Since Vannice (15) obtained with supported metal catalysts in most cases very small amounts of adsorbed H_2 at room temperature as compared with the adsorption of CO, the adsorptions of H_2 and CO were further studied in our laboratory.

A result similar to those of Vannice was also obtained with the adsorption of H_2 and CO at room temperature on a supported cobalt (16) catalyst (6.3% Co/ Al_2O_3). A more acceptable value of the H_2 -adsorption was obtained, when hydrogen was admitted to the reduced catalyst at the reduction temperature of 623 K. When, thereafter, the temperature was slowly lowered to room temperature, only on the supported cobalt catalyst, a higher adsorbed amount of H_2 was measured, than when the H_2 -adsorption was performed at room temperature (see table 3.V).

Table 3.V. Adsorption of H_2 and CO (in $\mu\text{mol/g cat}$).

catalyst	H_2 -adsorption		CO-adsorption	ref.
	room temperature adsorption (293 K)	admitted at reduction temperature (623 K)	room temperature adsorption (293 K)	
100% Fe	26.8	18.8	42.0	
100% Co	18.8	28.6	18.8	16
6.3% Co/ Al_2O_3	3.1	18.8	14.7	16
2% Co/ Al_2O_3	1	-	16.0	15
15% Fe/ Al_2O_3	0	-	21.5	15

The large difference of the adsorbed amounts of H_2 between the two adsorption methods on supported metal catalysts can be explained by an activated adsorption process of H_2 , as is recently also suggested by Topsøe (22). Because the two H_2 -adsorption methods agree rather well for bulk cobalt- and iron catalysts other trivial explanations such as a leakage in the adsorption equipment etc. are excluded. Emmett et al. (17) observed no adsorption of carbon monoxide on a fully carburized sample of $\chi\text{-Fe}_5C_2$.

In our laboratory the adsorption of CO at room temperature on a partially carburized Fe-catalyst was also studied. After the adsorbed amount of CO was determined on the fresh iron catalyst by the difference between two subsequently measured CO-adsorption isotherms, freshly reduced iron catalysts were heated at 513 K for various reaction periods with about 10 kPa carbon monoxide. The pressure drop in the adsorption vessel was followed with the membrane manometer and the consumption of CO by the catalyst was calculated. After the reaction at 513 K the adsorption vessel was quickly cooled down in CO and evacuated down to a pressure of 10^{-2} kPa.

Table 3.VI. Adsorption of CO on fresh and carburized iron catalysts.

reaction period in 10 kPa CO at 513 K (ksec)	CO consumption at 513 K ($\mu\text{mol/g Fe}$)	CO adsorption at room temperature ($\mu\text{mol/g Fe}$)
0	0	60.0
0.72	115.7	0.7
10.8	242.2	0.6

During this treatment only very small amounts of carbon species ($0.0002 - 0.0004$ mol % of iron) were deposited on the iron catalyst; but as table 3.VI indicates, the room temperature capacity for CO adsorption decreased tremendously by this carburization.

3.4. DISCUSSION

In our experiments four different iron carbides appeared to be formed. These carbides are the three well known ones $\theta\text{-Fe}_3\text{C}$, $\chi\text{-Fe}_5\text{C}_2$ and $\epsilon'\text{-Fe}_{2.2}\text{C}$, and one that has not been reported before, which we have called Fe_xC . The identification of $\theta\text{-Fe}_3\text{C}$ and $\chi\text{-Fe}_5\text{C}_2$ by means of X-ray diffraction as well as Mössbauer spectroscopy was possible in a straight forward manner. The identification of $\epsilon'\text{-Fe}_{2.2}\text{C}$ has been performed by means of the Mössbauer spectrum published by Amelse et al. (5).

Maksimov et al. (7) are the only authors who published a Mössbauer spectrum of ϵ -Fe₂C. They analyzed their spectrum as a combination of three different sextuplets with a maximum hyperfine field of 237 kOe at the Fe(II) site. We think it is not sure that their rather detailed analysis is completely correct, because the contribution of the ϵ -carbide phase to the spectrum is only small. Moreover, the velocity resolution of their spectrum seems to be rather poor. The Mössbauer spectrum of our sample prepared by carburization at T = 433 K for 24 hours (figure 3.4a) resembles the spectrum measured by Maksimov et al. (7), but our spectrum could not be characterized by three Lorentz sextuplets, because of the distribution of hyperfine fields up to 275 kOe at the Fe site with the highest hyperfine splitting. We assigned this Mössbauer spectrum to a carbide Fe_xC. It is noteworthy that this carbide Fe_xC appeared only together with α -Fe or shortly after the moment that α -Fe just had disappeared as can be seen in figure 3.7. No Fe_xC was found at a synthesis temperature higher than 513 K. The X-ray diffraction patterns of samples in which Fe_xC was present showed apart from the narrow α -Fe reflection only broad lines and their intensity was weaker than one would expect from the analysis of the Mössbauer spectra. From these results we suggest that Fe_xC represents a not well defined structure intermediate between α -Fe and the known carbide structures. The question remains, if any relation exists between Fe_xC and the ϵ -carbide of Maksimov et al. (7). For instance, Fe_xC might be a precursor of ϵ -carbide. More work will be done to clarify this.

In the Mössbauer spectrum of the χ -Fe₅C₂ sample measured at 4.2 K a contribution characteristic for α -Fe₂O₃ was found though the broad lines indicate a whole distribution in hyperfine fields (figure 3.4d). This contribution was not visible in the Mössbauer spectra measured at 77 K and 295 K, respectively. Apparently the fraction of the sample in which this oxide contribution is present has a recoilless fraction which decreases rapidly with increasing temperature. It is conceivable, therefore, that this might be an oxide layer on the surface of the catalyst. However, further experiments are necessary to clarify this definitely. The question whether this oxide layer has been formed during the Fischer-Tropsch synthesis or after removing the sample from the reactor can only be answered when Mössbauer experiments are performed on samples without a contact with air.

In the temperature dependent experiments we found that Fe_xC was formed during Fischer-Tropsch synthesis at 433 K and 463 K. Moreover Fe_xC was formed in an early stage in the time dependent experiments at 513 K. The carbides $\epsilon\text{'-Fe}_{2.2}\text{C}$ and $\chi\text{-Fe}_5\text{C}_2$ appeared in catalysts that had been subjected to synthesis at temperatures from 463 K up to 623 K. Cementite, $\theta\text{-Fe}_3\text{C}$, was formed at 623 K and 723 K and at the latter temperature it was the only carbide phase present. The temperature dependent formation of carbides in metallic iron does not fit in the scheme for promoted iron catalysts as published by Sancier et al. (10). As far as we are aware no literature is available about the formation of carbides in unsupported and unpromoted metallic iron. Only Le Caer et al. (12) and Bernas et al. (18) state that iron forms single phase $\chi\text{-Fe}_5\text{C}_2$ at 673 K and single phase $\theta\text{-Fe}_3\text{C}$ only at 823 K and in a gas mixture of 7 $\text{H}_2/3$ CO. As we found that $\theta\text{-Fe}_3\text{C}$ was formed already at 623 K, the former observation is not consistent with our results. Our sample of iron supported on a mixture of TiO_2 and CaO formed at 513 K almost exclusively $\epsilon\text{'-Fe}_{2.2}\text{C}$, which agrees with the results of Amelse et al. (5) for iron supported on SiO_2 . For a Fe/SiO_2 catalyst after 6 hours of Fischer-Tropsch reaction Raupp and Delgass (4) found a Mössbauer spectrum which they analyzed with 3 subspectra of $\chi\text{-Fe}_5\text{C}_2$, however with an intensity ratio which differs strongly from the expected ratio 2 : 2 : 1. They ascribe this deviation to surface effects or to the presence of unknown intermediate structures. From temperature dependent Mössbauer experiments it followed that the sample did not show a magnetic splitting above 505 K. Raupp and Delgass conclude from this result that the sample contains only $\chi\text{-Fe}_5\text{C}_2$, which has a Curie point of 525 K. However this conclusion is not necessarily correct, because a carbide with a Curie point higher than 505 K may be present in a superparamagnetic state with a transition temperature lower than 505 K. The Mössbauer spectrum of their sample looks almost identical with the Mössbauer spectra that we have measured with samples after 6 hours of Fischer-Tropsch reaction or longer. These spectra could straightforwardly be analyzed as combinations of $\chi\text{-Fe}_5\text{C}_2$ and $\epsilon\text{'-Fe}_{2.2}\text{C}$ spectra. Thus we suggest that the Mössbauer spectrum which Raupp and Delgass (4) measured with a Fe/SiO_2 catalyst after 6 hours of Fischer-Tropsch reaction

at 525 K does not represent some deformed $\chi\text{-Fe}_5\text{C}_2$, but a combination of $\chi\text{-Fe}_5\text{C}_2$ and $\epsilon'\text{-Fe}_{2.2}\text{C}$. The latter phase is likely to be present in small particles, with a superparamagnetic transition temperature below 505 K.

With an Fe/SiO_2 catalyst of an average particle diameter of 75 Å, which has been exposed to the Fischer-Tropsch synthesis mixture at 525 K for 6 hours, Raupp and Delgass (4) find a Mössbauer spectrum which is a combination of mainly $\epsilon'\text{-Fe}_{2.2}\text{C}$ and of some $\epsilon\text{-Fe}_2\text{C}$. Their temperature dependent Mössbauer experiments confirm the presence of $\epsilon'\text{-Fe}_{2.2}\text{C}$ and of some $\epsilon\text{-Fe}_2\text{C}$. The X-ray diffraction pattern shows three reflections which the authors ascribe to $\epsilon\text{-Fe}_2\text{C}$, but this contradicts their Mössbauer experiments. Unfortunately they do not present the diffraction parameters and we suspect that Raupp and Delgass have measured the same pattern as Barton and Gale (11). As we argued above this pattern has to be ascribed to $\epsilon'\text{-Fe}_{2.2}\text{C}$ instead of $\epsilon\text{-Fe}_2\text{C}$.

Nahon et al. (6) have recently studied the formation of carbides in $\text{Fe/Al}_2\text{O}_3$ catalysts at 523 K. The Mössbauer spectrum of the catalyst after 19 hours of Fischer-Tropsch reaction at 523 K has been ascribed by the authors to the carbide $\epsilon\text{-Fe}_2\text{C}$. However, this identification is not correct. From the observed effective hyperfine field of 184 kOe at $T = 4.2$ K it follows that the carbide formed is actually $\epsilon'\text{-Fe}_{2.2}\text{C}$.

Some authors (4) consider $\epsilon'\text{-Fe}_{2.2}\text{C}$ as a less stable carbide. However in our experiments $\epsilon'\text{-Fe}_{2.2}\text{C}$ was formed at a temperature as high as 623 K, while Amelse et al. (5) reported the thermal stability of $\epsilon'\text{-Fe}_{2.2}\text{C}$ on SiO_2 up to 673 K. So we conclude that $\epsilon'\text{-Fe}_{2.2}\text{C}$ is a stable carbide, at least as stable as $\chi\text{-Fe}_5\text{C}_2$.

In short, from the comparison of our results with those of various authors we conclude that apart from the temperature at which the reaction takes place, the nature of the catalyst (promoted, supported) is crucial for the type of carbide which will be formed under the synthesis conditions.

Analysis of the Mössbauer spectra of catalysts after various periods of Fischer-Tropsch reaction indicates that as soon as a mixture of carbon monoxide and hydrogen is passed over the catalyst metallic iron is rapidly converted into the carbides Fe_xC , $\epsilon'\text{-Fe}_{2.2}\text{C}$ and $\chi\text{-Fe}_5\text{C}_2$. Apparently, carbon atoms deposited at the surface by dis-

sociative adsorption of CO can migrate into the catalyst at a high rate. In the early stage of the synthesis, the catalyst will contain regions with α -Fe and regions where the carbides ϵ -Fe_{2.2}C and χ -Fe₅C₂ are formed. Probably, Fe_xC will be located in the boundary between those regions. When more and more metallic iron is converted into carbides the diffusion rate of carbon atoms into the catalyst will slow down with the result that progressively more carbon atoms remain on the surface, forming there spots of amorphous carbon and graphite. A similar mechanism has recently been proposed by Raupp and Delgass (19), based on their simultaneous kinetic and single velocity Mössbauer experiments. They noticed that during an experiment there is a linear relation between the amount of bulk carbides formed and the rate of hydrocarbon formation, and they suggest a causal relation between the two phenomena, which is - of course - not a necessary extrapolation. Another explanation is that the bulk carbide formation and the Fischer-Tropsch synthesis are in competition in such a way that a high rate of carbide formation entails a low rate of hydrocarbon formation. This is true when these two reactions have indeed a common precursor (e.g. some type of surface carbon) that is formed in an overall rate determining step. This model is supported by

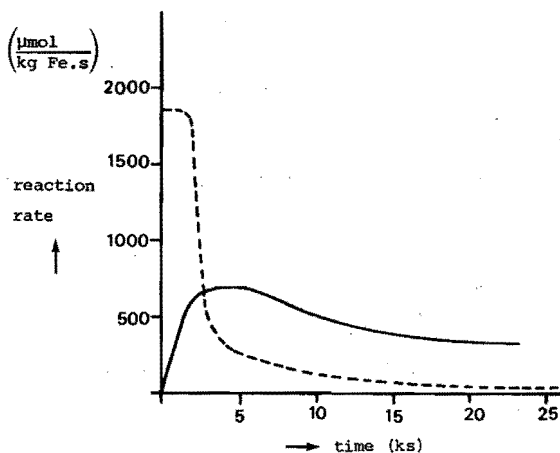


Figure 3.10. Conversion rate of CO into bulk carbides (-----) and into hydrocarbons (—) during Fischer-Tropsch synthesis over metallic iron catalysts at 513 K.

figure 3.10, where we have plotted the conversion of CO into bulk carbides together with the conversion of CO into hydrocarbons, both as a function of time. These results suggest that iron atoms at the surface of the catalyst form the sites that are active in Fischer-Tropsch synthesis. The increase of the initial activity by pretreating the catalyst with CO or C_2H_4 can be fully understood with this model. Depending on the duration of the pretreatment a certain amount of carbon has diffused into the iron lattice. When the pretreated catalyst is then subjected to the Fischer-Tropsch synthesis the diffusion rate of carbon into the bulk of the catalyst is already lower than with pure iron and the activity for the formation of hydrocarbons starts at a level well above zero. However, since evidence that the formation of surface carbon is the rate determining step for the reaction between carbon monoxide and hydrogen on iron catalysts is not available we cannot exclude the possibility that hydrogenation of carbon monoxide and bulk carbide formation are two more or less independent processes, each with its own rate determining step. A relatively slow activation of the iron surface would be the reason of the low activity for the formation of hydrocarbons during the early stage of the reaction process. More arguments, which support this activation of an iron catalyst, will be presented in chapter 5.

Let us consider adsorption studies of CO on the partially carburized iron catalyst. Although the activation energy of carbon diffusion (20) in iron is rather small (44 - 69 kJ/mol), a lot of deposited carbon stays on the surface at 513 K.

The induction period of the hydrocarbons synthesis can then be understood by assuming that more carbon atoms are required to form together with iron an active ensemble on which other carbon atoms are to be hydrogenated. This would be similar to the results of Araki and Ponc (21) who found that after ^{13}C was laid down on a nickel film the rate of $^{12}CH_4$ formation was initially about 6 times higher than on a clean nickel film.

Since the measured carbon content of catalysts after Fischer-Tropsch synthesis during 6.5 hours or longer is significantly higher than the carbon content of the bulk as calculated from the Mössbauer spectra, we conclude that the deactivation of the CO hydrogenation is caused by the formation of inactive carbon on the surface of the catalyst.

3.5. REFERENCES

1. C.D. Frohning, B. Cornils, Hydrocarbon Process. 53, 143 (1974)
2. H. Kölbl, K.D. Tillmetz, Deutsches Offenlegungsschrift 2 507 647 (1976)
3. B. Bössemeier, C.D. Frohning, G. Horn, W. Kluy, Deutsches Offenlegungsschrift 2 536 488 (1976)
4. G.B. Raupp, W.N. Delgass, J. Catal. 58, 348 (1979)
5. J.A. Amelse, J.B. Butt, L.H. Schwartz, J. Phys. Chem. 82, 558 (1978)
6. N. Nahon, V. Perrichon, P. Turlier, P. Bussiere, J. Physique (Orsay, Fr.) 41, C1-339 (1980)
7. Y.V. Maksimov, I.P. Suzdalev, R.A. Arents, S.M. Loktev, Kinet. Katal. 15, 1293 (1974)
8. S.M. Loktev, L.I. Makarenkova, E.V. Slivinskii, S.D. Entin, Kinet. Katal. 13, 1042 (1972)
9. L.J.E. Hofer, E.M. Cohn, W.C. Peebles, J. Am. Chem. Soc. 71, 189 (1949)
10. K.M. Sancier, W.E. Isakson, H. Wise, Symposium on Advances in Fischer-Tropsch Chemistry, Anaheim meeting, March (1978)
11. G.H. Barton, B. Gale, Acta Cryst. 17, 1460 (1964)
12. G. Le Caer, J.M. Dubois, J.P. Senateur, J. Solid State Chem. 19, 19 (1976)
13. H. Lipson, N.J. Petch, J. Iron Steel Inst. 142, 95 (1940)
14. J.P. Senateur, Ann. Chim. 2, 103 (1967)
15. M. Vannice, J. Catal. 37, 449 (1975)
16. A.O.I. Rautavuoma, prepared the cobalt catalyst
17. H.H. Podgurski, J.T. Kummer, T.W. de Witt, P.H. Emmett, J. Am. Chem. Soc. 72, 5382 (1950)
18. H. Bernas, I.A. Campbell, R. Fruchart, J. Phys. Chem. Solids 28, 17 (1967)
19. G.B. Raupp, W.N. Delgass, J. Catal. 58, 361 (1979)
20. R.T.K. Baker, Catal. Rev. - Sci. Eng. 19, 161 (1978)
21. M. Araki, V. Ponec, J. Catal. 44, 439 (1976)
22. H. Topsøe, N. Topsøe, H. Bohlbro, Int. Cat. Congress Tokyo (1980)

THE FISCHER-TROPSCH REACTION OVER PROMOTED IRON MANGANESE OXIDE CATALYSTS FOR THE PRODUCTION OF LIGHT OLEFINS

4.1. INTRODUCTION

An intensive research effort is at present directed towards the development of iron catalysts selective for the production of light olefins.

Kölbel et al. (1) prepared olefin selective catalysts with a low iron to manganese atomic ratio (1 : 9). Before the start of the Fischer-Tropsch synthesis, their catalysts were activated with carbon monoxide at 513 K.

Büssemeier et al. (2) developed an olefin selective catalyst, by fusing iron catalysts of an iron:manganese atomic ratio (1 : 1). They observed a low methane production deviating very strongly from the Schulz-Flory distribution.

Compared to a pure iron catalyst Yang and Oblad (3) observed in their iron manganese oxide catalysts an increased olefin selectivity even at a high iron to manganese atomic ratio (20 : 1).

In chapter 3 we discussed the behaviour of a pure iron catalyst (4) during the Fischer-Tropsch synthesis at 513 K and 100 kPa. The composition of the catalyst was investigated by Mössbauer spectroscopy and X-ray diffraction analysis. The carburized iron catalyst had an ethene/ethane ratio of about 5 in the steady-state(5),

while the product distribution nicely followed the Schulz-Flory distribution.

In the present investigation we have studied the promotor effect of manganese oxides on iron Fischer-Tropsch catalysts. Since it was already known for a long time, that the addition of small quantities of a sulfur containing compound resulted in an enhanced olefinic content of the products, we have tried to suppress the hydrogenation of olefins by poisoning the catalyst with a sulfur containing compound. However higher amounts than about 1% by weight of sulfur generally deactivate a Fischer-Tropsch catalyst completely.

4.2. EXPERIMENTAL

4.2.1. Catalyst preparation

The iron manganese oxide catalysts were prepared by slowly adding ammonium hydroxide (12% by wt ammonia, Merck P.A., 2.8 ml/min) to a solution (3 liter) of 0.25 kmol/m^3 iron(III)nitrate($\text{Fe}(\text{NO}_3)_3 \cdot 9\text{H}_2\text{O}$, Merck P.A.) and 0.16 kmol/m^3 manganese(II)nitrate($\text{Mn}(\text{NO}_3)_2 \cdot 4\text{H}_2\text{O}$, Riedel P.A.), which was heated to 363 K. An atomic ratio of Fe : Mn of 1.54 was used. The ammonia addition was stopped when a pH of 8 was reached. The precipitate was filtered off and washed with 200 ml distilled water. Then the catalyst was dried at 393 K for 24 hours and calcined at 673 K for one hour. In all experiments a sieve fraction of 0.2 - 0.6 mm was used.

In the same way a pure manganese oxide catalyst was obtained starting from only manganese(II)nitrate.

A sulfated catalyst was prepared by adding a suspension (3.8 kmol/m^3 Fe) of the iron manganese oxide catalyst to an ammonium sulfate solution ($0.01 \text{ kmol/m}^3 (\text{NH}_4)_2\text{SO}_4$, Merck P.A.) at 323 K. After the water was evaporated under thorough mixing, exactly the same procedure was followed as is described in the unsulfated catalyst preparation after the filtration. After reduction with H_2 the catalyst had atomic ratios of Fe : Mn : S = 1.54 : 1 : 0.008.

According to some electronmicroprobe records the sulfate (or sulfite) anions were present as large clusters on the catalyst surface.

4.2.2. Outline of experimental methods

The reactor system and the purification of the gases and the analysis of the products have already been discussed in chapter 3.

The standard reduction of the catalyst consisted of a treatment at 623 K in flowing hydrogen ($100 \text{ cm}^3/\text{min}$) for 16 hours. The Fischer-Tropsch reaction occurred at 100 kPa total pressure with 0.5 gram of catalyst and a gas mixture of $1\text{CO} : 1\text{H}_2 : 3\text{He}$ at a total gas flow rate of $100 \text{ cm}^3/\text{min}$.

The experiments have been executed under differential conditions (maximum conversion below 5%) to prevent possible heat transfer problems.

The hydrocarbon reaction rate r is defined as the number of μmoles of CO converted into C_1 through C_3 hydrocarbons per kg of iron and per second.

The selectivity S_j is defined as the ratio of the rate of formation of the product with j carbon atoms to the overall hydrocarbon reaction rate:

$$S_j = \frac{r_j}{\sum_{i=1}^3 r_i}$$

4.2.3. Catalyst characterization

For a characterization of the fresh catalyst as well as of the catalyst after various periods of Fischer-Tropsch reaction X-ray diffraction analysis, Mössbauer spectroscopy and a determination of the carbon content were used (4).

Mössbauer spectra were obtained with a spectrometer of the constant acceleration type, using a source of ^{57}Co embedded in a Rh-matrix. Isomer shifts are given relative to the NBS standard sodium nitroprusside (SNP or $\text{Na}_2\text{Fe}(\text{CN})_5 \cdot \text{NO} \cdot 2\text{H}_2\text{O}$) at room temperature, while hyperfine fields are calibrated against the 515 kOe field of $\alpha\text{-Fe}_2\text{O}_3$ at room temperature.

The following abbreviations will be used throughout this chapter:

I.S.: isomer shift; ΔE_Q : electric quadrupole splitting of a doublet; H_{eff} : magnetic hyperfine fields; ϵ' : line shift due to

the interaction of the nuclear quadrupole moment with the electric field gradient in a magnetically split spectrum; A total absorption of a spectrum.

Mössbauer spectra of the catalysts before and after reduction were analyzed by fitting sets of Lorentzian line shapes to the observed spectra with the aid of a least squares method. In order to obtain results of physical significance, a number of constraints was imposed on the final fits to the spectra:

- (I) Peaks belonging to the same subspectrum should have equal widths.
- (II) In case of a doublet peak intensities should be equal.
- (III) For a magnetically split spectrum or sextuplet the intensities of the first and the sixth, of the second and the fifth and of the third and the fourth peak should be pairwise equal.
- (IV) Distances between peaks in the same sextuplet should satisfy the ratios following from the different g-factors for the ground and excited level of the ^{57}Fe nucleus.
In the presence of an electric field gradient (EFG) these ratios must be corrected for the interaction of the nuclear quadrupole moment with the EFG.

The more complex Mössbauer spectra of catalysts after Fischer-Tropsch synthesis were analyzed by fitting a linear combination of single-phase spectra of the constituents. This procedure (4) has been described extensively in section 3.2.4.

4.3. RESULTS

4.3.1. The iron manganese oxide catalyst before reduction

Figure 4.1. shows the Mössbauer spectra of the catalyst before reduction, recorded at 4.2 K, 77 K and 295 K, respectively.

The spectra obtained at room temperature have been analyzed with the 'Lorentzian fitting procedure'; the results are listed in table 4.1. The spectra show two components, labeled I and II.

Component I has the I.S. and ϵ' of $\alpha\text{-Fe}_2\text{O}_3$, but H_{eff} (507 ± 2 kOe) is significantly lower than the 515 kOe field of bulk $\alpha\text{-Fe}_2\text{O}_3$.

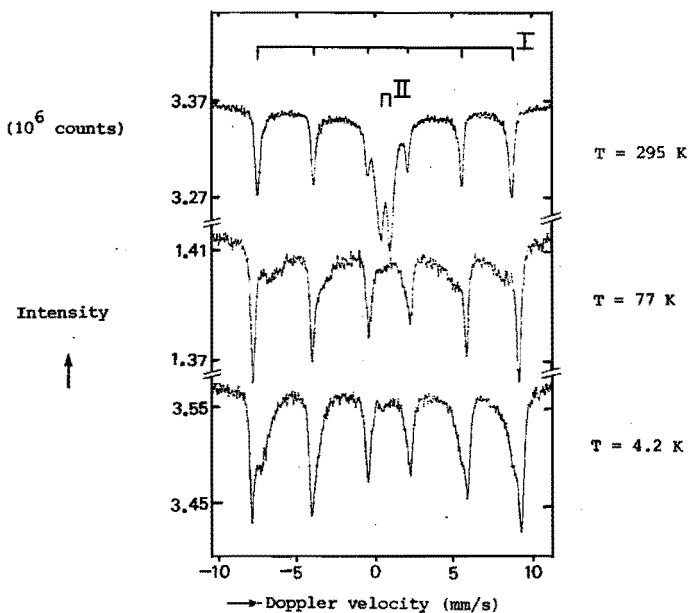


Figure 4.1. Mössbauer spectra of the manganese oxide promoted iron catalyst recorded at the indicated temperatures before the reduction.

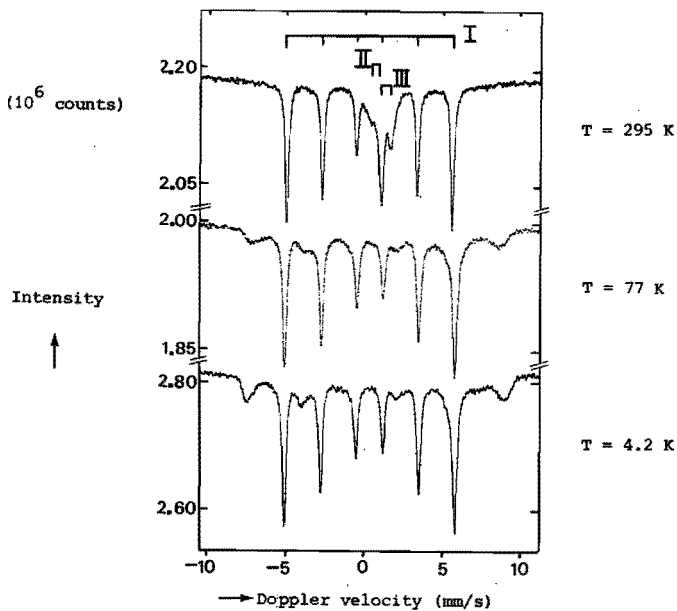


Figure 4.3. Mössbauer spectra of the manganese oxide promoted iron catalyst recorded at the indicated temperatures after the reduction.

The subspectrum of component I at $T = 295$ K is slightly asymmetrically broadened towards lower hyperfine splittings. This broadening and the reduced value of H_{eff} indicate that $\alpha\text{-Fe}_2\text{O}_3$ is present in small particles, with a distribution in particle diameters (11). Following Van der Kraan (11) an average diameter of 230 ± 20 Å can be estimated for these $\alpha\text{-Fe}_2\text{O}_3$ particles.

Component II shows a doublet at $T = 295$ K, but is magnetically split at $T = 77$ K and 4.2 K, with a broad distribution in H_{eff} . The average value of H_{eff} at $T = 77$ K and 4.2 K, and also the I.S. and ΔE_Q at $T = 295$ K, are characteristic for small particles $\alpha\text{-FeOOH}$, with a distribution in particle diameters. Based on the average hyperfine field and on the fact that the superparamagnetic transition temperature is lower than 295 K, it can be concluded (11) that the particle diameter is smaller than 85 Å.

Table 4.I. Mössbauer parameters at $T = 295$ K of catalysts before and after reduction

	Component	I.S. (mm/s)	ΔE_Q (mm/s)	ϵ' (mm/s)	H_{eff} (kOe)	Relative Area (%)
before reduction	I	.64 \pm .03	-	.09 \pm .03	507 \pm 2	54
	II	.59 \pm .02	.67 \pm .02	-	-	46
after reduction	I	.26 \pm .03	-	.00 \pm .01	332 \pm 2	80
	II	.48 \pm .06	.55 \pm .06	-	-	7
	III	1.35 \pm .06	.63 \pm .06	-	-	13

It should be noted that estimates of particle diameters are presented under the assumption that Van der Kraan's results, obtained with samples of small particles $\alpha\text{-Fe}_2\text{O}_3$ or $\alpha\text{-FeOOH}$, apply also to our samples.

According to X-ray diffraction data the unreduced catalyst consists of $\alpha\text{-Fe}_2\text{O}_3$, $\alpha\text{-FeOOH}$ and also Mn_2O_3 .

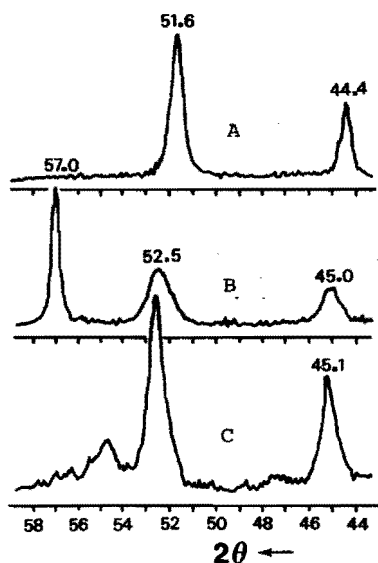


Figure 4.2. X-ray diffraction patterns of A) a reduced manganese oxide catalyst, B) a reduced manganese oxide promoted iron catalyst and C) id B) after 16 hours of Fischer-Tropsch reaction at 513 K.

4.3.2. The manganese oxide catalyst after reduction

The relevant part of the X-ray diffraction data of the reduced pure manganese catalyst is shown in figure 4.2a, data agree with the pattern of MnO, as follows from table 4.II.

Table 4.II. X-ray diffraction data of reduced Mn_2O_3 samples for angles 2θ between 40° and 80°

MnO			
this study		Swanson et al. (12)	
2θ	I (%)	2θ	I (%)
44.4	45	44.52	60
51.6	100	51.66	100
76.2	50	76.26	60

4.3.3. The iron manganese oxide catalyst after reduction

Mössbauer spectra of the catalysts after reduction are shown in figure 4.3. The spectrum obtained at room temperature was analyzed with the 'Lorentzian fitting procedure' as a combination of a sextuplet, labeled I, and two doublets, labeled II and III respectively. See table 4.I. for the numerical results.

Component I is easily identified as α -Fe. The parameters of component II are those of a paramagnetic Fe^{3+} compound, while the parameters of component III are more indicative for Fe^{2+} , although ΔE_Q is rather small for a Fe^{2+} compound. At temperatures of 77 K and 4.2 K components II and III are magnetically split, each with a distribution in hyperfine fields. Estimated averages of H_{eff} for component II are given in table 4.III, these values support the conclusion that II is a Fe^{3+} compound. The subspectrum of component III is very broad and difficult to observe at these low temperatures, so that even a rough estimation of its Mössbauer parameters seems hardly warranted. The contribution of α -Fe to the Mössbauer spectrum obtained at $T = 295$ K is $(80 \pm 3)\%$, so it can be concluded that the main part of the iron oxide that was present in the precipitated catalyst has been reduced.

Table 4.III. Hyperfine fields H_{eff} in the catalysts before and after reduction

	Component	H_{eff} (kOe)		
		$T = 295$ K	$T = 77$ K	$T = 4.2$ K
before reduction	I	507 ± 2	530 ± 2	537 ± 2
	II	-	$470 \pm 5^*$	$502 \pm 5^*$
after reduction	I	332 ± 2	339 ± 2	341 ± 2
	II	-	$495 \pm 5^*$	$513 \pm 5^*$

*) average value

The X-ray diffraction pattern (see figure 4.2b) showed clearly the diffraction line of reduced iron (at $2\theta = 57^\circ$), while the compounds containing Fe^{2+} and Fe^{3+} were probably not observed because of their small dimensions. A remarkable shift of the MnO diffraction lines occurred in the direction of the $\alpha\text{-Fe}$ diffraction line, which cannot be explained by spinel structures of iron- and manganese oxide.

It is likely that this shifted MnO pattern and the presence of the unreduced iron compounds containing Fe^{2+} and Fe^{3+} reflects the interaction between the iron compounds and the promotor MnO.

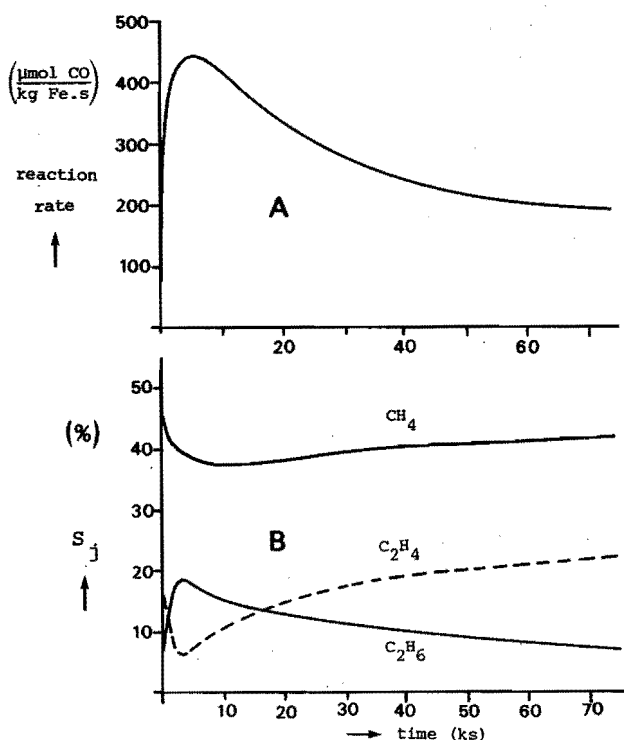


Figure 4.4. A) Reaction rate during Fischer-Tropsch synthesis on a Fe/MnO catalyst at 513 K.

B) The corresponding methane, ethane and ethene selectivities.

4.3.4. The Fischer-Tropsch synthesis on an iron manganese oxide catalyst at 513 K

The experiments on the manganese oxide promoted catalyst at 513 K were performed in the same way as those described in chapter 3. The composition of the catalyst during the synthesis was studied by Mössbauer spectroscopy and X-ray diffraction analysis; for this a number of catalysts after various periods of reaction were compared. For each experiment a fresh catalyst was used from the same batch of unreduced material.

With the promoted catalyst used we found differences of about 10% in the reaction rate between the various experiments at corresponding intervals. The accuracy of the product analysis itself was better than 1%. Probably the differences observed were due to a not too good reproducibility of the reduction of these promoted catalysts. Because the product distributions did not differ and the general shape of the curves of the reaction rate were comparable, these experiments still gave a good qualitative picture of the catalyst behaviour during the Fischer-Tropsch reaction.

The reaction rate and the selectivities for methane, ethane and ethene are shown in figure 4.4.

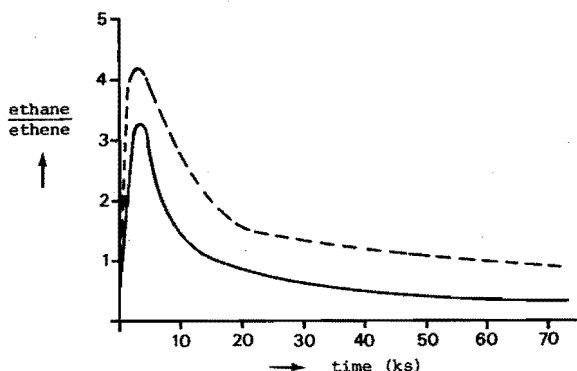


Figure 4.5. Ethane to ethene ratio during Fischer-Tropsch synthesis over an unsulfated (—) and a sulfated (-----) Fe/MnO catalyst at 513 K.

This catalyst needed about 1.5 hour before the maximum activity was reached; in that period the ethane to ethene ratio increased drastically, as is shown in figure 4.5. During the deactivation of the catalyst the ethane to ethene ratio decreased again.

As opposed to an iron catalyst a cobalt catalyst has a high initial activity; on these cobalt catalysts a slow deactivation is immedi-

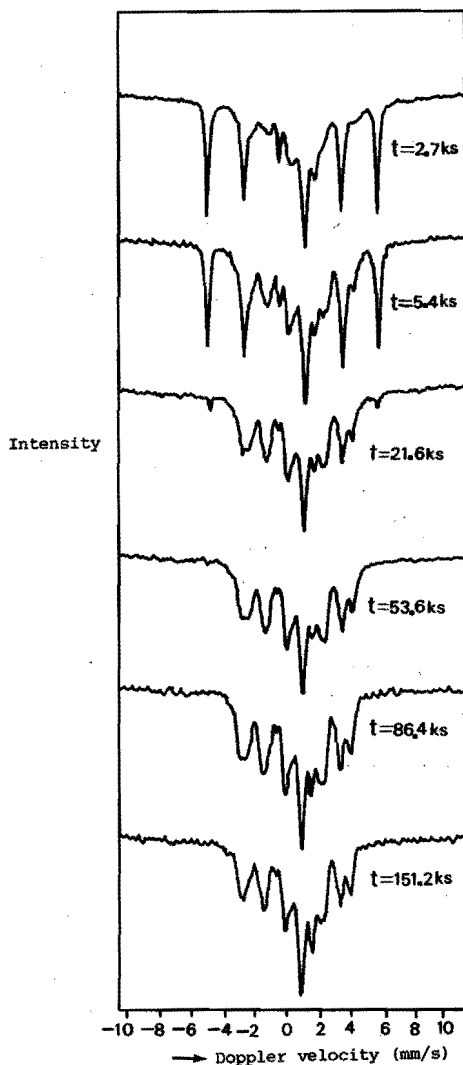


Figure 4.6. Mössbauer spectra of the reduced Fe/MnO catalyst after different periods of Fischer-Tropsch synthesis at 513 K. Spectra were recorded at room temperature.

ately observed, which is also coupled with a decreasing ethane to ethene ratio (13).

The ethene selectivity of the promoted and pure iron catalysts were about equal at corresponding reaction periods.

Since there was no relation at 513 K between the olefin selectivity of the catalyst and the amount of manganese oxide added, the manganese oxide itself was not considered as an effective promotor for the production of light olefins.

Mössbauer spectra of the catalyst after various periods of Fischer-Tropsch synthesis at 513 K are shown in figure 4.6. The spectra were analyzed by fitting a linear combination of base spectra to the measured spectra. The Mössbauer spectra which were used as a base are the single phase carbide spectra from ref.(4), completed with the spectra of α -Fe and the subspectra of doublets belonging to the unreduced iron phases in the catalyst after reduction. Results of this analysis are shown in figure 4.7.

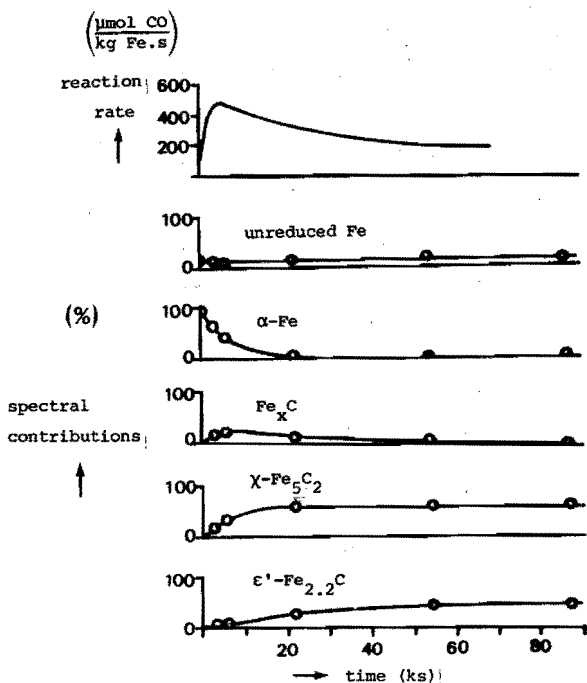


Figure 4.7. Reaction rates (upper curve) and relative contributions of reduced Fe, unreduced Fe and the various carbides to the Mössbauer spectra during the Fischer-Tropsch synthesis over a reduced Fe/MnO catalyst at 513 K.

According to the Mössbauer spectra and the X-ray diffraction pattern (see figure 4.2c) the α -Fe is converted into the carbides ϵ -Fe_{2.2}C and χ -Fe₅C₂. In this conversion Fe_xC, which is known from our Mössbauer and X-ray investigation to represent poorly defined structures somewhere between α -Fe and a crystallographically well defined carbide, appears as an intermediate.

The X-ray diffraction lines of MnO are still the same as those in figure 4.2b; because the contribution of the unreduced iron phases Fe²⁺ and Fe³⁺ is also constant during the time interval studied, these results indicate, that during the Fischer-Tropsch synthesis no further reduction or oxidation of the catalyst occurs.

If the synthesis gas mixture is led over a pure MnO catalyst, no reaction products are formed at 513 K.

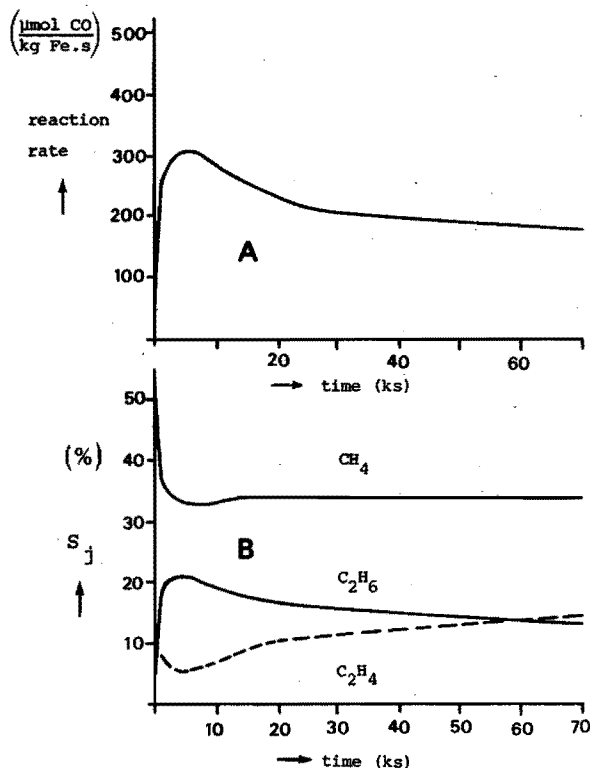


Figure 4.8. A) Reaction rate during Fischer-Tropsch synthesis on a sulfated Fe/MnO catalyst at 513 K.

B) The corresponding methane, ethane and ethene selectivities.

4.3.5. The Fischer-Tropsch synthesis on a sulfur containing iron manganese oxide catalyst at 513 K

The reaction rate and the selectivities of the sulfate impregnated iron manganese oxide are shown in figure 4.8. The maximum reaction rate is lower than the maximum rate of the original iron manganese oxide catalyst; but as the final activities are about equal, evidently the sulfated catalyst also deactivates less. The smaller deactivation parallels the higher ethane to ethene ratio during the complete time interval studied, as is shown in figure 4.5.

The Mössbauer spectrum of the reduced sulfated catalyst contains contributions of the same subspectra as the unsulfated catalyst, only the contribution of α -Fe for the former is less. So the degree of reduction is somewhat lower for the sulfated catalyst.

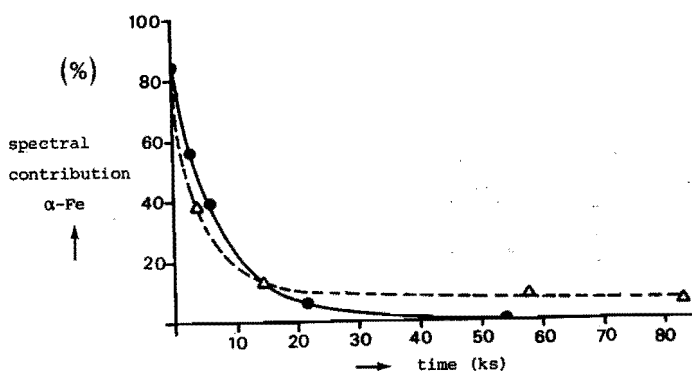


Figure 4.10. Relative contributions from reduced α -Fe to the Mössbauer spectra during Fischer-Tropsch synthesis over

- A) an unsulfated Fe/MnO catalyst (●)
- B) a sulfated Fe/MnO catalyst (Δ) at 513 K.

However after a reaction period of 30 ks iron is still present in the sulfated catalyst (see figure 4.10); probably the sulfur compounds prevent that this iron is reached by the synthesis gas. The composition of the spectra with respect to the carbides is not essentially different. Here also the phase Fe_xC remains visible in the spectra as long as α -Fe is present.

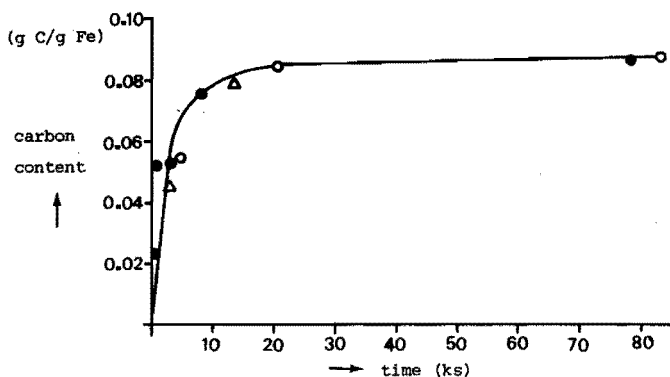


Figure 4.9. Carbon content during Fischer-Tropsch synthesis at 513 K over

- A) a reduced α -Fe catalyst (●)
- B) reduced unsulfated Fe/MnO catalyst (○) and
- C) reduced sulfated Fe/MnO catalyst (Δ).

For a comparison between the behaviour of a pure iron catalyst, a manganese oxide promoted iron catalyst and the sulfated iron manganese oxide catalyst during the Fischer-Tropsch synthesis at 513 K, the carbon content (in gram C/gram Fe) of those three catalysts is shown in figure 4.9 as a function of reaction time. During the time interval of 15 ks no noticeable difference is found between the three catalysts. The same result is obtained from Mössbauer spectra, when the contribution of α -Fe to the spectra of the sulfated catalyst during the Fischer-Tropsch synthesis is displayed together with the corresponding values for the unsulfated catalyst (see figure 4.10).

4.3.6. Olefin selective catalysts at 623 K

In the introduction we mentioned manganese oxide as an effective promotor of Fischer-Tropsch catalysts to produce light olefins. Because the unsulfated as well as the sulfated catalysts behave at 513 K in about the same way as a pure iron catalyst, the catalysts were further studied at the higher reaction temperature of 623 K.

At the reaction temperature of 623 K the reaction rate of the pure iron catalyst increased very quickly, but the catalyst was com-

pletely deactivated within 1 hour by the formation of inactive graphitic carbon species (the carbon deposition (5) increased already after a short initial period of a few minutes at a constant rate of 3% by weight carbon/hour). The methane selectivity varied between 80 and 90%.

The manganese oxide promoted iron catalyst behaved at 623 K just as the pure iron catalyst, while the main product was also methane (see figure 4.11).

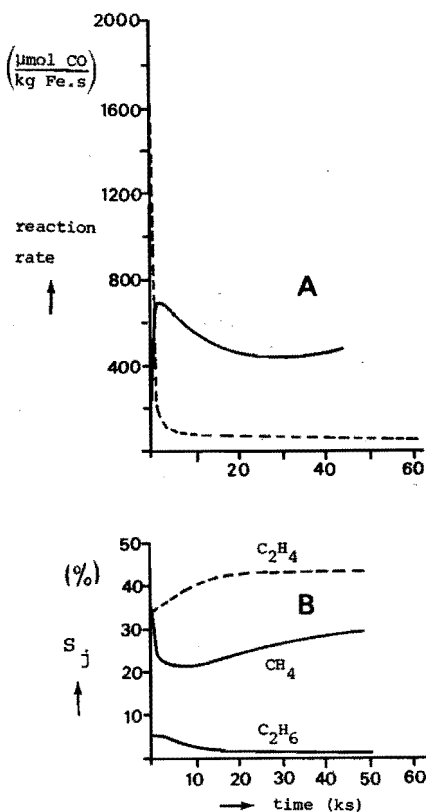


Figure 4.11. Reaction rates during Fischer-Tropsch synthesis at 623 K over

- A) an unsulfated Fe/MnO catalyst (-----) and over a sulfated Fe/MnO catalyst (———)
- B) the methane, ethane and ethene selectivities on a sulfated Fe/MnO catalyst.

However, the sulfate impregnated iron manganese oxide catalyst behaved totally different at 623 K, as is shown in figure 4.11. The catalyst was again quickly activated, but the reaction rate remained rather high. Even more remarkable is the observation, that the main product was not methane anymore, but ethene.

The ethene/ethane ratio leveled out to a value of about 30 after 50 ks Fischer-Tropsch reaction at 623 K.

Unfortunately, the mechanical strength of this sulfated catalyst was much lower than the unsulfated iron manganese oxide catalyst. On the sulfated as well as the unsulfated catalyst very much carbon was deposited at 623 K, but only the sulfated catalyst particles broke up to a fine powder after a few hours; this effect resulted in an increase of the reaction rate after 25 ks.

Since the mechanical strength of the sulfated catalyst is that unsatisfactory, the catalyst were not yet characterized with Mössbauer spectroscopy and X-ray diffraction analysis as in the experiments at 513 K.

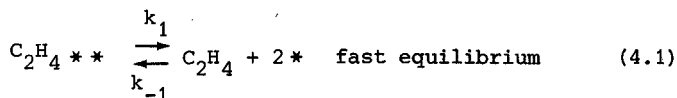
The addition of higher quantities of ammonium sulfate to the iron manganese oxide catalyst resulted in a better resistance against the deposition of carbon, while the olefin selectivity remained very high. The amounts of sulfate added had to be restricted, because otherwise the catalyst is completely deactivated. In our laboratory Kieffer (14) has obtained quantitative data about the optimum addition of sulfate to Fe/ZnO catalyst.

4.4. DISCUSSION

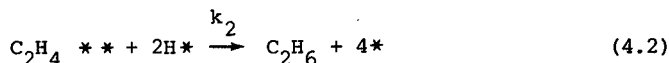
The degree of reduction of the sulfated and unsulfated catalysts varied between 75 and 80%. The unreduced small Fe^{2+} and Fe^{3+} compounds were observed as superparamagnetic phases in Mössbauer spectroscopy; these compounds also caused the shift of the X-ray diffraction lines of MnO. During the Fischer-Tropsch reaction the amount of unreduced iron did not change. These unreduced iron compounds are probably associated with the MnO phase of the catalyst. Reduction at higher temperatures did lead to a lower activity presumably due to surface sintering.

The increase of the reaction rates on unsulfated and sulfated catalysts during the activation period at 510 K was accompanied by an

increase of the ethane to ethene ratio. This was also observed on pure iron catalysts in our laboratory (5) and also by Ott and Delgass (15). If we assume that ethane and ethene are formed according to the following reactions:



and



the formation rates of these products can be expressed as:

$$r_{\text{C}_2\text{H}_4} = (\text{C}_2\text{H}_4) \cdot \frac{F}{W} = \frac{K \cdot \theta_{\text{C}_2\text{H}_4}}{\theta_e^2} \cdot \frac{F}{W} \quad (4.3)$$

and

$$r_{\text{C}_2\text{H}_6} = \frac{d(\text{C}_2\text{H}_6)}{dt} = (k_2 \cdot \theta_{\text{C}_2\text{H}_4} \cdot \theta_{\text{H}}^2) \quad (4.4)$$

where F is the gas rate in m^3/sec ,
 W the catalyst weight in kg,
 (C_2H_4) the concentration of ethene in kmol/m^3 ,
and K the ratio between k_1 en k_{-1} .

As (4.1) and (4.2) are parallel reactions starting from the same substrate we can write:

$$\frac{r_{\text{C}_2\text{H}_6}}{r_{\text{C}_2\text{H}_4}} = k' \cdot \theta_e^2 \cdot \theta_{\text{H}}^2 \cdot \frac{W}{F} \quad (4.5)$$

The surface coverage of empty sites θ_e can initially not be (very) low, as will be further discussed in chapter 5. The low ethane to ethene ratio is then caused by either a low surface coverage of hydrogen θ_{H} or by a low number of ensembles of sites, that can perform the hydrogenation reaction. Since we expect, that the equilibrium of

the dissociative hydrogen adsorption is quickly reached, we suggest that the iron surface requires first some kind of activation by which action the hydrogenation ensembles are formed.

The deactivation of the catalysts is accompanied by a decrease of the ethane to ethene ratio. This decrease can be caused by carbon deposition, that results in a decrease of either the hydrogenation ensembles mentioned above or of the empty sites θ_e or even of both. The former factor influences k' of equation (4.5), whereas the latter has its influence on both θ_e and θ_H .

As during the overall deactivation process the rate of ethene formation actually increases, we are inclined to ascribe this deactivation to a decrease in empty sites, for that would, according to equation (4.3) nicely explain the observed rate increase for ethene. This explanation is in agreement with the one that has been offered by McCarty et al. (16) for the deactivation of reactive carbonaceous species on nickel which they studied with temperature programmed reduction experiments.

In the activation/deactivation process the sulfated catalyst is always somewhat less active than the unsulfated catalyst, although in the final pseudo steady state the difference in activity is small.

It is noteworthy that during the whole activation/deactivation process at 510 K the ethane to ethene ratio was higher for the sulfated catalyst than for the unsulfated catalyst.

The average bulk composition of the unsulfated and sulfated catalysts did not differ significantly from the pure iron catalyst during the Fischer-Tropsch synthesis at 510 K. According to the results of the carbon analysis by which carbon was determined as a function of time, the same process of carbon deposition operates for all three catalysts.

Addition of various quantities of manganese oxide to iron catalysts showed no improvement of the olefin selectivity. This is not in agreement with the results of Kölbl (1), Bössemeier (2) and Yang (3). We also did not observe any influence of manganese oxide additions on the molecular mass distribution of the product mixture. A fully carburized iron manganese oxide catalyst revealed a Schulz-Flory distribution which was quite similar to that of a carburized iron catalyst without manganese oxide.

However a major difference between sulfated and unsulfated catalysts

is observed at higher temperatures. The sulfated catalysts were stable at 625 K and gave a product with a high olefin content and a relatively low CH_4 -production, whereas the unsulfated catalyst deactivated quickly and produced only methane.

The same results as we obtained with our sulfated catalyst at 625 K were also obtained by Bössemeier (2) with manganese oxide promoted iron catalysts. In connection with our negative results with manganese oxide alone we are inclined to think that the catalysts of Bössemeier also contained small quantities of sulfur containing compounds.

4.5. REFERENCES

1. H. Kölbel, K.D. Tillmetz, Deutsches Offenlegungsschrift 2 507 647 (1976)
2. B. Bössemeier, C.D. Frohning, G. Horn, W. Kluy, Deutsches Offenlegungsschrift 2 518 964 (1976)
3. C.H. Yang, A.G. Oblad, Symposium on advances in F.T. chemistry, Anaheim meeting, March (1978)
4. J.W. Niemantsverdriet, A.M. van der Kraan, W.L. van Dijk, H.S. van der Baan, J. Phys. Chem., 84(25), 3363 (1980)
5. W.L. van Dijk, University of Technology Eindhoven, unpublished data
6. I.G. Farbenindustrie Aktiengesellschaft British patent 322, 284 (1929)
7. W.W. Myddleton, British patent 509, 325 (1939)
8. E.T. Layng, U.S. patent 2, 446, 426 (1948)
9. R.B. Anderson, F.S. Karn, J.F. Schulz, J. Catal. 4, 56 (1965)
10. R.A. Dalla Betta, A.G. Piken, M. Shelef, J. Catal. 40, 173 (1975)
11. A.M. van der Kraan, thesis University of Technology Delft (1972)
12. M. Swanson et al., NBS circular 539 5 45 (1955)
13. A.O.I. Rautavuoma, thesis University of Technology Eindhoven (1979)
14. E.Ph. Kieffer, thesis University of Technology Eindhoven (1981)
15. G.L. Ott, T. Fleisch, W.N. Delgass, J. Catal. 65, 253 (1980)
16. J.G. Mc Carty, P.R. Wentreck, H. Wise, J. Catal. 57, 406 (1979)

THE FORMATION OF ACTIVE HYDROGENATION ENSEMBLES DURING THE ACTIVATION OF AN IRON FISCHER-TROPSCH CATALYST

5.1. INTRODUCTION

Already in the early days of Fischer-Tropsch synthesis it was a customary procedure to pretreat the iron catalyst with carbon monoxide before the start of the Fischer-Tropsch synthesis.

Pichler et al. (1) suggested that this treatment was necessary, because - according to him - the hexagonal iron carbide was the actual active catalyst. The industrial iron catalysts (2) at SASOL (South Africa) as well as the iron catalysts recently developed by K  lbel (3) need about the same pretreatment conditions: namely a treatment with 0.1 MPa of carbon monoxide at 600 K.

Raupp and Delgass followed the Fischer-Tropsch reaction on a supported iron catalyst with in-situ M  ssbauer spectroscopy and performed simultaneously reaction rate measurements. The increase of the Fischer-Tropsch reaction rate appeared to be directly proportional to the formation rate of the iron carbides.

Since the diffusion of carbon in α -Fe is very fast, as is shown by the low activation energy (69 kJ/mol) and the high frequency factor (4), we suggested in chapter 3, that this fast diffusion of carbon is possibly the reason for the initial inactivity of an iron catalyst. Another explanation was proposed in chapter 3 and 4,

namely that the iron surface had to be activated with carbon monoxide, which activation occurs in an autonomous process parallel to the diffusion of carbon into the bulk of the iron.

Various authors claimed (5, 6, 7) they have found with Ni-catalysts, that hydrogen assists the dissociation of carbon monoxide; hence they suggest, that the dissociation of CO is possibly involved in the rate determining step of the Fischer-Tropsch reaction.

Recently Unmuth (8) also observed on iron catalysts an enhanced CO-dissociation rate, when hydrogen was added to the carbon monoxide feed. However Unmuth could not discriminate for the rate determining step between the assistance of hydrogen in the dissociation of CO and the hydrogenation of C to CH_2 as is advocated by Biloen et al. (9) and Rautavuoma (10).

As the reactivity of carbon and its formation play a central role in all models of the Fischer-Tropsch reaction, we have studied the formation and reactivity of carbon on an iron catalyst in more detail. For the study of the bulk composition of an iron catalyst we have augmented the results of chapter 3 with thermomagnetic measurements in equipment as described by Sancier (11). As these bulk techniques can hardly say anything useful about the surface composition, we have applied temperature programmed surface reaction (TPSR) with hydrogen to obtain a better insight in the reactivity of the different (potential) intermediates of surface species. This is the same method as the one Mc Carty (12) applied in his study of the methanation reaction on $\text{Ni}/\text{Al}_2\text{O}_3$ catalysts. The TPSR spectra obtained allowed us to determine the reactivities of the various carbon species on the surface and in the bulk of the catalyst. When the hydrogenation was carried out under isothermal conditions, further information was obtained about the nature of the surface intermediates, especially when the carbon- and oxygen containing products were analyzed carefully.

5.2. EXPERIMENTAL

5.2.1. Catalyst preparation

The preparation of a pure iron catalyst is described in 3.2.1. A sieve fraction of 0.2 - 0.6 mm from the same batch of unreduced precipitated material was used in all experiments.

Standard reduction of the catalyst was at 623 K in flowing hydrogen ($1.7 \text{ cm}^3/\text{s}$), that resulted in a completely reduced iron catalyst, as is shown in 3.3.1.

5.2.2. Magnetic susceptibility apparatus

The rate of carbon deposition and the magnetic properties of the iron catalyst at 510 K were studied during the Fischer-Tropsch reaction in the magnetic susceptibility apparatus of Sancier et al (11) equipped with an electronic micro balance (Cahn Model RS), as is shown in figure 5.1. A modified Faraday technique was used to measure the magnetization of the sample; the vertical magnetic-field gradient was provided by a set of electromagnetic gradient coils (13, 14), further indicated as Lewis coils, which were mounted on the flat pole faces of a 30 cm magnet. The assembly of the gradient coils, its power supply and the tube with furnace for heating the sample in a controlled gas atmosphere were supplied by George Associates. A bipolar current regulator delivered an oscillating square wave current of 0.50 A to the Lewis coils at a frequency of 1 Hz. The electrical ac signal from the micro balance was determined by the mass changes and by the oscillating magnetization forces on the catalyst. To record the magnetization, a lock-in amplifier was used to convert the 1 Hz component in the micro balance ac signal to a dc voltage. After the 1 Hz component in the micro balance signal was removed by filtering, the resulting dc signal represented the weight change of the sample, and could be recorded simultaneously with the magnetization of the catalyst. Because the pure iron catalyst is a highly magnetic substance, a rather low magnetic field (0.3 kOe) had to be used, as otherwise the catalyst was lifted out of the catalyst basket.

Two thermocouples were used; one in the gas stream just below the catalyst sample to measure the catalyst temperature and one near the furnace to control its temperature.

Catalyst samples (about 50 mg) were placed in a small quartz container suspended from the micro balance by a quartz fiber.

The CO (Matheson, U.C.P. >99.8%) and the premixed CO/H₂ mixtures were purified by passing the gases through a copper tube packed with molecular sieves cooled in a bath of dry ice and acetone. Hy-

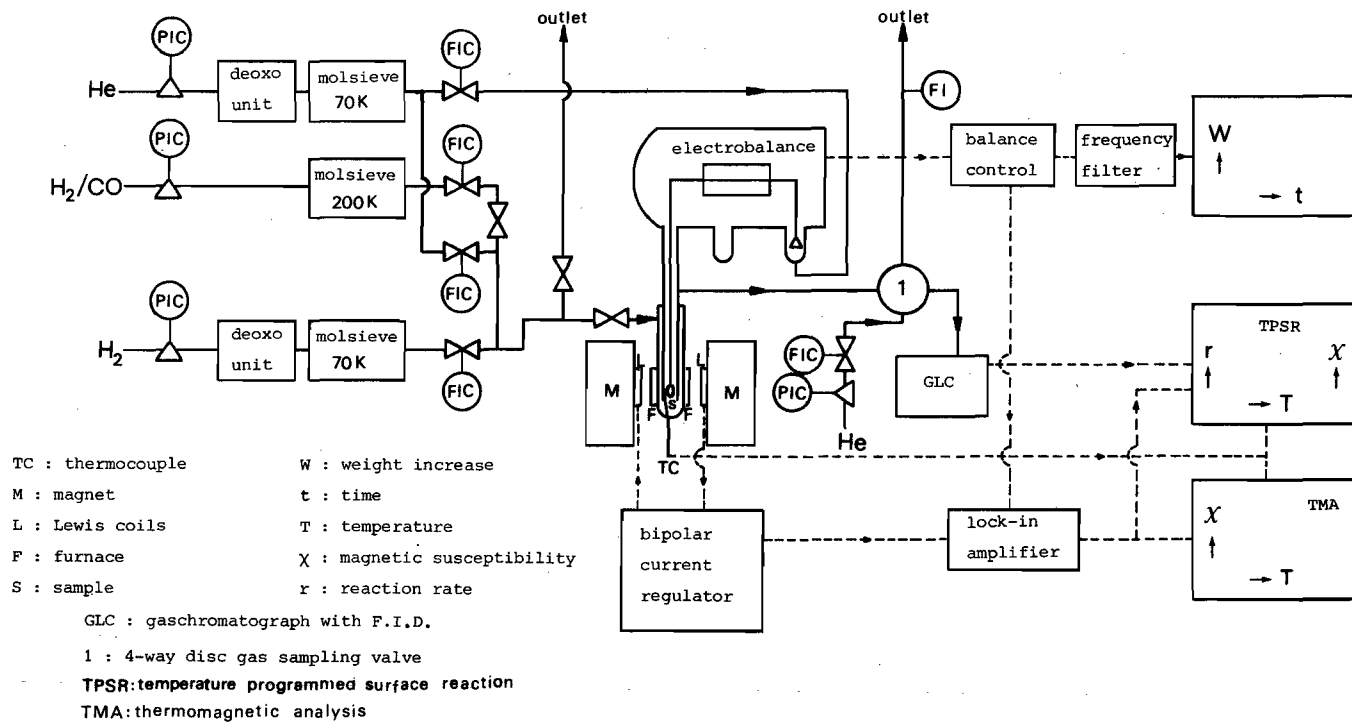


Figure 5.1 The reactor system for magnetic susceptibility experiments

drogen and helium (Matheson, prepurified) were passed through copper tubes packed with molecular sieves cooled in liquid nitrogen.

Thermomagnetic analysis (TMA) was performed by recording the magnetization of the sample as a function of the temperature that was raised from 300 to 925 K at a heating rate of 0.42 K/s in a flow of $0.5 \text{ cm}^3/\text{s}$ of helium.

Temperature programmed surface reactions (TPSR) with hydrogen were also carried out in this apparatus; after the carburization of the iron catalyst the sample was quickly cooled in helium to room temperature, whereafter a hydrogen flow ($0.5 \text{ cm}^3/\text{s}$) was led over the catalyst, while the temperature was slowly increased with a heating rate of 0.10 K/s. The hydrocarbons formed were analyzed on a Hewlett Packard 5700 gas chromatograph equipped with a FID detector. The weight change, the magnetic susceptibility and the production of various hydrocarbons were determined simultaneously during the TPSR-experiment.

5.2.3. Temperature programmed surface reaction (TPSR) apparatus

Some TPSR experiments were also conducted in the apparatus of MC Carty et al. (12) as a check of the TPSR-results in the magnetic susceptibility apparatus. The TPSR apparatus of Mc Carty contained a small quartz micro reactor, in which approximately 30 mg of catalyst was placed.

During the Fischer-Tropsch reaction and the TPSR experiment a fraction of the reactor outlet flow was admitted to a quadrupole analyzer via a variable leak valve. In this way the gas composition was monitored continuously.

Since the active carbon species can deactivate during the heating of the catalyst in the TPSR-experiment, a fast linear heating rate of 0.9 K/s was used.

5.2.4. Thermobalance

The course of the carburization of the catalyst was further studied with various H_2/CO mixtures in a Dupont thermogravimetric balance. The temperature was regulated within 0.2 K and measured with a chromel-alumel thermocouple, placed just above the quartz sample boat.

Carbon monoxide, hydrogen and helium were purified separately over a reduced copper catalyst (BASF RJ-11, BTS catalyst) at 425 K and a molecular sieve (5A, Union Carbide) at room temperature.

The production of carbon dioxide and water was measured continuously and quantitatively with a CO₂ monitor (Unor CO₂ monitor, Maihak) and a H₂O monitor (Panametrics hygrometer 3000), respectively.

5.2.5. Isothermal flushing reactions

After the catalyst was subjected to the Fischer-Tropsch reaction for a certain period in a continuous flow fixed-bed reactor (see section 3.2.2), the synthesis mixture was replaced by helium and subsequently by hydrogen at the reaction temperature of 510 K and at gas rates of 1.7 cm³/s. Besides hydrocarbons, water and carbon dioxide were continuously measured with the monitors mentioned above.

5.3. RESULTS

5.3.1. Thermomagnetic analysis

Before a thermomagnetic curve was recorded, the flowing synthesis gas was replaced by helium and the reaction temperature lowered to 350 K. Subsequently the magnetic susceptibility was measured by increasing the catalyst temperature at a linear heating rate of 0.42 K/s in helium. To the observed Curie temperatures we

Table 5.1. Curie temperatures of ferromagnetic phases of iron and iron compounds (14).

phase	Curie temperatures (K)
θ -Fe ₃ C (cementite)	478 - 493
χ -Fe ₅ C ₂ (Hägg)	520 - 540
ε -Fe ₂ C	653
ε' -Fe _{2.2} C	723
Fe ₃ O ₄ (magnetite)	838 - 868
α -Fe	1041

assigned specific ferromagnetic phases in accordance with the data of Loktev (15), as is given in table 5.I. A strong decrease of the magnetic susceptibility was observed above the Curie temperature of each ferromagnetic phase, because thereafter the ferromagnetic material changed into a paramagnetic compound.

The fraction of the total magnetization force attributable to a given phase was estimated by extrapolating the TMA curve of a given

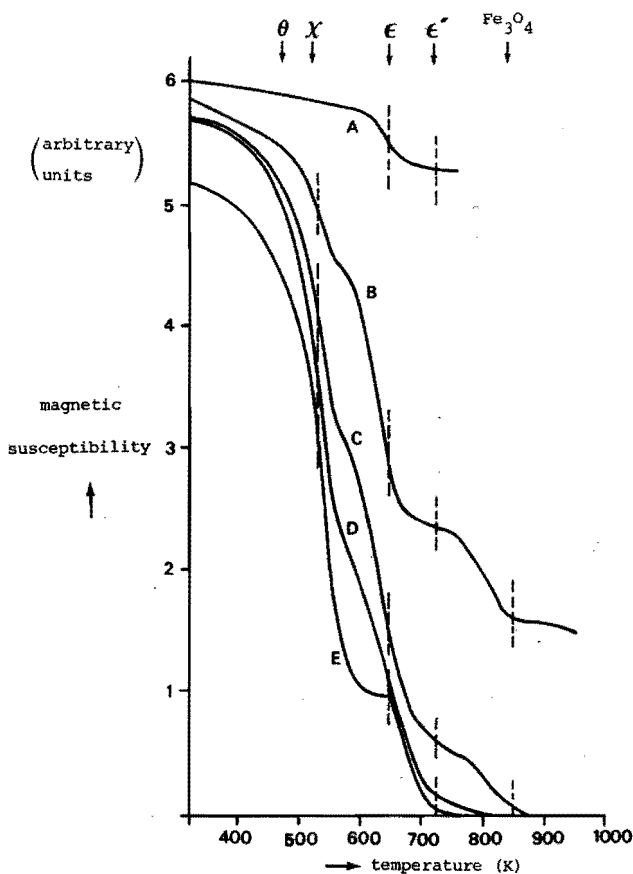


Figure 5.2. TMA curves after the Fischer-Tropsch synthesis at 513 K on an Fe catalyst during

- | | |
|---------------|---------------|
| A) 0.6 ksec; | D) 19.1 ksec; |
| B) 3.6 ksec; | E) 56.9 ksec |
| C) 11.9 ksec; | |

($\theta, \chi, \epsilon, \epsilon'$ and Fe_3O_4 indicate the Curie temperature of these iron compounds)

ferromagnetic phase to 300 K. The magnetization attributable to the various ferromagnetic phases can only be estimated semi quantitatively. Firstly, because of the unknown domain size, which at sufficiently small values could give rise to superparamagnetism rather than ferromagnetism (16). Secondly, because of the uncertainty about the identity of the ϵ' -Fe_{2.2}C phase and the stoichiometry of the Fe_xC phase as is discussed in chapter 3.

Thermomagnetic analysis (TMA) experiments were carried out on reduced iron catalysts that were carburized at 513 K to increasing extents with a gas mixture of 50 vol % H₂/50 vol % CO and a total gas rate of 0.4 cm³/s. For each carburization experiment a new catalyst sample was used.

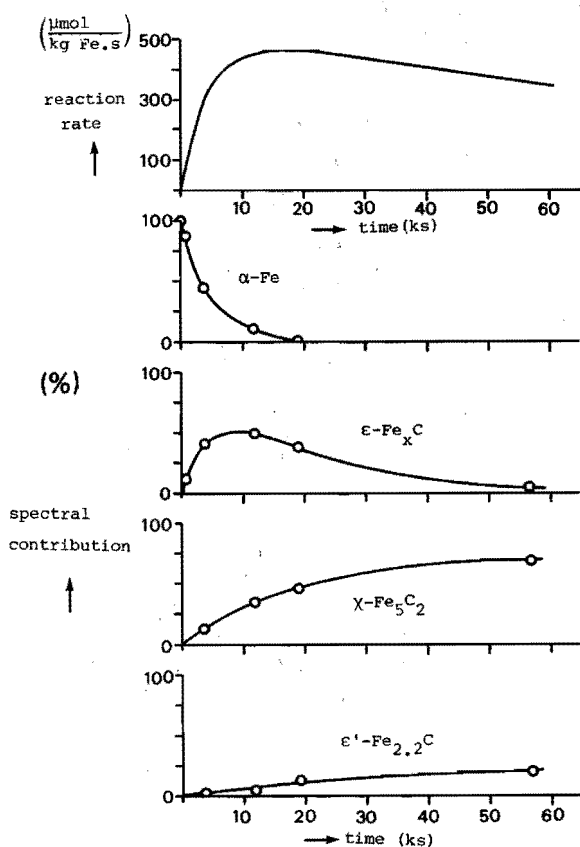
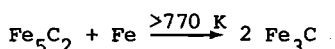


Figure 5.3. Reaction rates (upper curve) and relative contributions of α -Fe and the various carbides to the TMA curves during Fischer-Tropsch synthesis over an Fe catalyst at 513 K

When the catalyst was exposed for 0.6 ks to the Fischer-Tropsch gas mixture, a TMA curve was obtained, as is shown in figure 5.2a. A small amount of a pure ferromagnetic carbide was observed, which is ascribed to ϵ -Fe₂C according to table 5.I. When a new sample was prepared in the same way and cooled down in helium, the Mössbauer spectrum of this sample at 295 K contained besides reduced α -Fe a small contribution of the previously mentioned Fe_xC compounds. So, the Fe_xC compounds detected by Mössbauer spectroscopy correspond with the ϵ -carbide observed in TMA. TMA of the catalyst samples exposed to the Fischer-Tropsch gas mixture for longer periods of time are also shown in figure 5.2.

The χ -Fe₅C₂, ϵ' -Fe_{2.2}C and Fe_xC carbides were clearly observed. A decrease of the magnetic susceptibility was sometimes observed above 775 K. Sancier (11) who observed the same phenomenon ascribed this to a solid phase reaction between the iron carbides and α -Fe:



Since the decrease of the magnetic susceptibility at 775 K was not too far away from the Curie temperature of Fe₃O₄, the possible presence of Fe₃O₄ was checked by measuring the magnetization while the temperature was lowered from 950 K to 350 K. No increase of the magnetization was observed until 490 K, when the Curie temperature of θ -Fe₃C was reached.

In figure 5.3 the catalytic reaction rate ($\mu\text{moles CO/kg iron.s}$ converted to C₁ - C₃ hydrocarbons) is plotted together with the relative spectral contributions to the TMA spectra of α -Fe and the different carbides as a function of reaction time. The results will be discussed in the following section.

5.3.2. Carburization followed in the thermobalance

The experiments in the thermobalance were carried out at 510 K with about 35-40 mg of catalyst and a total gas rate of 3.5 cm³/s.

The relations between the carburization rates and the partial pressures of hydrogen and of carbon monoxide were obtained from two series of experiments, in which the partial pressure of either hydrogen or carbon monoxide was kept constant at 57 kPa and 9.5 kPa,

respectively, while that of the other was varied between 0 and 60 kPa.

First, the carburization of the iron catalyst was studied with various concentrations of carbon monoxide in helium. The weight increase is plotted as a function of time in figure 5.4. We see

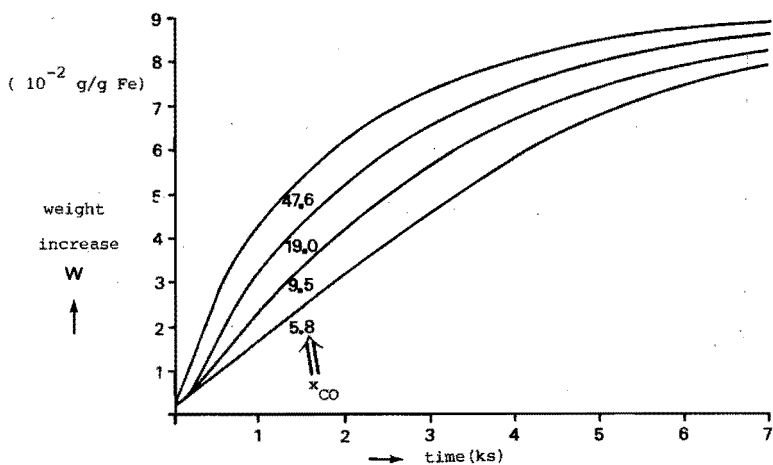


Figure 5.4. Weight increases of a metallic iron catalyst during carburization at 513 K for various mole fraction of carbon monoxide (total pressure of 10^5 Pa)

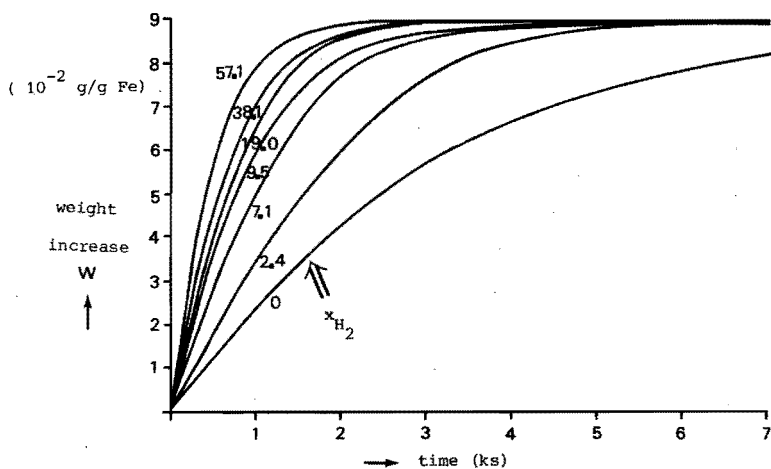


Figure 5.5. Weight increases of a metallic iron catalyst during carburization at 513 K for various mole fractions of hydrogen (constant mole fraction of carbon monoxide $x_{CO} = 0.095$; total pressure of 10^5 Pa)

that initially a small weight increase is observed, that is nearly constant for the various carbon monoxide concentrations. This 'step'-increase of the weight was of the same order of magnitude as the room temperature adsorption of carbon monoxide on a fresh iron catalyst. After this 'step' the weight increased linearly with time for a period varying between 0.5 and 1.0 ks depending on the CO concentrations until the weight approached about 0.025 g/g Fe; the rate of weight increase diminished then continually for the various gas mixtures. The slope of the linear part of the weight curves increased with the partial pressure of carbon monoxide.

In figure 5.5 corresponding curves are shown for the case that the partial pressure of carbon monoxide is kept constant at 9.5 kPa and the partial pressure of hydrogen was varied between 0 and 57 kPa. The above mentioned first 'step' was only observed at low hydrogen partial pressures. It was interesting to note that in this case the initial rate of weight increase also enhanced with the partial pressure of hydrogen. Also in this case there is a linear part in the weight curves until the weight approaches about 0.027 g/g Fe. At longer reaction periods the weight curves all leveled off to a carbon content of about 9.0%, which agrees rather well with the calculated carbon content of ϵ' -Fe_{2.2}C carbide (8.9%).

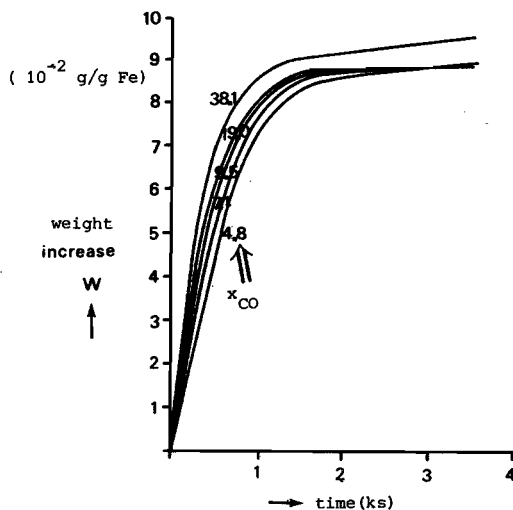


Figure 5.6. Weight increases of a metallic iron catalyst during carburization at 513 K for various mole fractions of carbon monoxide (constant mole fraction of hydrogen $x_{H_2} = 0.57$; total pressure of 10^5 Pa)

In figure 5.6 the weight gain is shown, as a function of time, when the partial pressure of H_2 was kept constant at 57 kPa and the partial pressure of carbon monoxide was varied between 4.8 and 38 kPa. During the carburization of the iron catalysts water and carbon dioxide production were monitored continuously; low concentrations of hydrocarbons could not be measured accurately, but from our experiments in a continuous flow fixed-bed reactor an estimate of the rate of hydrocarbon formation could be made (c.f. section 5.3.1). An oxygen mass balance for the carburization results in:

$$r_{CO, in} = r_{CO, out} + 2 r_{CO_2} + r_{H_2O} + r_{O, ads} + r_{CO, ads} \quad (5.1)$$

A corresponding carbon mass balance results in:

$$r_{CO, in} = r_{CO, out} + r_{CO_2} + r_{F.T.} + r_{C, ads} + r_{CO, ads} \quad (5.2)$$

It must be noted that $r_{O, ads}$ represents not only oxygen but also oxygen in oxygen containing compounds, except CO, that are adsorbed. A corresponding note can be made regarding $r_{C, ads}$.

An expression for $r_{C, ads}$ is obtained, when equation (5.2) is subtracted from equation (5.1):

$$\begin{aligned} r_{C, ads} &= r_{CO_2} + r_{H_2O} - r_{F.T.} + r_{O, ads} \\ &= r_C^{calc} + r_{O, ads} \end{aligned} \quad (5.3)$$

where r_C^{calc} represents the carbon deposition rate calculated from the carbon dioxide, water and hydrocarbon production only. If we neglect the very small weight of hydrogen that may be present in adsorbed water and hydrocarbons, we can say that the experimental rate of weight increase is determined by both carbon deposition and by oxygen and CO adsorption:

$$r^{exp} = r_{O, ads} + r_{C, ads} + r_{CO, ads} \quad (5.4)$$

or, because we assume that $r_{CO, ads}$ i.e. the rate of change of the

amount of CO adsorbed, is negligible after a very short period:

$$r^{\text{exp}} = 2 r_{\text{O, ads}} + r_{\text{C}}^{\text{calc}} \quad (5.5)$$

We shall call this simply the 'experimental carburization rate'.

The difference of $2r_{\text{O, ads}}$ between the experimental carburization rate r^{exp} and the calculated carburization rate $r_{\text{C}}^{\text{calc}}$ is noticed in figure 5.7, when the carburization is carried out with a 9.5/9.5 H_2/CO mixture. A considerable amount of oxygen is adsorbed by the catalyst during the initial reaction period of about 1 ks. It is curious that the rate of oxygen deposition $r_{\text{O, ads}}$ becomes zero after that period. This suggests that the formation of iron-carbon compounds actually prevents further deposition of oxygen or oxygen containing compounds.

All the weight increases leveled off for various gas mixtures at a weight of about 0.025-0.027 g/g Fe and in this period reasonable amounts of carbon- and oxygen were deposited on the catalyst.

As the bulk of the catalyst becomes partly saturated at a weight of 0.025 g/g Fe, the carburization rate becomes limited by the diffusion of carbon in the bulk. This is experimentally observed by

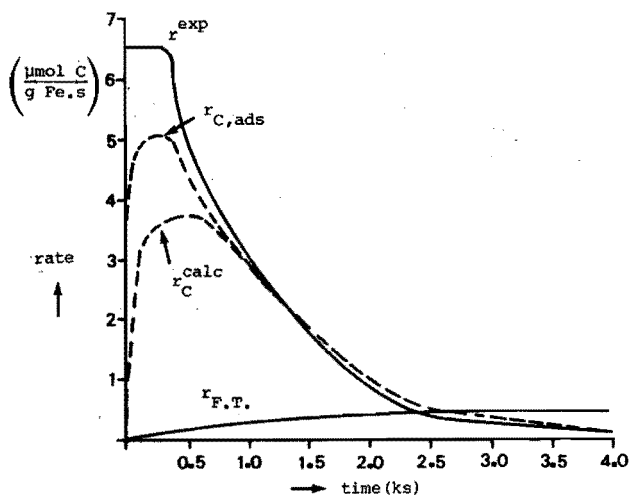


Figure 5.7. Various rates during the reaction at 513 K with a 9.5 kPa $\text{CO}/9.5$ kPa $\text{H}_2/81.0$ kPa He mixture on an Fe catalyst (see text for definitions of various rates)

the deviation from the linear weight increase; the rate of weight increase $\frac{dW}{dt}$ can then be described by a semi-empirical equation:

$$r_C = \frac{dW}{dt} = k \cdot f(p_{H_2}, p_{CO}) \cdot \left(1 - \frac{W}{W_{\max}}\right) \quad (5.6)$$

where W is the weight increase at time t and W_{\max} the maximum weight increase.

An integration of equation (5.6) results in:

$$\ln \left(1 - \frac{W}{W_{\max}}\right) = K \cdot t + C \quad (5.7)$$

The left-hand side of equation (5.7) is shown as a function of time for various partial pressures of H_2 and CO in figure 5.8; a maximum weight increase W_{\max} of $8.9 \cdot 10^{-2}$ is used, that agrees with the theoretical carbon content of ϵ' - $Fe_{2.2}C$. A linear relation is obtained after the period, where the linear weight increase is observed.

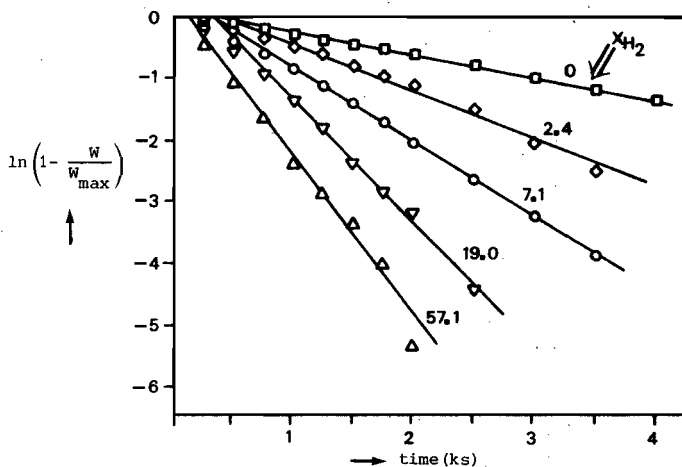


Figure 5.8. $\ln(1 - W/W_{\max})$ as a function of time for various mole fractions of hydrogen (constant mole fraction of carbon monoxide $x_{CO} = 0.095$; total pressure of 10^5 Pa)
Catalyst : Fe ; $T = 513$ K ; $W_{\max} = 0.089$

5.3.3. Reactivity of carbon species determined with TPSR experiments

Carbon species were deposited on a clean, freshly reduced iron catalyst at 510 K in the TPSR-apparatus of Mc Carty from two gas mixtures of different compositions (50 vol % H_2 /50 vol % CO and 90 vol % H_2 /10 vol % CO).

Since the formation of methane is a good indication for the activity for all Fischer-Tropsch reactions, we have plotted in figure 5.9 only the partial pressure of methane in the outgoing stream as a function of time. Since we could monitor methane continuously with a quadrupole mass spectrometer following the mass $m/e=15$, it appeared that for the high H_2 to CO ratio the iron catalyst was at the very beginning of the experiment already active. Thereafter, deactivation was observed for a period of about 0.5 ks followed by an activation.

With the 50/50 H_2 /CO mixture initially a very low activity was found, but activation of the catalyst was observed almost from the beginning of the experiment.

Since the methane production rate at a high H_2 /CO ratio appears to be a complex function of time, we used TPSR-experiments to study the reactivity of carbon surface species produced after various periods of Fischer-Tropsch reaction.

The catalyst was cooled down within 45 sec to 300 K in a helium stream immediately after the deposition of carbon from a 90/10 H_2 /CO mixture. Thereafter the gas flow was switched to 100 kPa hydrogen and

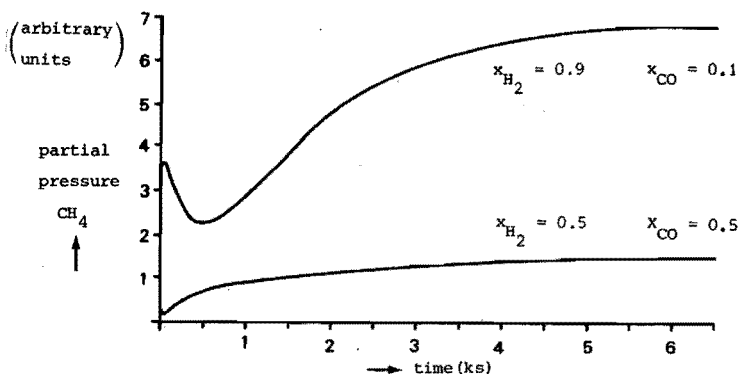


Figure 5.9. Formation of methane on an Fe catalyst during the Fischer-Tropsch synthesis at 513 K for different gas mixtures (total pressure of 10^5 Pa)

the temperature was raised at a linear heating rate of 0.9 K/s. As shown in figure 5.10 a number of carbon species with different reactivities were observed. The initial activity is coupled with (or caused by) a small quantity of surface species with a TPSR maximum at about 475 K. A lower activity is obtained after a reaction period of 600 s, which is coupled to a much larger quantity of much less active carbon with a TPSR maximum above 600 K. The deactivation observed in between is caused by the loss of the first type of surface species.

That the TPSR results do not explain the complete picture follows from TPSR-experiments after treatment with a 90/10 and with a 50/50 H_2/CO mixture. In figure 5.11 we have compared the TPSR results after 60 s treatment with both gas mixtures. We see that the quantity of carbon that hydrogenated at or below 475 K is the same in both

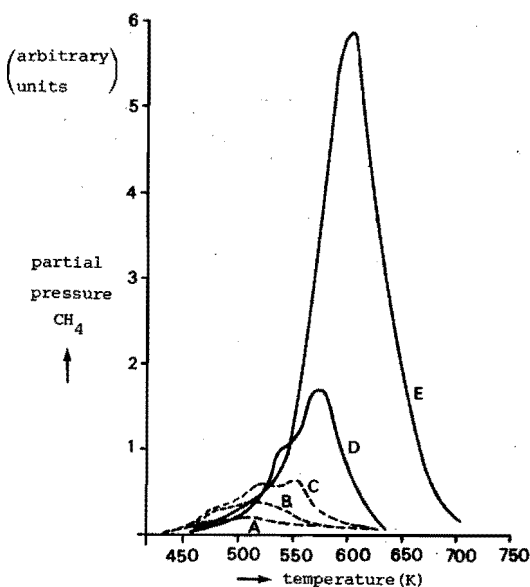


Figure 5.10. Temperature programmed reduction with hydrogen of carbonaceous material deposited after different periods of synthesis at 513 K on an Fe catalyst.

- A) 5 s;
- B) 60 s;
- C) 100 s;
- D) 300 s;
- E) 600 s;

cases. Nevertheless the Fischer-Tropsch activity after 60 s (see figure 5.9) with a 50/50 mixture is almost 15 times lower than with the 90/10 mixture. This difference can not be explained by the difference in hydrogen pressure only. We must also assume that the number of hydrogenation ensembles (as discussed in chapter 4) increases much faster with the 90/10 mixture than with the 50/50 feed.

TPSR experiments were also carried out in the magnetic susceptibility apparatus. When we compared the weight increase during the Fischer-Tropsch reaction with the weight loss during the TPSR run, it appeared that all the deposited material was removed from the catalyst at 750 K.

The magnetic susceptibility apparatus was very well suited for a determination of the nature of the desorbed carbon species, since the magnetic susceptibility could be measured simultaneously with the weight loss and the CH_4 -production.

In figure 5.12 we show the results obtained after the catalyst had been treated for 16 hours at 513 K with a 50/50 H_2/CO mixture. Because the heating rate had to be lower (0.1 K/s) in this apparatus than in the TPSR reactor, a better resolution of the CH_4 -peaks was obtained, although some conversion of carbon to a less active form is possible (see section 5.2.3).

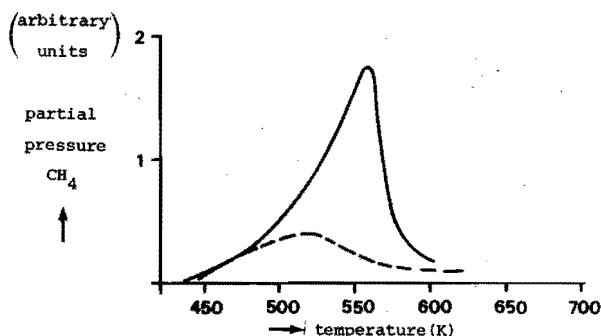


Figure 5.11. Temperature programmed reduction with hydrogen of carbonaceous material deposited during 60 s of Fischer-Tropsch synthesis at 513 K on an Fe catalyst

- A) $x_{\text{H}_2} = 0.90$; $x_{\text{CO}} = 0.10$ (-----)
 B) $x_{\text{H}_2} = 0.50$; $x_{\text{CO}} = 0.50$ (———)

A small amount of reactive carbon species is present at the TPSR temperature of 510 K, probably representing the reactive surface intermediates. When the thermomagnetic analysis in helium (figure 5.2e) of a sample, that was obtained after an almost equal reaction period, was compared with the magnetic susceptibility curve during the TPSR experiment, hardly any difference is found until a temperature of 625 K. This means that the 600 K peak pre-sumable is not related to the bulk structure but represents surface carbon (rather inactive in the Fischer-Tropsch reaction) that can be removed without changing the bulk composition of the material. Above 625 K a tremendous increase of the magnetic susceptibility is observed, that appears simultaneously with the large 670 K peak in the TPSR run. The increase of the magnetic susceptibility is caused by the reaction of the carbides with hydrogen, which results in the formation of hydrocarbons. Almost all the carbides are paramagnetic at 625 K, however iron is then still ferromagnetic compound (Curie temperature of 1041 K).

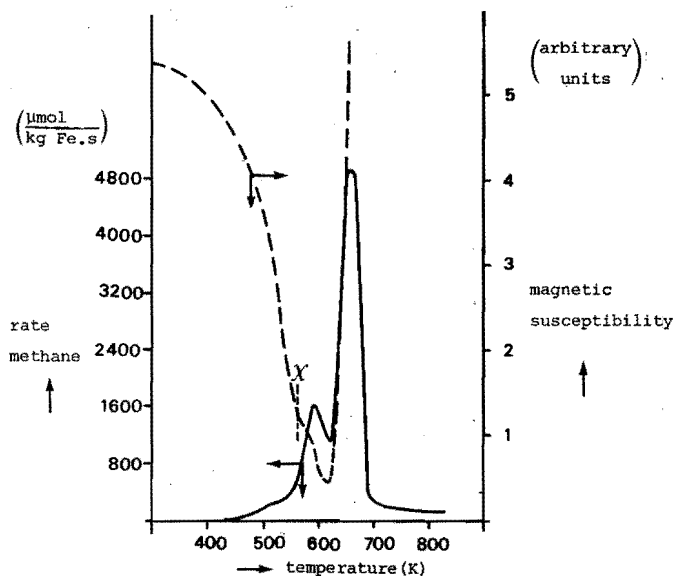


Figure 5.12. The magnetic susceptibility (-----) and the rate of formation of methane (——) during the temperature programmed reduction with hydrogen of carbonaceous material deposited during the synthesis ($x_{\text{H}_2} = 0.50$; $x_{\text{CO}} = 0.50$) at 513 K on an Fe catalyst

5.3.4. Isothermal flushing reactions

From the experiments described above we obtained mainly information about the reactivities of the different carbon species on the catalyst, but little information about the nature of the surface species.

Therefore we performed a number of flushing experiments with helium and hydrogen in the continuous flow fixed-bed reactor filled with about 500 mg of catalyst.

The Fischer-Tropsch reaction rate $r_{F.T.}$ was defined in this case, as the number of μ moles of carbon monoxide converted into C_1 through C_2 hydrocarbons per kilogram of iron and per second.

The Fischer-Tropsch reaction rates are shown in figure 5.13a for the reactions with either a mixture composed of $H_2 : CO : He$ as 20 : 20 : 60 respectively or the mixture with a composition of $H_2 : CO$ as 90 : 10. When the maximum activity is reached after about 6 ks, the synthesis gas is switched to helium for 1.2 ks and subsequently to hydrogen for about 2-3 ks at 510 K.

When the catalyst is flushed with helium after the Fischer-Tropsch reaction, the carbon dioxide rate increased with both gas mixtures (figure 5.13b). The total amount of CO_2 formed was somewhat larger, when a higher H_2/CO ratio was used during the Fischer-Tropsch reaction. As was expected the hydrocarbons and water clearly decreased during the flushing with helium.

The total quantity of carbon hydrogenated during these flushing experiments corresponded to the equivalent of about 40 to 60 monolayers. From the most reactive surface species, which were hydrogenated in the beginning of the hydrogen flushing methane and ethane were formed. Later on only methane was formed from the less active bulk carbon.

The quantity of water produced corresponded to about 0.8 and 0.7 monolayers of oxygen for the 20/20 and the 90/10 H_2/CO mixtures, respectively.

So although the Fischer-Tropsch reaction rate was much lower for the 20 kPa H_2 /20 kPa CO mixture than for the 90 kPa H_2 /10 kPa CO mixture, about equal amounts of CO_2 were produced during the flushing with helium and about the same initial rates of water and hydrocarbons during the following hydrogenation.

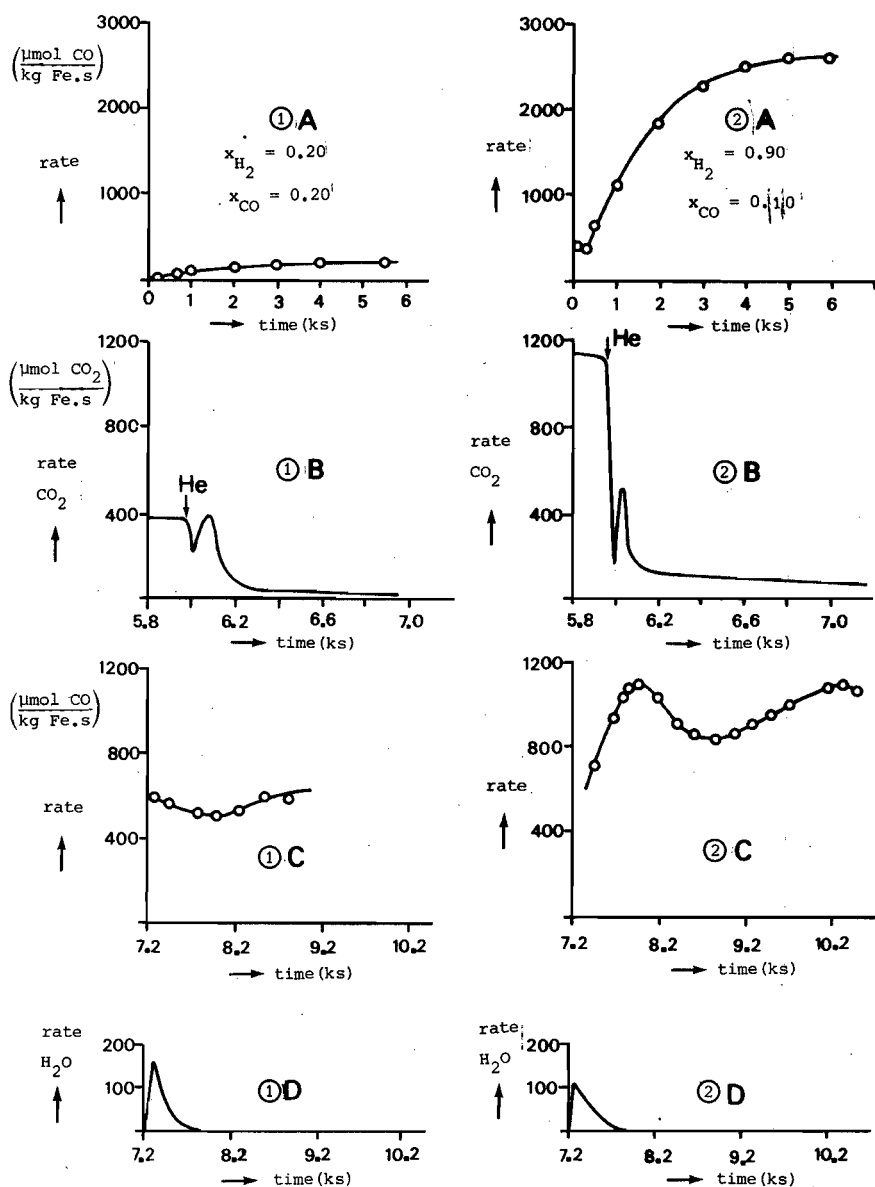


Figure 5.13. A) Reaction rate during the synthesis at 513 K

B) Rate of formation of carbon dioxide at 513 K during a consecutive treatment by helium

C) Rate of formation of methane during hydrogenation of carbonaceous materials at 513 K

D) Rate of formation of water (total pressure of 10^5 Pa)

This again indicates that the Fischer-Tropsch activity is not only caused by the quantity of surface carbon species and the hydrogen partial pressure, but also by the presence of active (hydrogenation) ensembles.

5.4. DISCUSSION

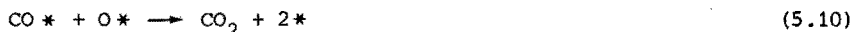
We determined in our experiments with the magnetic susceptibility apparatus the quantities of the various iron carbides and α -Fe and parallel the Fischer-Tropsch reaction rate, all as a function of the progress of reaction with a 50 vol % CO/50 vol % H₂ gas mixture. When these results are compared with the results observed in the continuous flow fixed-bed reactor (chapter 3), the following points can be noticed:

- 1) The activation of the catalyst in the magnetic susceptibility apparatus appears to be slower than in the continuous flow fixed-bed reactor. We think, that this phenomenon is caused by the construction of the sample holder. The greatest part of the gas passes the catalyst basket and the reactants can enter and leave the mass of catalyst particles only by diffusion. In the continuous flow fixed-bed reactor mass transport is much more effective because of the forced convection of the gases through the catalyst bed.
- 2) However, the quantities of the various compounds and the Fischer-Tropsch reaction rate, which are observed in the two systems, are similar. The course of the quantity of ϵ -carbide, as is determined with thermomagnetic analysis, corresponds with the course of the Fe_xC compounds, as determined in chapter 3 with Mössbauer and X-ray diffraction techniques.

Since our sample of pure ϵ -carbide used in the magnetic susceptibility apparatus showed the same Mössbauer spectrum as the Fe_xC compound, we are inclined to believe that the ϵ -carbides prepared by Hofer (17) are when found experimentally often wrongly interpreted: either as a compound with a completely hexagonal structure (17), which is however the ϵ' -Fe_{2.2}C carbide (see chapter 3) or as a carbide with a stoichiometry Fe₂C (11, 15, 18), which we do not think to exist at all.

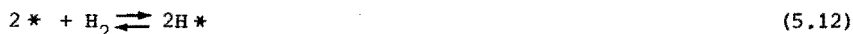
In the TMA experiments we observed no formation of Fe_3O_4 , although a magnetization drop near the Curie temperature of Fe_3O_4 was noticed. This magnetization decrease was only observed, when reduced iron was still present. This can react with the various bulk carbides near the Curie temperature of Fe_3O_4 (838 - 868 K). The stable carbide $\theta\text{-Fe}_3\text{C}$ formed is a paramagnetic compound at these temperatures. It is therefore possible that instead of the Fe_3O_4 formation, used by Anderson et al. (19) and Loktev et al. (15) to explain the results of their TMA experiments, the above mentioned reaction is the cause of their observations.

Since we observe in all thermobalance experiments a period of linear weight increase, we must assume that during that period a steady state exists on the surface. If one looks at the sequence of reactions



\square = bulk vacancy for carbon

to which, if hydrogen is present, the following equations must be added



one might assume that the surface steady state rate (under constant reaction conditions) is governed by the rate of equation (5.10), as long as the rate of equation (5.11) is not limiting. In the case that no hydrogen is present, only small enhancements of the linear weight increases are observed, when the partial pressure of carbon monoxide increases. However, if hydrogen is added to the carbon monoxide feed much larger linear weight increases are observed, as can be concluded from table 5.II.

This small influence of the partial pressure of carbon monoxide is also observed, when the partial pressure of hydrogen is high (57 kPa).

Since the rate of removal of carbon will increase when the partial pressure of hydrogen is increased, the interaction between C* and H* can only result in a lower rate of weight increase. So, the positive effect of hydrogen on the rate of weight increase must be governed by the rate of removal of oxygen by hydrogen (equation (5.13)) and with a small contribution by the rate of removal of oxygen by carbon monoxide (equation (5.10)), which is the only contribution in the absence of hydrogen.

Table 5.II.

feed	addition	weight increase (g/g Fe) after 1 ks
9.5 kPa CO	-	0.0235
9.5 kPa CO	9.5 kPa CO	0.0320
9.5 kPa CO	9.5 kPa H ₂	0.0615

This qualitative model for the linear weight increases is supported by adsorption studies of section 2.5, where it was shown that the adsorption of CO is inhibited on oxidized Fe-surfaces.

When the weight is increased to a level of about 0.026 g/g Fe the rate of weight increase diminishes. This can be explained by assuming that the surface carburization rate is then not determined anymore by the rates of equation (5.10) and (5.13) (i.e. by the removal of surface oxygen), but becomes limited by the rate of carbon diffusion in the bulk (equation (5.11)) i.e. by the removal of surface carbon.

When the weight increase is expressed as:

$$r_C = \frac{dw}{dt} = k \cdot f(p_{H_2}, p_{CO}) \cdot \left(1 - \frac{W}{W_{\max}}\right) \quad (5.15)$$

the plot of $\ln(1 - W/W_{\max})$ vs. time for constant hydrogen and carbon monoxide pressures indicates, that this equation derived on basis of a 'diffusion' model, predicts the observed weight increase accurately after the linear weight increase of about 0.026 g/g Fe, as is shown in figure 5.8.

Unmuth (8) has also observed, albeit qualitatively, a positive order effect of hydrogen on the carburization reaction on supported iron catalysts.

However for nickel and cobalt catalysts the addition of hydrogen to the carbon monoxide feed results in a strongly decreased carburization rate, as was observed for nickel by Goodman (20) and for cobalt by Rautavuoma (10). This different (from Fe) behaviour of nickel and cobalt is probably caused by the good hydrogenation properties of these materials and by their lower tendency to form carbides, as compared with iron.

In chapter 3 we discussed the low initial activity of an iron catalyst during the Fischer-Tropsch reaction on basis of the evidence available at the time, that chapter 3 was published. We mentioned there Raupp and Delgass (18) who suggested, that the Fischer-Tropsch reaction rate is linearly proportional to the carburization rate. However, our present results do not support their model: when the partial pressure of hydrogen was increased at a constant partial pressure of carbon monoxide, the increase of the initial carburization rate was certainly not as high as the increase of the Fischer-Tropsch reaction rate. The increase of the Fischer-Tropsch reaction rate showed a first order behaviour in hydrogen (21), whereas the influence of H_2 on the carburization is less pronounced.

The second model suggested in chapter 3 was as follows. The Fischer-Tropsch activity is related to the difference between the limited CO dissociation rate and the rate of diffusion of carbon in the bulk. The low initial Fischer-Tropsch rate is thus explained by the high initial rate of carbon diffusion into the lattice. However, this model becomes improbable on basis of the evidence discussed in the previous sections of this chapter 5. With the experimental results presented in this chapter we are inclined to abandon this competitive diffusion model as a possible explanation for the low initial activity, because:

- 1) from section 5.3.2 and figure 5.7 we see, that the carbon deposition rate $r_{C, ads}$ and the Fischer-Tropsch reaction rate $r_{F.T.}$ increase both during the 'activation' period.

This shows that the CO dissociation rate is not a limiting factor for the sum of the Fischer-Tropsch rate and the rate of carbon diffusion into the bulk, but that the latter two processes are more or less autonomous.

- 2) The TPSR-experiments indicate (figure 5.11), that on the initially inactive iron catalyst at the beginning of the synthesis with the 50/50 H_2/CO mixture about the same quantity of very reactive C-species are formed as with the 90/10 H_2/CO mixture. This shows that the Fischer-Tropsch rate is not only governed by the quantity of active surface species, as assumed in the second model, but that also the appropriate active centers, on which this active carbon can be converted into hydrocarbons, have to be formed.

Consequently we suggest, that the activation of an iron Fischer-Tropsch catalyst is caused by the formation of active Fischer-Tropsch surface ensembles, whereas the formation of bulk carbides is a more or less unrelated parallel process.

The higher activity at the beginning of the experiments, most noticeable in the 90/10 H_2/CO experiment requires separate discussion. We think that the higher activity and its decline can be explained by the hydrogen coverage of the catalyst. As figure 5.11 shows the initial activity for both H_2/CO ratios is coupled to almost the same quantity of reactive carbon surface species with a TPSR maximum of 475 K. In the beginning of both experiments the catalyst is fully covered by hydrogen from the preceding reduction, and thus can react at a high rate with the first carbon atoms formed on the surface. This activity generally decreases very fast because hydrogen is quickly replaced by CO and products formed from it.

However this replacement process is retarded when a high H_2/CO ratio is used. As a result we see in figure 5.11 a much higher carbon content after 60 s in the 50/50 H_2/CO experiment than in the 90/10 H_2/CO experiment. We think that this initial hydrogen effect is a transient phenomenon, superimposed on the normal activation. The latter starts from an almost zero activity at the beginning of the experiments and develops slowly in a period of around 5 ks to its maximum. As carbon monoxide and carbon hinder the adsorption of hydrogen, and a high surface coverage by carbonaceous material is reached in a short period (less than 0.5 ks for a 90/10 H_2/CO ratio and less than 0.1 ks for a 50/50 H_2/CO ratio; figure 5.9), the increased Fischer-Tropsch activity after that period can not be explained by an increase of surface carbon, nor by an increase of hydrogen adsorbed on normal iron sites. This means that either the adsorption of hydrogen is enhanced

by changing the nature of the iron surface or that the reactivity of the sites on which the rate determining hydrogenation step of the Fischer-Tropsch reaction takes place is increased. In both cases a change in the nature or number of the surface ensembles operative in the activation of reaction steps connected with hydrogen is necessary.

In short the activation of iron Fischer-Tropsch catalysts can be described as an increase in the number or the activity of the hydrogenation ensembles. It is very well possible that oxygen plays a role in this activation. Figure 5.7 indicates that sizeable quantities of oxygen are adsorbed on the catalyst. In the next chapter we will show further evidence that adsorbed oxygen can improve the Fischer-Tropsch activity on iron.

5.5. REFERENCES

1. H. Pichler, H. Merkel, U.S. Bureau of Mines Techn. Paper, 718 (1949)
2. J.C. Hoogendoorn, Symposium on clean fuels from coal, Chicago Meeting (1973)
3. H. Kölbels, K.D. Tillmetz, Deutsches Offenlegungsschrift 2 507 647 (1976)
4. J. Askill, Traces diffusion data for metals, alloys and simple oxides, Plenum, New York, N.Y. (1970)
5. P. Wentrcek, B.J. Wood, H. Wise, J. Catal. 43, 363 (1976)
6. S. van Ho, P. Harriott, J. Catal. 64, 272 (1980)
7. C.H. Bartholomew, D.C. Gardner, J. Catal. in press
8. E.E. Unmuth, thesis Northwestern University Illinois (1979)
9. P. Biloen, J.M. Helle, W.M.H. Sachtler, J. Catal. 58, 95 (1979)
10. A.O.I. Rautavuoma, thesis University of Technology Eindhoven (1978)
11. K.M. Sancier, W.E. Isakson, H. Wise, Symp. on Advances in Fischer-Tropsch Chemistry, Anaheim Meeting, March (1978)
12. J. Mc Carty, P. Wentrcek, H. Wise, J. Catal. 57, 406 (1979)
13. R.T. Lewis, Rev. Sci. Instrum. 42, 31 (1971)
14. R.T. Lewis, J. Vac. Sci. Technol. 11, 404 (1974)
15. S.M. Loktev, L.I. Makarenkova, E.V. Slivinskii, S.D. Entin, Kinet. Katal. 13, 1042 (1972)

16. P.W. Selwood, Adsorption and collective paramagnetism, Chapter 3, 35-50, Academic, New York (1962)
17. L.J.E. Hofer, E.M. Cohn, W.C. Peebles, J. Am. Chem. Soc. 71, 189 (1949)
18. G.B. Raupp, W.N. Delgass, J. Catal. 58, 361 (1979)
19. R.B. Anderson, L.J.E. Hofer, E.M. Cohn, B.J. Seligman, J. Am. Chem. Soc. 73, 944 (1951)
20. D.W. Goodman, R.D. Kelley, T.E. Madey, T. White, J. Catal 64 (2), 479 (1980)
21. L. Steffanie, M.Sc. report University of Technology Eindhoven (1980)

CHAPTER 6

A STUDY ON THE FISCHER-TROPSCH SYNTHESIS AT LOW PRESSURES

6.1. INTRODUCTION

During the activation of an iron catalyst under atmospheric pressure conditions a considerable absorption of carbon and oxygen by iron occurs. This process is rather fast and in order to study it in more detail, we have followed the activation of the Fischer-Tropsch catalyst at low pressures. In this way we hoped to obtain more insight in possible relations between the activation, bulk diffusion of carbon and the formation of C* and O* surface species.

For this study a high vacuum system was built, with the reactor coupled to a quadrupole mass spectrometer where quantitative data could be obtained at low reactant pressures. Tillmetz (1) already gave a certain quantitative description of the reaction at very low pressures (10^{-2} - 10^{-5} Pa) on fully carbided iron catalysts. On rhodium polycrystalline foils Somorjai (2) was not able to produce meaningful data at such low pressures, because the amounts of higher hydrocarbons produced were too small for a reliable detection by a quadrupole analyzer. At extremely low pressures also our experiments with reduced iron catalysts were unsuccessful. Therefore our experiments were carried out at pressures between 10 and 10^4 Pa.

A second reason for building a low pressure reaction system was, that in this way we could possibly reduce the rates so much, that the low turnover numbers for chain growth, as observed by Dautzenberg et al. (3) for ruthenium, could also be observed on iron. In the meantime, however Kieffer (4) has already shown that on iron the chain growth is a fast reaction.

6.2. EXPERIMENTAL

6.2.1. High vacuum apparatus

A general scheme of the HV-apparatus is shown in figure 6.1. The system consists of:

- a) 'feed' section
- b) reactor section
- c) quadrupole section.

The reaction mixture is prepared in the 'feed' section. The reactor operates as a flow fixed-bed reactor at 25 Pa and as a batch reactor at 9 kPa. The gas is evacuated by a pumping system, consisting of a turbomolecular pump (Leybold-Heraeus, Turbovac 220, pump capacity 220 l/s) and a two-stage oil rotary vane pump (Leybold Heraeus, Trivac D16 A). The turbomolecular pump produced a hydrocarbon free background.

The complete HV-apparatus was made of stainless steel (AISI 316/321) Leybold-Heraeus equipment parts and the connections were sealed by copper gaskets. All the equipment in the system could be baked out at 573 K with Pilz heating tape. In a well baked out system the lowest attainable pressure in the reactor was about 10^{-5} Pa. During Fischer-Tropsch synthesis the whole system is kept at 420 K, except the reactor which is kept at 523 K.

Feed section

Gas mixtures of H_2 , CO and Ne are prepared by separate regulation of each gas stream with mass flow controllers (Brooks 5841-1). The mixture of the three compounds flows for about 30 min through the feed vessel to a vent. Any desired pressure in this feed volume can be obtained by the use of the oil rotary vane pump ORP.

The absolute pressure in the feed volume is determined by a membrane

differential pressure gauge PD 1.0 (Hottinger Baldwin Messtechnik, measuring range 10^2 to 10^5 Pa), with its reference chamber connected to the vacuum of the oil rotary vane pump. When the reactor was used as a continuous flow fixed-bed reactor, the gas feed rate (in mol/sec) in the reactor is calculated from the rate of pressure decrease in the known feed volume. The pressure decrease is followed by the PD 0.01 differential pressure gauge (measuring range 1 to 10^3 Pa), with its reference chamber filled with the initial pressure of the feed volume.

The gases hydrogen (Matheson, U.H.P. > 99.999%), carbon monoxide (Matheson, purity > 99.997%) and neon (Hoekloos purity, > 99.9%) were of such a high purity, so that no further purification was applied.

Reactor section

When the reactor operates as a fixed-bed flow reactor at 25 Pa the gas flows from the feed section to the reactor section via a variable (Leybold-Heraeus) leak valve A, which controls a constant leak rate (in mol/s) into the reactor, as long as the pressure in the feed section does not change too much. The pressure in the reactor is controlled by a second variable leak valve B, that connects the reactor to the quadrupole section.

At the higher pressure of 9 kPa the pumping system, operating at 10^{-4} Pa was unable to maintain an acceptable flow rate through the reactor. We therefore decided to operate the reactor at this pressure as a batch reactor. When the reactor operates in this way, the pressure of 9 kPa is established by bringing the feed section to the appropriate pressure and then opening valve A. The total reactor volume was 1.8 dm^3 . Via the variable leak valve B (see figure 6.1) a small gas stream flows to the quadrupole.

The reactor is made of quartz glass and has an inside diameter of 10 mm. The reactor is heated by a furnace, and the temperature is measured with a chromel-alumel thermocouple and controlled by an Eurotherm thyristor. The bypass line around valve B is used for fast evacuation of the reactor section e.f. after reduction or after the Fischer-Tropsch synthesis or during baking out of the apparatus.

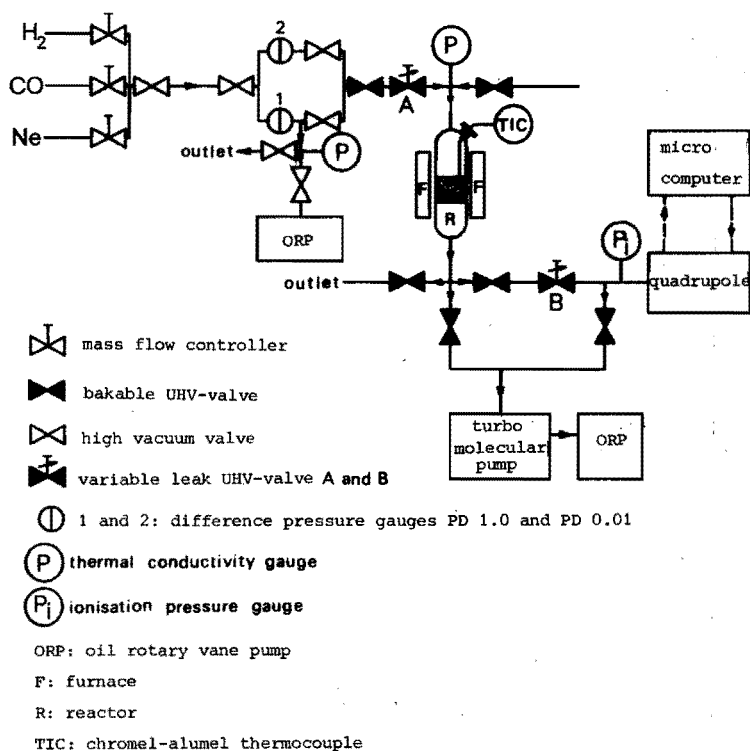


Figure 6.1. A scheme of the high vacuum apparatus

The pressure in the reactor is measured with a thermal conductivity vacuum gauge (Leybold-Heraeus, Thermotron 11/12, range 1 to 10^4 Pa).

Quadrupole section

A simple quadrupole mass spectrometer (Leybold-Heraeus, Quadruvac Q 200, mass range 0-200 a.m.u.) was chosen as analyzer, because a complete scan over 100 a.m.u. could be done with it within 100 s, while the sensitivity was high ($\sim 10^{-11}$ Pa).

As the output of the mass spectrometer is very complex, computerized data extracting, handling and storing is essential to obtain maximal benefit from this analytical tool. We adapted a 6502-microcomputer to control the scan over a selected mass range of the quadrupole and to choose for each mass signal the appropriate amplifier range, providing a total dynamic range of 10^5 over the complete mass spectrum. Another advantage of the use of the microcomputer is the improved reproducibility, as the intensity at each mass was measured 16 times and the mean value was printed in the output.

However, mainly due to the electronics of the mass spectrometer this averaging operation resulted in a reduced scan rate of 600 s/100 a.m.u.

At high sensitivities the leading edge of a strong peak extended into the region of the preceding small peak. A mathematical procedure was applied then to obtain an estimate of the small peak.

6.2.2. Evaluation of mass spectra

The quadrupole mass spectrometer is calibrated by admitting mixtures of known compositions into the quadrupole section. The intensities (relative to neon) for the main peak of each component are presented in table 6.I.

Table 6.I. Sensitivities of a quadrupole equipped with a multiplier for the main peak of various compounds with respect to neon.

component	sensitivity	component	sensitivity
xylene	3.5*	propene	2.9
toluene	3.5*	ethane	3.4
benzene	3.5*	ethene	3.4
heptane	3.4*	methane	3.6
heptene-1	3.4*	argon	3.7
hexane	3.3*	water	3.3*
hexene-1	3.3*	neon	1.0
pentane	3.3*	carbon dioxide	2.6
pentene-1	3.3*	carbon monoxide	4.2
butane	3.2	nitrogen	3.3
butene-1	3.2	hydrogen	5.0
propane	2.9		

*estimated values

Analysis of a mass spectrum is usually based on the selection of a characteristic peak for each component expected in the sample.

It is then customary to start from one side of the spectrum, subtracting for each component its characteristic peak and proportional parts of the other peaks of that component from the mass spectrum. In this way inaccuracies are apt to add up on the other side of the spectrum. Furthermore, if the sample contains components with the

same characteristic peak, the results may be in considerable error. A computer program that gives quantitative data for the composition of the sample has been developed by Henriquez (5). This program is based on a modification of a stepwise regression program (6). Linear regression analysis is concerned with finding an approximate linear relation between a variable (y_1, \dots, y_n) and the quantities of one or more components ($1, \dots, p$). The regression function has the following form:

$$\begin{bmatrix} \bar{y} \\ \hat{y} \\ \vdots \\ \hat{y}_n \end{bmatrix} = b_0 + b_1 \begin{bmatrix} x_1 \\ x_2 \\ \vdots \\ x_n \end{bmatrix} + b_2 \begin{bmatrix} x_1 \\ x_2 \\ \vdots \\ x_n \end{bmatrix} + \dots + b_p \begin{bmatrix} x_1 \\ x_2 \\ \vdots \\ x_n \end{bmatrix}$$

com-
pound
1
com-
pound
2
com-
pound
p

The regression procedure in our case is a mathematical method of choosing from a library of reference spectra (compounds $1, \dots, q$) a group of spectra p each with its own fragmentation spectrum (x_1, \dots, x_n), the sum of which, after each is multiplied by its concentration coefficient (b_0, \dots, b_p), will give the best fit to the measured spectrum (y_1, \dots, y_n), i.e. the sum of the squares of the residuals

$$\sum_{i=1}^{i=n} (y_i - \hat{y}_i)^2 \quad (6.1)$$

must be minimal.

The regression program operates in such a way, that at each step one spectrum is added to or rejected from the set of p spectra, at that moment in the program. That change is chosen each time, that gives the greatest reduction in the value of the sum of squares residuals. We have tested this stepwise regression procedure by evaluating a mass spectrum from the study of Tillmetz (1). For the evaluation of his spectra Tillmetz uses for each component only the intensity of one atomic mass peak. As our program did not choose acrolein and acetaldehyde (see table 6.II) we must conclude, that there is no statistical indication that these compounds were present in Tillmetz's mixture.

Table 6.II. Difference between evaluated mass spectrum of Tillmetz (1) by characteristic intensities and by stepwise regression procedure.

components	concentration coefficients in arbitrary units	
	characteristic intensity	stepwise regression
benzene	2	0
acrolein	10	0
acetaldehyde	14	0
carbon dioxide	205	195
argon	448	440
propene	42	39
ethene	172	170
carbon monoxide	43400	39900
water	23	25
neon	2310	2240
methane	363	290

During our experiments we applied the wide dynamic range to determine all the products up to the C₈-hydrocarbon fraction. Since oxygen containing hydrocarbons were not chosen from the library by the stepwise regression procedure, these compounds were also in our experiments not present in statistically significant quantities.

6.2.3. Outline of the experimental methods

An iron manganese oxide catalyst with an iron to manganese atomic ratio of 4 : 1 was used in all the experiments.

The preparation of this catalyst has been described in section 4.2.1. About 1 gram of catalyst with a sieve fraction of 0.2 - 0.6 mm was used in all experiments.

Standard reduction of the catalyst was carried out at 623 K in flowing hydrogen (100 cm³/min) for 20 hours. Thereafter the reactor was quickly evacuated via the bypass line and cooled down to the reaction temperature of 523 K. The evacuation was continued for about 4 hours until a pressure of about 10⁻⁴ Pa was obtained in the reactor. In the meantime the Fischer-Tropsch mixture of hydrogen, carbon monoxide and neon was prepared at the required pressure in the feed section.

For the experiments at very low pressures (25 Pa) the reactor system operates as a continuous flow fixed-bed reactor. The gas mixture is admitted in the reactor by the variable leak valve A, and the feed rate (in mol/sec) into the reactor is calculated from the pressure decrease in the feed section. The ratio of the concentrations of the various components to neon, determined with the quadrupole, was used to calculate the mole fractions at the outlet of the reactor. The reaction rate was calculated by multiplying these mole fractions by the gas feed rate.

At the higher pressure (9 kPa) the reactor system operates as a batch reactor. The gas mixture in the feed volume was completely expanded to the reactor. From the reactor a small gas flow was admitted via the variable leak valve B to the quadrupole section (pressures between 10^{-3} and 10^{-4} Pa) and the turbomolecular pump. The absolute quantities (in μmol) of the various components in the reactor were calculated by multiplying the ratio of the concentration of the various components to neon by the known initial concentration of neon.

In this mode of operation concentration gradients over the complete reactor system cannot be ruled out completely. However from the fast stepwise increase of some concentrations at the beginning of an experiment we conclude that these concentration gradients are marginal.

6.3. RESULTS

6.3.1. CO hydrogenation over clean reduced iron catalysts at very low pressures in a continuous flow fixed-bed reactor

The Fischer-Tropsch reaction was investigated at 523 K and at a reactant pressure of 24 Pa with a mixture of H_2 , CO and Ne with a volumetric ratio of 60 : 15 : 25, respectively. The pressure in the reactor and the feed flow rate were controlled by adjusting the leak valves A and B. During the initial synthesis period of about 30 ks the carbon monoxide was mainly converted into benzene and toluene, while the rate of formation of methane was much lower. It increased slowly (see figure 6.2) with time.

Besides this initial formation of aromatic compounds the olefins propene and butene were also formed. Formation of ethene could not be determined accurately, because the main peak coincided with that of carbon monox-

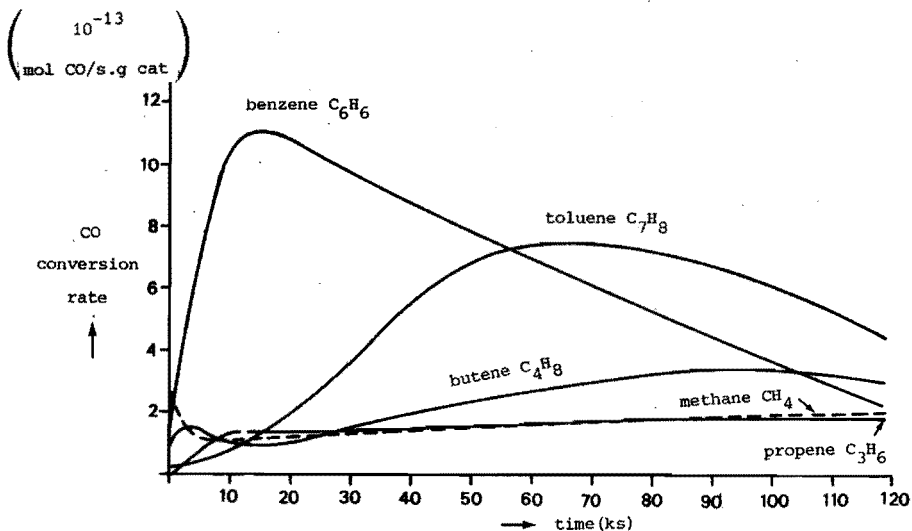


Figure 6.2. Conversion rate of CO into various hydrocarbons during Fischer-Tropsch synthesis in a continuous flow fixed bed reactor.

Synthesis: $T = 523 \text{ K}$; $P_{H_2} = 10.0 \text{ Pa}$; $P_{CO} = 2.5 \text{ Pa}$.

ide. Production of benzene and toluene was much higher than derived from a Schulz-Flory relation between the C_1 , C_3 and C_4 hydrocarbon formation rates. Since all products and carbon monoxide were analyzed during the course of the synthesis, a mass balance for carbon and for oxygen could be obtained.

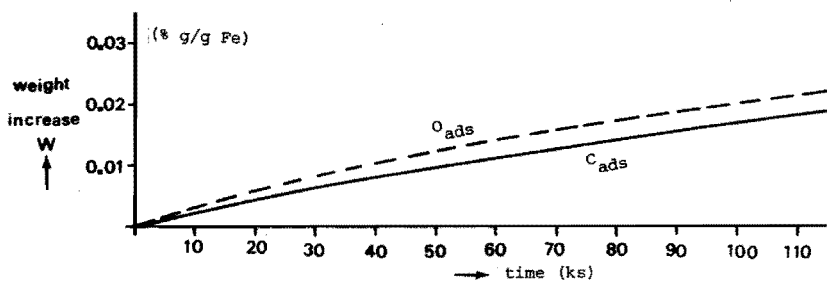


Figure 6.3. Weight increase by carbon and oxygen during Fischer-Tropsch synthesis in a continuous flow fixed bed reactor.

Synthesis: $T = 523 \text{ K}$; $P_{H_2} = 10.0 \text{ Pa}$; $P_{CO} = 2.5 \text{ Pa}$.

As figure 6.3 indicates, the catalyst absorbed only small quantities of carbon and oxygen. If the quantity of CO adsorbed at room temperature ($\sim 0.1\%$ g/g Fe) is indicative of one monolayer, we find the equivalent of about 1/5 monolayer of carbon and of oxygen adsorbed or absorbed at the end of the experiment. It is remarkable that although the surface coverage was small, the catalyst converted more carbon monoxide into higher hydrocarbons than e.g. into methane, except at the very beginning, when, presumably with the aid of the hydrogen left on the catalyst after reduction, the methane production is the highest. We are of the opinion that since for the formation of olefins and especially of aromatics less hydrogen is needed than for the formation of methane, the high fraction of olefins and aromatics in the output can be explained partly by an initial lack of sufficient hydrogenation ensembles.

This however cannot be the complete story. Because the aromatics formation is not at all in agreement with the Schulz-Flory distribution we do not think that these products are formed according to the customary chain growth model, but that they are formed from six membered carbon rings laid down on the surface. In this connection it is worthy of mention that the carbon atoms of a benzene ring fit exactly on a layer of close packed iron atoms, when the carbon atoms are located in the valleys between two adjacent iron atoms, as is shown in figure 6.4.

At the maximum of the benzene formation rate there is only a small fraction (5% or less) of the surface covered by carbon. A random distribution of the carbon would contain only a very small fraction of C_6 rings. The relatively very high rate of benzene formation thus suggests that a selective adsorption process is operative in which adsorption next to occupied sites is favoured.

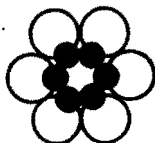


Figure 6.4. Formation of a six membered carbon ring (●) on a layer of close packed iron atoms (O).

It is often noted during the Fischer-Tropsch synthesis, in particular when the Schulz-Flory constant is .5 or lower, that the production of the higher fractions tends to be above the Schulz-Flory line (7). This is also the case in the experiments to which figure 6.8 refers. Possibly a part of these products is formed by hydrogenation of preformed carbon chains.

As the amount of carbonaceous deposits approaches a weight increment of about 0.02% g C/g Fe, the rates of formation of 'normal' Fischer-Tropsch products like methane, propene and butene, increase, while the rate of formation of benzene and toluene, decrease.

As for the increased normal Fischer-Tropsch products more hydrogen is needed than for the aromatics we conclude again, that in the course of the experiment more hydrogenation ensembles became available on the catalyst surface. This is in agreement with the results for atmospheric pressure conditions discussed in chapter 5.

6.3.2. CO hydrogenation over clean reduced iron catalysts at low pressures in a batch reactor

The Fischer-Tropsch reaction was also investigated at 523 K and at a pressure of 9.2 kPa. As discussed in section 6.2 the reactor operated in this case as a batch reactor. We used the same 60 : 15 : 25 gas composition of H_2 , CO and Ne as in the previous experiment.

The composition of the content of the reactor was determined by leaking a small gas stream to the quadrupole.

Methane and to a much smaller extent hydrocarbons up to C_4 were formed immediately after the introduction of the synthesis mixture (see figure 6.5), possibly again with the hydrogen left on the catalyst after reduction. During the subsequent period of about 15 ks no further product was formed, although much carbon and oxygen were deposited during this period on the catalyst as followed from the mass balances (see figure 6.6). This deposition continued until about 1.0% by weight C/Fe and 0.8% by weight O/Fe was deposited on the catalyst. This quantity corresponds to about 10 monolayers of carbon and about 6 monolayers of oxygen, but we assume that most of the deposited material is transferred to the bulk of the catalyst.

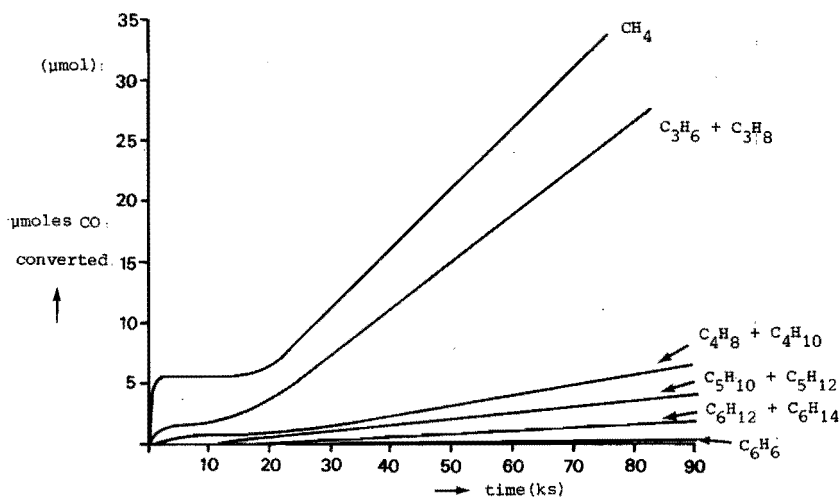


Figure 6.5. Formation of various hydrocarbons during Fischer-Tropsch synthesis in a batch reactor.

Synthesis: $T = 523 \text{ K}$; $P_{\text{H}_2} = 5.5 \text{ kPa}$; $P_{\text{CO}} = 1.4 \text{ kPa}$.

Although the CO concentration in the reactor decreased considerably (figure 6.7), the rates of formation of hydrocarbons remained reasonably constant as follows from the straight lines in figure 6.5. This can be ascribed to the zero order of the reaction rate in carbon monoxide. We found this zero order also at atmospheric conditions.

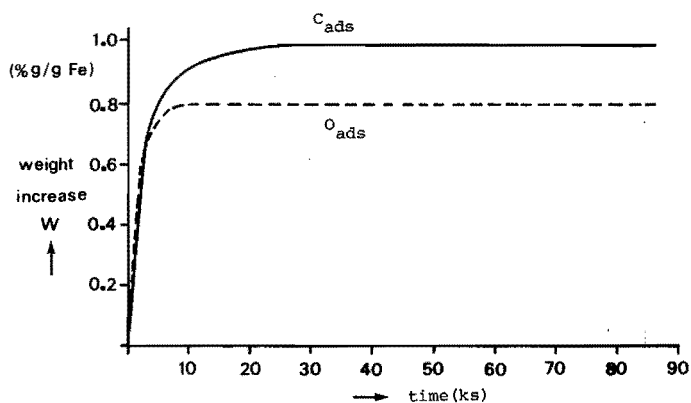


Figure 6.6. Weight increase by carbon and oxygen during Fischer-Tropsch synthesis in a batch reactor.

Synthesis: $T = 523 \text{ K}$; $P_{\text{H}_2} = 5.5 \text{ kPa}$; $P_{\text{CO}} = 1.4 \text{ kPa}$.

From a hydrogen mass balance we can conclude that the hydrogen concentration decreased only marginally during the experiment. Consequently the hydrogen to carbon monoxide ratio increased drastically to an estimated value of about 15 after 15 ks.

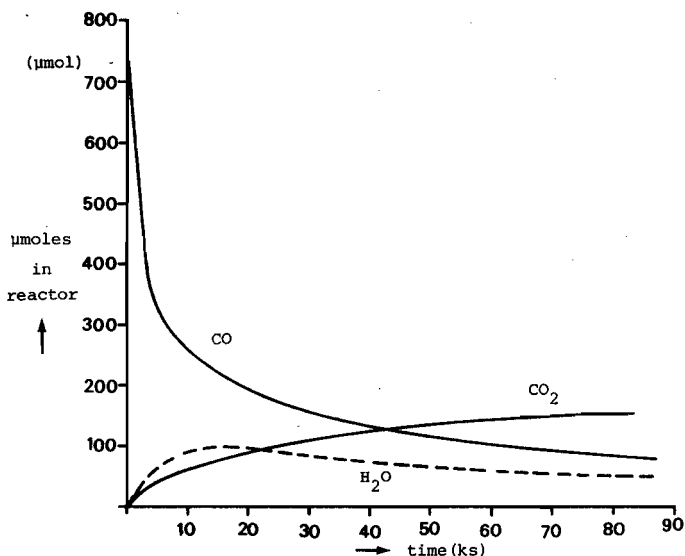


Figure 6.7. Concentration of the products H_2O and CO_2 and the reactant carbon monoxide during Fischer-Tropsch synthesis in a batch reactor.

Synthesis: $T = 523 \text{ K}$; $P_{\text{H}_2} = 5.5 \text{ kPa}$; $P_{\text{CO}} = 1.4 \text{ kPa}$.

Two reasons may be offered as explanation of the almost negligible rate of benzene formation. One is, that so much carbon is present on the surface, that almost no isolated 6 membered rings are present, i.e. no benzene precursors are formed and the other is that the higher (hydrogen) pressure enhanced the formation of paraffins and olefins at the cost of the formation of aromatics. For instance the rate of methane formation increased from $2 \cdot 10^{-13} \text{ mol/g cat.s}$ at a total pressure of 25 Pa to $4 \cdot 10^{-10} \text{ mol/g cat.s}$ at a local pressure of 9.2 kPa. During the 'induction' period of about 15 ks predominantly olefinic C_3 and C_4 hydrocarbons were observed, but the paraffin/olefin ratio increased during the consecutive activation period, as was also found in chapter 4 at atmospheric pressure. At the higher pressure of 9.2 kPa, the 'normal' Fischer-Tropsch reaction pattern was obtained as

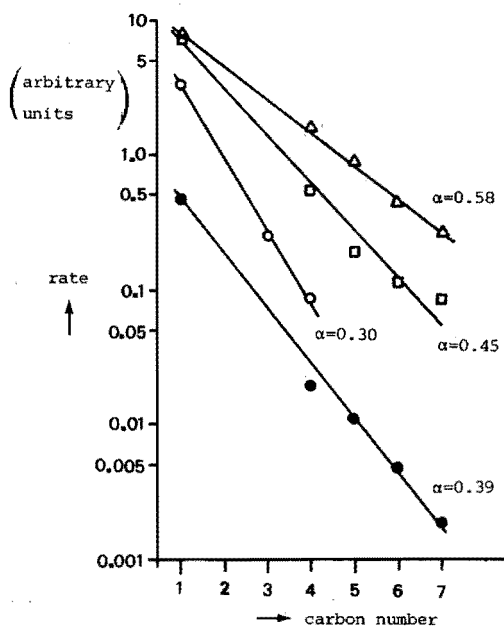


Figure 6.8. Schulz-Flory plot of the hydrocarbon product distribution

after Fischer-Tropsch synthesis in a batch reactor.

Synthesis: $T = 523 \text{ K}$; $P_{\text{H}_2} = 5.5 \text{ kPa}$; $P_{\text{CO}} = 1.4 \text{ kPa}$.

● on a reduced catalyst

▲ on an oxygen pretreated catalyst

(40 $\mu\text{mol O}_2$ for 28 min)

□ on an oxygen pretreated catalyst

(78 $\mu\text{mol O}_2$ for 195 min)

● on a reduced catalyst at 35 ks synthesis

} at 1 ks synthesis

can be concluded from the fact that the product distribution after 35 ks of Fischer-Tropsch synthesis obeys almost exactly the Schulz-Flory distribution, as is shown in figure 6.8, from which we also derive a Schulz-Flory constant $\alpha = 0.39$.

Initially more oxygen was removed in the form of water than as carbon dioxide. After about 15 ks the concentration of water in the reactor started to fall, while carbon dioxide concentration continued to increase. From the oxygen mass balance we conclude, that after 10 ks no oxygen was consumed anymore by the catalyst, so that the observed decrease of the water content had to be coupled to the increase of the carbon dioxide concentration. Possibly the very long reaction time allowed equilibration of the water-gas shift reaction and this equilibrium lies under our conditions on the CO_2 side (8).

6.3.3. CO hydrogenation over preoxidized iron catalysts at low pressures in a batch reactor

When the Fischer-Tropsch synthesis was performed at atmospheric pressure conditions (see chapter 5) or at lower pressures (see section 6.3.2), we observed during the activation of the catalyst not only the deposition of carbon but also a considerable absorption of oxygen. In this respect it must be mentioned that in the Mössbauer spectroscopic and the thermomagnetic experiments some effects were found, that could be ascribed to oxygen in the catalyst. However only the mass balances gave a clear indication of oxygen absorption. To investigate the influence of oxygen on the Fischer-Tropsch reaction, a series of experiments was performed on preoxidized iron catalysts.

The oxidation was carried out at room temperature by expanding a diluted 1.8% O_2 /Ne mixture from the 'feed' volume into the closed reactor.

Two different gas mixtures, which contained 40 and 78 μmol of oxygen, $^{16}O_2$ and $^{18}O_2$ respectively, were contacted with 1 gram of reduced iron manganese oxide catalyst at 6.5 kPa for a period of 28 and 195 min, respectively. At the end of the pretreatment the gases in the reactor were quickly evacuated via the bypass line. Thereafter the reactor was heated to the reaction temperature of 523 K in 0.5 hour. During the evacuation little or no oxygen was found in the stream pumped off.

The Fischer-Tropsch synthesis was carried out again at 9.2 kPa and 523 K in the batch reactor system with a 60 : 15 : 25 gas mixture of H_2 , CO and Ne.

In experiments in which an unreduced Fe_2O_3/Mn_2O_3 precipitated catalyst was directly exposed to the same gas mixture at 9.2 kPa and at 523 K, no hydrocarbon formation and only a slow reduction were observed.

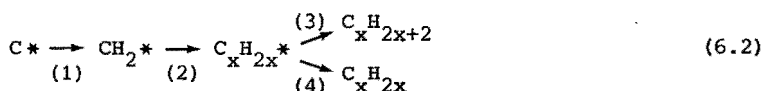
The reduced but preoxidized catalysts however produced immediately methane, the production of which increased during the consecutive reaction period. No induction period occurred as observed with the untreated reduced iron catalyst.

In figure 6.8 the product distribution on the preoxidized iron catalysts are shown after a reaction period of 1 ks. We see that the activity levels of the two preoxidized catalysts were higher than

of the untreated one, but that the influence of the smaller quantity of oxygen was more pronounced than of the higher quantity. This means that two opposing effects are operating: an activating one at low oxygen content and a deactivating one at higher oxygen content. The inactivity of an unreduced iron catalyst must be mentioned in this connection.

Another interesting observation follows from the comparison of figures 6.9 and 6.10. Figure 6.9 shows the normal behaviour of an untreated reduced iron catalyst viz. slow activation and an increase in both olefinic and paraffinic products. The rate of increase is greater for the paraffin than for the olefin.

In figure 6.10 we see that olefins are only formed at the very beginning of the experiment, and that they are formed at a rather high rate. This means that in the sequence:



all steps except step (3) proceed in the beginning stage of the synthesis at a high rate. But as follows from figure 6.8 the methane rate is not depressed at all. This suggests that the two steps:

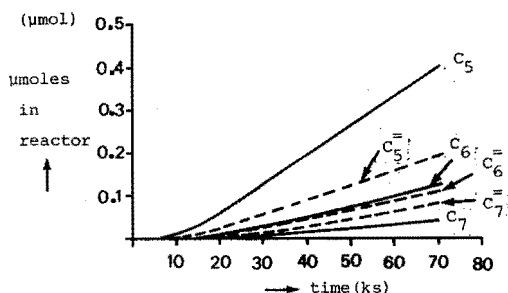
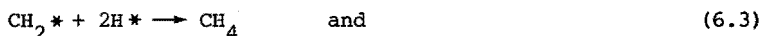


Figure 6.9. $\text{C}_5 - \text{C}_7$ olefin (C_n^-) and paraffin (C_n) concentrations during Fischer-Tropsch synthesis on a reduced iron catalyst in a batch reactor.

Synthesis: $T = 523 \text{ K}$; $P_{\text{H}_2} = 5.5 \text{ kPa}$; $P_{\text{CO}} = 1.4 \text{ kPa}$

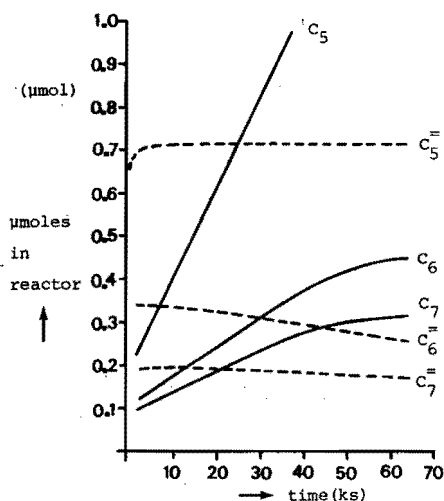


Figure 6.10. $C_5 - C_7$ olefin ($C_n^=$) and paraffin (C_n) concentrations during Fischer-Tropsch synthesis in a batch reactor on a reduced iron catalyst after a pretreatment with 40 $\mu\text{mol O}_2$ for 28 min.

Synthesis: $T = 523 \text{ K}$; $P_{H_2} = 5.5 \text{ kPa}$; $P_{CO} = 1.4 \text{ kPa}$.

are different in nature: the rate of equation (6.3) has a normal rate on a lightly oxidized catalyst whereas the rate of equation (6.4) is very much inhibited. The slight decrease in the concentrations of hexene and heptene, shown in figure 6.10, indicate the possibility of readsorption of these olefins followed by hydrogenation.

When a reduced iron catalyst is pretreated with a O_2/Ne mixture containing 78 μmol of isotopic labeled oxygen $^{18}O_2$ (Rohstoff GMBH, purity $\sim 99.8\%$) for 195 min at 6.5 kPa, about 25 $\mu\text{mol } ^{18}O$ (12.5 $\mu\text{mol } ^{18}O_2$) are desorbed from the surface rather quickly (see figure 6.11) The formation of $C^{18}O$ must occur according to an equilibrium reaction as:



The rate of formation of $C^{18}O$ in the initial period is high ($6.5 \cdot 10^{-9} \text{ mol/g cat.s}$) as compared with the Fischer-Tropsch reaction rate on such a catalyst. From figure 6.5 we calculate a total Fischer-Tropsch rate under the same conditions of about $1 \cdot 10^{-9} \text{ mol CO converted/g cat.s}$.

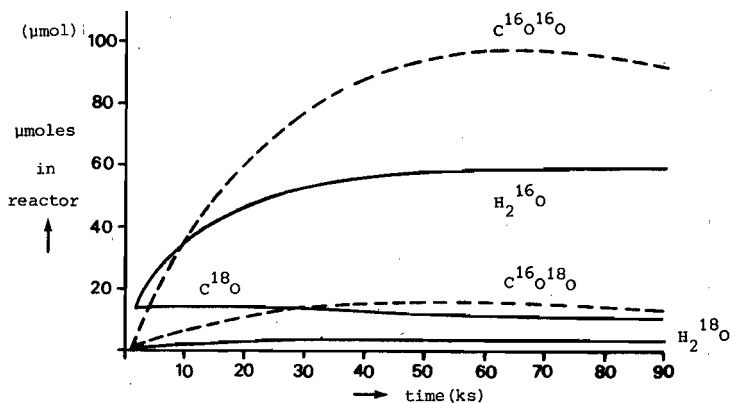


Figure 6.11. Concentrations of unlabelled and ^{18}O -labelled products during Fischer-Tropsch synthesis in a batch reactor on a reduced iron catalyst after a pretreatment with $78 \mu\text{mol } ^{18}\text{O}_2$ for 195 min.
 Synthesis: $T = 523 \text{ K}$; $P_{\text{H}_2} = 5.5 \text{ kPa}$; $P_{\text{CO}} = 1.4 \text{ kPa}$.

This shows that the CO dissociation rate is much higher than the Fischer-Tropsch reaction rate under most of the conditions applied in this thesis. This shows at the same time that the interaction of gaseous carbon monoxide with surface oxygen is more complex than assumed by Van Ho and Harriott (see chapter 2). For as follows from figure 6.11, the $\text{C}^{16}\text{O}^{18}\text{O}$ formation rate is much lower than the C^{18}O formation rate. Thus it is very well possible that also in the Van Ho and Harriott's case the rate of CO_2 formation was not at all indicative of the CO dissociation rate.

As far as the carbon dioxide and water formation rates are concerned, we see, that the rates of the unlabeled products are much higher than those of the products containing an ^{18}O atom, while for labeled and unlabeled products the carbon dioxide formation is higher than the water formation. From the former observation we conclude that much less ^{18}O than ^{16}O is available for exchange.

A comparison of the quantities of carbon and oxygen adsorbed during the Fischer-Tropsch synthesis on a reduced and on the ^{18}O -pretreated catalyst is shown in figure 6.12. We see that the presence of oxygen hinders the carbon deposition on the catalyst. From the exchange experiments shown in figure 6.11 we estimate that 0.85 mg O/gr Fe (corre-

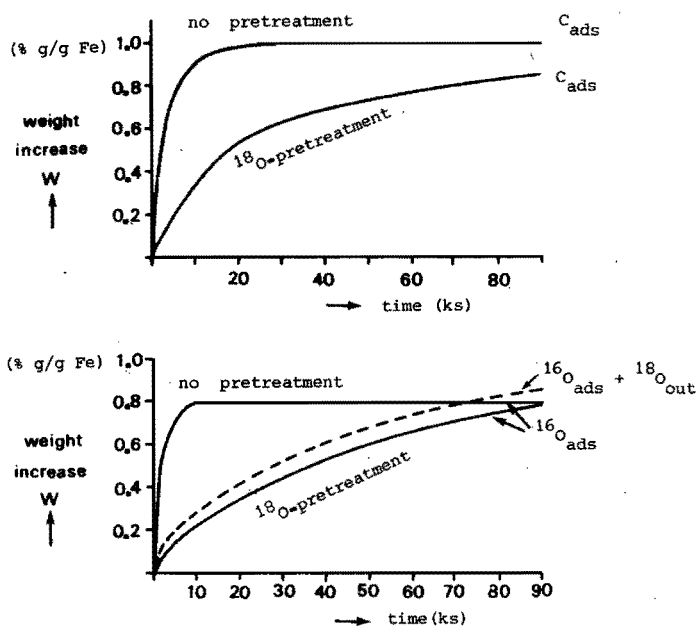


Figure 6.12. Weight increase by carbon and oxygen during Fischer-Tropsch synthesis in a batch reactor on a
 A) reduced iron catalyst
 B) with 78 μmol $^{18}\text{O}_2$ pretreated iron catalyst.
 Synthesis: $T = 523 \text{ K}$; $P_{\text{H}_2} = 5.5 \text{ kPa}$; $P_{\text{CO}} = 1.4 \text{ kPa}$.

sponding to about one monolayer) is available for exchange. From hydrogen stripping experiments at 523 K we have found that at that temperature only part of the oxygen deposited on and in a catalyst can be recovered as water. Since the exchange reaction was fast, the exchanged oxygen must be present in the outer layers of the catalyst.

6.4. DISCUSSION

The experiments at 25 Pa showed, that only small amounts of hydrocarbons up to C_4 were immediately produced by a fresh Fe surface, but that the largest amount of carbon monoxide was converted under these conditions into benzene and toluene, although the surface coverage by C was very small (about 5% of a monolayer). Because the aromatic C_6 -rings are probably bound to 6 C-adsorption sites, while the Fischer-Tropsch hydrocarbons are generally assumed to be bonded to only one or two C-adsorption sites, it is very remarkable, that these aromatics

are formed at such a low surface carbon coverage. The formation of the C_6 -rings indicates, that new carbon coming atoms are either absorbed preferentially on a site next to one already occupied by a carbon atom or that carbon atoms migrate over the catalyst surface to a site adjacent to one already occupied. We rather prefer the first explanation because the sticking coefficient of CO on an average surface site is small, and on the other hand we do not think that the migration, which has to overbridge rather long distances on the scarcely covered surface could cope with the aromatics formation rate.

We believe, that because of the low partial pressure of hydrogen a small number of 'hydrogenation ensembles' were active, which caused a low production rate of methane and of the olefins up to C_4 . The product distribution did not follow satisfactorily the Schulz-Flory distribution, because there was now a separate route towards the higher - aromatic - products.

At higher pressures formation of aromatics was not observed anymore. The formation of the precursors of the aromatics is in this case possibly coupled to the deactivation of the catalyst, when much more carbon (and oxygen) is deposited on the catalyst.

At 9 kPa in the batch reactor (see figure 6.5) methane and hydrocarbons up to C_4 were immediately produced, although the amount of carbon deposited was still relatively low (0.5% by weight C/Fe) compared to the atmospheric pressure reaction conditions (about 9 - 10% by weight C/Fe). This initial effect is ascribed to the surplus hydrogen left on the catalyst after reduction.

The direct formation of higher hydrocarbons in the initial stage of the synthesis agrees with the results from the pulse experiments performed by Kieffer (4) on Fe/ZnO catalysts. He concludes, that the chain growth is a fast reaction on iron catalysts.

When the equivalent of about 10 and 6 monolayers of C and O respectively, were absorbed by the catalyst, the concentration of carbon monoxide was reduced strongly which increased the H_2/CO ratio to about 15 after 15 ks. As a consequence increased quantities of paraffinic hydrocarbons were produced.

When we summarize our results with preoxidized catalysts, we notice:

- a) oxygen inhibits the deposition of carbon on the catalyst (see figure 6.12)

b) oxygen brings the system faster into an active state (see figure 6.8 and 6.10)

c) the probability of chain growth (α) during the Fischer-Tropsch synthesis is initially higher on an oxygen pretreated catalyst than on a reduced iron catalyst.

Dwyer and Somorjai (9) observe also a higher initial reaction rate with preoxidized iron catalysts and also a small shift towards higher molecular weight products. Somorjai et al. (2, 10) observe the same phenomena on Rh-polycrystalline foils. The increased reaction rate after an oxygen pretreatment is also observed by various authors on several other metals, like on nickel and cobalt (11) and on ruthenium (12, 13).

The increased activity of the Fischer-Tropsch synthesis is often explained by a redispersion or roughening of the catalyst surface by the oxygen treatment. Since we observe that the rate of exchange of the predeposited oxygen is much lower than the rate of exchange of oxygen coming from the normal Fischer-Tropsch reaction (see figure 6.11) we do not think that this explanation is really acceptable for our case.

It is known, that extensive penetration of oxygen can already occur at -195°C in the lattice of iron (14, 15).

Boudart (16) has suggested that oxygen which penetrated into the outer layers of the catalyst causes, as follows from photoelectric measurements, a lowering of the work function. This can result in an increased adsorption of hydrogen. This last phenomenon is also observed on Fe-catalysts by Burshtein et al. (17).

Furthermore it has been observed by various authors (4, 18, 19) that the presence of negative ions (halides, sulfides, oxides) reduces the carbon metal bond strength and this way hamper the formation of carbon deposits. This allows a stable operation of the catalyst at higher temperatures.

We suggest that the higher hydrogen availability due to subsurface oxygen increases the formation rate of all products except the higher paraffins, and further that for the formation of the higher paraffins certain hydrogenation surface ensembles have to be developed, and that carbon is a necessary component of these hydrogenation surfaces ensembles.

In the case that we have a pure reduced catalyst, an initial activity can only be brought about by a high initial hydrogen pressure, which corresponds to the effect of the oxygen described in the previous section. Otherwise active sites have to be developed by the adsorption of oxygen and of carbon.

The influence of oxygen on the carbon-metal bond strength results in an increased olefin-to-paraffin ratio as follows i.e. from figure 6.9 and 6.10.

The influence of the various process parameters on the Schulz-Flory constant is very complex e.g. hydrogen can increase chain growth rate by producing more CH_2^* species but can also increase the termination rate by increasing paraffin formation.

6.5. REFERENCES

1. K.D. Tillmetz, thesis University of Technology Berlin (1976)
2. B.A. Sexton, G.A. Somorjai, J. Catal. 46, 167 (1977)
3. F.M. Dautzenberg, J.N. Helle, R.A. van Santen, H. Verbeek, J. Catal. 50, 8 (1977)
4. E.Ph. Kieffer, thesis University of Technology Eindhoven (1981)
5. L. Henriquez, M.Sc. report University of Technology Eindhoven (1980)
6. M.A. Efroymsen, R.I. Jenrich, Statistical methods for digital computers, Vol. 3, ed. by A.Ralston & H.S. Wilf
7. A.O.I. Rautavuoma, H.S. van der Baan, to be published
8. R.B. Anderson, Catalysis, Vol. IV, ed. by P.H. Emmett, Reinhold Publishing Corporation, Baltimore, 1 (1956)
9. D.J. Dwyer, G.A. Somorjai, J. Catal. 52, 291 (1978)
10. R.G. Castner, R.L. Blachader, G.A. Somorjai, J. Catal. 66, 257 (1980)
11. R.L. Palmer, D.A. Vroom, J. Catal. 50, 244 (1977)
12. R.A. Dalla Betta, M. Shelef, A.G. Piken, J. Catal. 35, 54 (1974)
13. D.L. King, J. Catal. 51, 386 (1978)
14. C.M. Quinn, M.W. Roberts, Trans. Faraday Soc. 58, 569 (1962)
15. R.B. Anderson, Klemperer, Proc. Roy. Soc. A. 258, 350 (1960)
16. M. Boudart, J. Am. Chem. Soc. 74, 3556 (1952)
17. R.K. Burshtein, M.D. Surova, Doklady. Akad. Nauk SSSR 61, 75 (1948)
18. H.G. Davis, T.P. Wilson, U.S. patent 2717259, 2717260 (1955)
19. H. Hammer, D. Bittner, Erdoel und Kohle 31, (8), 369 (1978)

SUMMARIZED CONCLUSIONS

The results discussed in this thesis demonstrate that the rate and the product distribution of the Fischer-Tropsch (F.T.) reaction on iron catalysts at 513 K are governed by the partial pressures of carbon monoxide and hydrogen and by the composition of the catalyst. As carbon monoxide and hydrogen are adsorbed dissociatively on iron and the reaction steps occur on the surface of the catalyst, a more precise discussion must take into account the formation of and the surface reactions between carbon- oxygen- and hydrogen- ad species. Also the interactions between these species and the catalyst, both on the surface and in the bulk, are of importance as they may change the catalytic properties of the surface.

In experiments at very low pressures we have observed a preference for the formation of aromatics. From this we tentatively conclude that CO adsorption on sites next to an occupied site is favoured as compared with adsorption on a clean part of the surface.

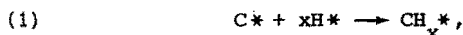
From experiments with catalysts preoxidized with $^{18}\text{O}_2$ we conclude, that the dissociation of carbon monoxide is a fast reaction on iron catalysts.

As far as the surface carbon is concerned the TPSR-experiments demonstrate that carbon on the surface can have very different reactivities towards hydrogen (TPSR maxima varying between 450 K and 670 K) and further that this carbon can enter the bulk of the catalyst at a very high rate to form a series of carbides. Tentatively we have even ascribed the initially low F.T. activity in chapter 3 to a low degree of surface coverage by carbon due to this high carburization rate. More precise measurements of the rate of carburization and of the F.T. reaction rate (chapter 5) revealed however that the F.T. rate and the carburization rate both increase during the 'activation' period. This means that the rate of formation of the precursor of these two reactions, i.e. the active carbon surface species, is not a limiting factor for the sum of the carburization rate and the F.T. rate.

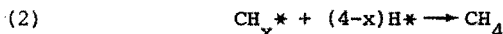
Finally it has been demonstrated that active carbonaceous surface species can be converted into less active carbon species that can cover part of the catalyst surface and thus decreases the catalyst activity.

The TPSR-experiments on an iron catalyst indicate, that at the beginning of the synthesis with a 1 : 1 H₂/CO mixture about the same quantity of very reactive C-species is formed as with a 9 : 1 H₂/CO mixture. This shows, that although the quantities of very reactive C-species are about equal for both gas mixtures, the F.T. rate is also governed by the appropriate rate of formation of these active species.

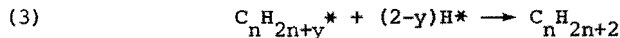
The role of hydrogen in the F.T. process is complex. We can distinguish at least three different reactions between surface hydrogen and carbonaceous ad species namely:



i.e this reaction is often considered as rate determining for the F.T. reaction



for the methane formation and



for the formation of higher paraffins.

The two latter reactions deal with hydrogenolysis of carbon-iron bonds. It seems that the rate of these two latter reactions are more or less independent, as we can have relatively high methane yields together with low paraffin/olefin ratios for the higher hydrocarbons. Also the reactions (1) and (3) seem to be independent as we can have a decreasing total activity coupled with an increasing paraffin/olefin ratio for the higher hydrocarbons.

If reaction (1) is rate determining, the rate of the F.T. reaction depends on the surface concentrations and the reactivities of the C* and H* ad species.

From the TPSR-experiments we see that initially the activity of the surface carbon is high. If we have then a relatively high coverage by H^* a high initial activity is obtained. If this coverage by H^* is low on an iron surface the activity is practically zero. As in the activation period of a F.T. reaction run the reactivity of the carbon decreases and as we have no reason to assume that the hydrogen coverage increases during that period, we must assume that the surface hydrogen ad species become more active.

We ascribe this hydrogen activation or this formation of hydrogenation surface ensembles to the role of oxygen present in the catalyst. In experiments with preadsorbed oxygen already from the beginning of the F.T. synthesis we noticed a noticeable activity under circumstances where we would have no or almost no activity without oxygen pretreatment.

SUMMARY

Synthesis gas, a mixture of carbon monoxide and hydrogen, can be obtained when coal is gasified with steam and/or oxygen. This gas can be applied in many ways. In our laboratory we are particularly interested in converting this synthesis gas selectively via the Fischer-Tropsch process to the most important petrochemical: ethene.

This route from coal to ethene can become more attractive in the near future, because the prices of hydrocarbons and particularly of naphtha, the customary feed stock for ethene manufacture rise much more quickly than the price of coal.

Since iron catalysts are better than any other metal catalyst for the production of hydrocarbons with a high olefin content, this metal is chosen as the active component of the catalyst in our study.

Such a study of iron catalysts during the Fischer-Tropsch synthesis however is complicated by the fact that the metal is unstable during the synthesis, as the bulk of the catalyst can be completely converted into carbidic phases. Furthermore iron catalysts are initially almost inactive for the Fischer-Tropsch synthesis and during the process activity develops. Industrial iron catalysts are therefore very often activated by a pretreatment of a carbon monoxide mixture. This initially transient behaviour of iron catalysts has been studied in a differential plug flow reactor. Especially the possible relations between the composition of the bulk or of the surface of the catalyst and the activity has been extensively investigated during that activation period.

The bulk composition of the catalysts has been studied by three different bulk techniques: Mössbauer spectroscopy, X-ray diffraction analysis and thermomagnetic analysis. Besides the three well known carbides χ -Fe₅C₂, θ -Fe₃C and ϵ' -Fe_{2.2}C a compound Fe_xC not mentioned earlier is observed. This compound has a composition intermediate between the one of α -Fe and the one of χ -Fe₅C₂. However, our thermomagnetic and Mössbauer measurements indicate, that this Fe_xC compound is often

(wrongly) thought to be a carbide with a stoichiometry Fe_2C and with a purely hexagonal structure. The latter structure belongs however to the carbide $\epsilon\text{'-Fe}_{2.2}\text{C}$. With the three carbides $\chi\text{-Fe}_5\text{C}_2$, $\theta\text{-Fe}_3\text{C}$ and $\epsilon\text{'-Fe}_{2.2}\text{C}$ and the compound Fe_xC the bulk composition of our iron catalysts and those mentioned in the literature can be better explained than when Fe_xC is thought to be Fe_2C , as is often done in the literature.

Although it is claimed in a number of patents that a marked increase of the olefin selectivity is obtained if an unreducible oxide such as MnO is added to an iron catalyst, we have been unable to confirm these claims in runs at 513 K. At 623 K such a catalyst shows a fast deactivation and a very selective methane production. However, the addition of a sulfate salt to an iron manganese oxide catalyst leads to a catalyst that produces very selectively short olefins, while the deposition of carbon is much less than on not sulfated catalysts. The deposition of carbon on pure iron catalysts from carbon monoxide and carbon monoxide/hydrogen mixtures is further studied in the thermobalance. A linear weight increase is always observed in the beginning of the exposure. Since the slope of the linear part of the weight curves is more influenced by the partial pressure of hydrogen than by the partial pressure of carbon monoxide, we think that oxygen removal is the rate determining step during this period of linear weight increase. After a certain weight increase has been reached, the subsequent slower weight increase is explained as being governed by the rate of carbon diffusion into the iron lattice.

To obtain further information about the activation of our catalysts a number of experiments have been carried out in a micro flow reactor. At a low H_2/CO ratio hydrogen, which is left on the catalyst from the previous reduction, is quickly replaced by carbon monoxide and C(and/or O)-containing products. In that case initially almost no hydrogenation ensembles are available and the activity is very low. At a high H_2/CO ratio this replacement of surface hydrogen by carbonaceous species can be retarded for a larger period of time. This means a noticeable activity from the very beginning of the synthesis followed by a slow deactivation. After this initial period the catalyst shows the same 'normal activation' with both gas mixtures, that is ascribed to the formation of special hydrogenation ensembles.

In chapter 6 of this thesis Fischer-Tropsch experiments at low pressures (9 kPa) in a batch reactor are described. Also here very little activity is found initially. However, when the catalyst is pre-treated with a small quantity of oxygen (equivalent to 2 to 3 monolayers), hydrocarbons (even up to C_6 and C_7) are immediately produced, while the deposition of carbon and oxygen is retarded compared to the not preoxidized catalyst. Since subsurface oxygen can increase the adsorption of hydrogen, the increased reaction rate can possibly be explained by the fast formation of hydrogenation ensembles. The reduced iron catalyst is initially inactive for the Fischer-Tropsch mixture, because the hydrogenation ensembles have to be formed during the synthesis.

Finally, the reactivity of the oxygen laid down during such a pre-treatment is investigated by the adsorption of $^{18}O_2$ and the subsequent exposure of this surface to unlabeled synthesis gas. The main part of the deposited ^{18}O -atoms exchanges then quickly with carbon monoxide to form $C^{18}O$, while the formation of $C^{16}O^{18}O$ and $H_2^{18}O$ proceeds at a much lower rate. As dissociation of the unlabeled carbon monoxide must precede the formation of $C^{18}O$, the CO dissociation rate is in this case much higher than the carbon dioxide formation rate.

SAMENVATTING

Synthesegas, een mengsel van koolmonoxide en waterstof kan verkregen worden door vergassing van kolen met stoom en/of zuurstof. Dit gas kan op vele manieren gebruikt worden. In ons laboratorium wordt vooral aandacht besteed aan dit synthesegas door middel van het Fischer-Tropsch proces selectief om te zetten in een van de belangrijkste grondstoffen voor de chemische industrie: etheen.

De bereiding van etheen uit kolen via deze route kan in de naaste toekomst steeds aantrekkelijker worden, omdat de prijzen van koolwaterstoffen in het bijzonder die van nafta, waaruit momenteel etheen wordt bereid, veel sterker stijgen dan de kolenprijzen.

Aangezien ijzerkatalysatoren beter geschikt zijn voor de bereiding van koolwaterstoffen met een hoog olefine gehalte dan ieder andere metaal katalysator, is dit metaal gekozen als actieve component van de door ons bestudeerde katalysator.

Een dergelijke studie van ijzer katalysatoren tijdens de Fischer-Tropsch synthese wordt echter bemoeilijkt, doordat het metaal niet stabiel is tijdens de synthese, hetgeen blijkt uit de volledige omzetting van de bulk van de katalysator in verschillende carbidische fasen. Daarnaast zijn ijzer katalysatoren initieel vrijwel inactief in de Fischer-Tropsch synthese en neemt de activiteit in de loop van het proces toe. Daarom worden industriële ijzer katalysatoren zeer vaak geactiveerd door de voorbehandeling met een koolmonoxide mengsel.

De geleidelijke veranderingen van ijzer katalysatoren tijdens de aktiveringsperiode zijn bestudeerd in een differentiële propstroom reactor.

Daarbij is vooral aandacht besteed aan mogelijke relaties tussen de bulk- en oppervlakte samenstelling van de katalysator en de activiteit tijdens die aktiveringsperiode.

De bulk samenstelling van de katalysatoren is bestudeerd door middel van drie verschillende bulk technieken: Mössbauer spectroscopie, Röntgen diffractie opname en thermomagnetische analyses. Naast de drie

bekende carbiden $\chi\text{-Fe}_5\text{C}_2$, $\theta\text{-Fe}_3\text{C}$ en $\epsilon'\text{-Fe}_{2.2}\text{C}$ is een nog niet eerder vermelde verbinding Fe_xC waargenomen. Deze verbinding heeft een samenstelling tussen die van $\alpha\text{-Fe}$ en het carbide $\chi\text{-Fe}_5\text{C}_2$. Uit onze thermomagnetische en Mössbauer metingen is echter gebleken, dat deze Fe_xC verbinding vaak (foutief) voorgesteld wordt als een carbide met een stoichiometrie Fe_2C en met een volledige hexagonale structuur. Deze laatste structuur behoort echter bij het carbide $\epsilon'\text{-Fe}_{2.2}\text{C}$. Met de drie carbiden $\chi\text{-Fe}_5\text{C}_2$, $\theta\text{-Fe}_3\text{C}$ en $\epsilon'\text{-Fe}_{2.2}\text{C}$ en de verbinding Fe_xC kunnen we de bulk samenstelling van onze en in de literatuur vermelde ijzer katalysatoren beter verklaren dan bij de vervanging van Fe_xC door Fe_2C , hetgeen vaak in de literatuur gebeurt.

Hoewel een aantal patenten claimen, dat een duidelijke verbetering van de olefine selektiviteit verkregen wordt, indien een slecht reduceerbaar oxide, zoals MnO , toegevoegd wordt aan een ijzer katalysator, is dit niet waargenomen tijdens onze experimenten bij 513 K. Bij 623 K vertoont een dergelijke katalysator een snelle deaktivering gepaard gaande met een zeer selektieve methaan produktie. De toevoeging van een sulfaat verbinding aan deze katalysator resulteert in een zeer selektieve produktie van korte olefinen, terwijl de afzetting van koolstof veel minder is dan op katalysatoren, die geen sulfaat bevatten.

De koolstof afzettingssnelheden op zuivere ijzer katalysatoren zijn nader bestudeerd met koolmonoxide en koolmonoxide/waterstof mengsels in de thermobalans. In alle gevallen wordt tijdens de beginperiode een lineaire gewichtstoename waargenomen. Omdat de helling van het lineaire gedeelte van de gewichtstoename sterker beïnvloed wordt door de partiaalspanning van waterstof dan door die van koolmonoxide, denken we, dat de verwijdering van oppervlakte zuurstof de snelheids bepalende stap is gedurende de periode waarin het gewicht lineair toeneemt. Nadat een bepaalde gewichtstoename bereikt is, neemt deze langzaam af, hetgeen verklaard wordt door de gelimiteerde diffusiesnelheid van koolstof in het ijzer rooster.

Om nadere informatie te krijgen over de aktivering van ijzer katalysatoren zijn een aantal experimenten uitgevoerd in een micro propstroom reaktor. Bij een lage H_2/CO verhouding wordt waterstof, dat nog afkomstig is van de reductie, snel door koolmonoxide en door C(en/of O) bevattende produkten verdrongen van het katalysator oppervlak. Zodoende zijn er initieel bijna geen hydrogenerings ensembles aanwezig en is de aktiviteit zeer laag. Bij een hoge H_2/CO verhouding kan dit verdring-

ingsproces van oppervlakte waterstof door koolstofhoudende verbindingen worden tegengehouden gedurende een langere periode, hetgeen is gebleken uit de langzame deaktivering na een hoge initiële activiteit bij de aanvang van de synthese. Na deze initiële periode vertoont de katalysator dezelfde "normale aktivering" voor beide gas mengsels, hetgeen toegeschreven wordt aan de vorming van speciale hydrogenerings ensembles.

In hoofdstuk 6 van dit proefschrift worden Fischer-Tropsch experimenten beschreven bij lage druk (9 kPa) in een batch reaktor. Ook onder deze omstandigheden wordt een zeer lage activiteit waargenomen in het begin van de synthese. Indien de katalysator echter voorbehandeld wordt met een kleine hoeveelheid zuurstof (overeenkomend met 2 à 3 monolagen) worden koolwaterstoffen (zelfs tot C_6 en C_7) onmiddellijk geproduceerd, terwijl de afzetting van koolstof en zuurstof geremd wordt in vergelijking met de afzetting bij een niet voorbehandelde katalysator. Omdat de adsorptie van waterstof verhoogd kan worden door vlak onder het oppervlak gelegen zuurstof, kan de toegenomen reactie snelheid mogelijk verklaard worden door de snelle vorming van hydrogenerings ensembles. De gereduceerde ijzer katalysator is initieel inactief voor het Fischer-Tropsch mengsel, omdat de hydrogenerings ensembles gevormd moeten worden tijdens de synthese.

Tenslotte is de reaktiviteit van zuurstof, die afgezet wordt bij zo'n voorbehandeling, onderzocht door na de adsorptie van $^{18}O_2$ niet gemerkt synthesegas te laten reageren op dit oppervlak. Het grootste gedeelte van de afgezette ^{18}O atomen wisselt dan snel uit met koolmonoxide en vormt daarbij vooral $C^{18}O$, terwijl de vorming van $C^{16}O^{18}O$ en $H_2^{18}O$ met een veel lagere snelheid plaatsvindt. Aangezien de dissociatie van niet gemerkt koolmonoxide vooraf gaat aan de vorming van $C^{18}O$, is in dit geval de CO dissociatie snelheid veel hoger dan de CO_2 vormingssnelheid.

CURRICULUM VITAE

De schrijver van dit proefschrift werd op 10 mei 1952 geboren te Amsterdam. Het diploma HBS-B werd in 1970 behaald aan het Triniteitslyceum te Haarlem.

In hetzelfde jaar begon hij met de studie scheikunde aan de Rijksuniversiteit te Leiden. Het kandidaatsexamen (S1) werd in 1973 behaald. Het doctoraalexamen werd afgelegd in 1976 met als hoofdvak Heterogene Katalyse (Prof. Dr. V. Ponec), bijvak Theoretische Organische Chemie (Prof. Dr. L.J.E. Oosterhoff) en als derde richting Econometrie (Prof. Dr. M. van Praag). In de genoemde periode werd tevens de bevoegdheid tot het geven van scheikunde lessen behaald. Gedurende 1 jaar was hij part-time werkzaam als docent scheikunde aan de Henricus MAVO te Heemstede.

Vanaf november 1976 tot mei 1981 was hij als wetenschappelijk medewerker werkzaam bij de vakgroep Chemische Technologie van de Technische Hogeschool Eindhoven. Hier werd, in de groep van Prof. Drs. H.S. van der Baan, het onderzoek uitgevoerd, dat beschreven is in dit proefschrift.

Dit onderzoek werd in 1980 gedurende een half jaar onderbroken voor een verblijf aan het Stanford Research Institute te Menlo Park (U.S.A.), nadat hij een Fulbright beurs had ontvangen. Het onderzoek in de groep van Dr. H. Wise is eveneens in dit proefschrift vermeld.

Op 1 juli 1981 zal hij in dienst treden van Esso Nederland B.V.

DANKWOORD

Op deze plaats wil ik gaarne mijn dank betuigen aan allen, die hun medewerking hebben verleend aan het tot stand komen van dit proefschrift. Een aantal personen wil ik met name noemen.

In het bijzonder gaat mijn dank uit naar mijn promotor Prof. Drs. H.S. van der Baan, die door zijn stimulerende en kritische houding heeft bijgedragen in mijn technologische ontwikkeling.

Voorts ben ik mijn co-promotor Prof. Dr. V. Ponec zeer erkentelijk voor de consciëntieuze en plezierige wijze, waarop hij mij heeft begeleid tijdens mijn scheikunde studie.

Zeër veel dank ben ik verschuldigd aan de heren A. Sommen en W.P.Th. Groenland, die met veel toewijding aan het onderzoek hebben bijgedragen.

De heren D. Francois en R.J.M. van der Wey ben ik zeer erkentelijk voor de technische assistentie en de constructie adviezen bij de ontwikkeling van nieuwe reactor opstellingen.

De heer W.J.G. van Lith bedank ik voor de prettige samenwerking tijdens de ontwikkeling van onze microcomputer.

Voorts dank ik de afstudeerders Ir. L. Henriquez en Ing. L. Steffanie voor de enthousiaste medewerking en plezierige samenwerking gedurende hun onderzoek.

Vele praktikanten en stagiaires dank ik voor de bijdrage, die zij aan dit proefschrift hebben geleverd.

Het korte doch vruchtbare verblijf aan het Stanford Research Institute in Californië zal een onvergetelijke herinnering blijven. In het bijzonder dank ik Dr. H. Wise en Dr. K. Sancier voor de prettige samenwerking en voor hun geweldige gastvrijheid. Tevens dank ik Dr. J. Mc Carty voor de bereidwilligheid bij het beschikbaar stellen van zijn apparatuur.

Dr. A.O.I. Rautavuoma en Dr. E.Ph. Kieffer bedank ik voor hun collegialiteit.

De kontakten met Dr. A.M. van der Kraan en Drs. J.W. Niemantsverdriet van het Interuniversitair Reactor Instituut te Delft was in mijn ogen een toonbeeld van optimale samenwerking.

Voorts dank ik Dr. G.J. Visser voor de visuele weergave van de katalysator structuren.

Bij de vormgeving van het proefschrift dank ik de heren A. Sommen voor het ontwerpen van het omslag, R.J.M. van der Wey voor de uitstekende uitvoering van de tekeningen en H.N.A.M. van der Meyden voor de prettige samenwerking in deze. De lay-out en het typewerk werden door Ineke, mijn vrouw, met veel toewijding en geduld verzorgd.

STELLINGEN

1. De lage adsorptie van waterstof bij kamertemperatuur op een bij 725 K gereduceerde Ni/TiO₂ katalysator wordt in de literatuur (1,2) verklaard door een sterke metaal/drager-interactie. Deze waarneming kan echter ook veroorzaakt worden door een gedeeltelijke reoxidatie van het nikkeloppervlak tijdens de evacuatie bij hoge temperatuur voorafgaande aan de waterstofadsorptie-meting (3).

1. M.A. Vannice, R.L. Garten, J. Catal. 56, 236 (1979)
2. D.G. Mustard, C.H. Bartholemew, J. Catal. 67, 206 (1981)
3. G.C.A. Schuit, N.H. de Boer, Rec. Trav. Chim. 70, 1067 (1951)

2. De methaniseringsexperimenten van Araki en Ponec (1) met ¹²CO/H₂ mengsels en ¹³C-bedekte nikkeloppervlakken hebben veel bijgedragen tot de opheldering van het mechanisme van de Fischer-Tropsch synthese. De auteurs hebben echter weinig aandacht besteed aan hun eveneens zeer belangrijke waarneming dat de initiële vormingssnelheid van ¹²CH₄ op deze ¹³C-bedekte oppervlakken aanzienlijk groter is dan op een gereduceerd nikkeloppervlak (2).

1. M. Araki, V. Ponec, J. Catal. 44, 439 (1976)
2. E.G.M. Kuijpers, G. Werner, A.J.H.M. Kock, J.W. Geus, KNCV Katalyse Symposium, Vlaardingen (1981)

3. De door Uda et al. (1) gemeten overall activeringsenergie van de reductie van γ-bismuth-molybdaat met propeen bij temperaturen beneden 673 K is niet in overeenstemming met hun isotherme reoxidatie experimenten en sluit niet aan bij hun theorie over de verschuiving van de snelheidsbepalende stap bij de omzetting van propeen in acroleïne over deze katalysator bij temperaturen beneden 673 K.

1. T. Uda, T.T. Lin, G.W. Keulks, J. Catal. 62, 26 (1980)

4. De door Yermakov (1) bereide geankerde Pd-komplexen met een variabele hoeveelheid Pd-atomen kunnen een goede methode opleveren om het aantal plaatsen in de actieve ensemble voor een katalytische reactie te bepalen. Dan dient echter bewezen te worden, dat tijdens de bereiding van het complex geen metallisch palladium gevormd wordt.

1. Yu.I. Yermakov, 7th Int. congress on Catalysis, Tokyo (1980)

5. Door de bewering dat tweewaardige overgangsmetaal ethercomplexen niet erg stabiel zijn, geven Newkome et al. (1) blijk van een onvolledige kennis van de hun ter beschikking staande literatuur (2).

1. G.R. Newkome, D.K. Kohli, F. Fronczek, J.C.S. Chem. Comm. 9 (1980)

2. M. den Heijer, W.L. Driessen, Inorg. Chim. Acta 39, 43 (1980)

6. De bewering van Isbell (1), dat zijn berekende relatieve snelheidskonstante van fructose ten opzichte van glucose niet overeenkomt met die van De Wilt (2), berust op een misverstand. Indien de snelheidskonstanten worden weergegeven in een Arrhenius plot, blijken de resultaten goed met elkaar overeen te komen (3).

1. H.S. Isbell, ACS Symposium on Carboh. Chem. Washington DC (1971)

2. H.G.J. de Wilt, B.F.M. Kuster, Carbohyd. Res. 19, 5 (1971)¹

3. J.A.W.M. Beenackers, proefschrift TH Eindhoven (1980)

7. Indien de huidige resultaten (1) met "high resolution solid state" ¹³C-NMR met behulp van "Magic Angle Spinning" technieken worden uitgebreid (2,3) met de bestudering van ²⁹Si-NMR en ²⁷Al-NMR, kan hieruit, met name voor zeolieten, een veelbelovende techniek ontstaan om de aard van de reactieve sites en de verandering daarvan tijdens een katalytische reactie nader te bepalen.

1. J.P. Wolthuizen, J.P. v.d. Berg, J.H.C. van Hooff, Catal. Zeol. (ed. B. Imelik et al.), Amsterdam, 85 (1980)
2. G.E. Maciel, D.W. Sindorf, J.A.C.S. 102, 7607 (1980)
3. E. Lippmaa, M. Mägi, A. Samoson, G. Engelhardt, A.R. Grimmer, J.A.C.S. 102, 4893 (1980)

8. Door bij de vloeistofchromatografie van suikers alleen brede pieken te combineren met mutarotatie, suggereren McGinnis (1) en Fang ten onrechte, dat bij de smalle pieken mutarotatie afwezig zou zijn.

1. G.D. McGinnis, P. Fang, J. of Chromatography 153, 107 (1978)

9. Het feit, dat in 1979 meer dan de helft van de door de overheid aan energie-onderzoek bestede gelden terecht is gekomen bij kernenergie-onderzoek, doet vermoeden, op grond van het te verwachten aandeel van kernenergie in de totale energievoorziening, dat de verdeling van gelden niet op een verstandige én economisch verantwoorde wijze heeft plaatsgevonden.
10. De aanleg van volkstuintjes in de nabijheid van drukke autowegen bewerkstelligt niet het beoogde doel van vele eigenaren om onbespoten groenten te telen.